DOT/FAA/TC-14/32

Federal Aviation Administration
William J. Hughes Technical Center
Aviation Research Division
Atlantic City International Airport
New Jersey 08405

Aircraft Performance in Slippery Runway Conditions: A Simulation Study of the Accuracy and Limitations of Real-Time Runway Friction Estimation Based on Airplane Onboard Data

April 2015

Final Report

This document is available to the U.S. public through the National Technical Information Services (NTIS), Springfield, Virginia 22161.

This document is also available from the Federal Aviation Administration William J. Hughes Technical Center at actlibrary.tc.faa.gov.

U.S. Department of Transportation
Federal Aviation Administration

Technical Report Documentation Page

1. Report No.	2. Government Accession No.	3. Recipient's Catalog No.
DOT/FAA/TC-14/32		

4. Title and Subtitle	5. Report Date
AIRCRAFT PERFORMANCE IN SLIPPERY RUNWAY CONDITIONS: A SIMULATION STUDY OF THE ACCURACY AND LIMITATIONS OF REAL-TIME RUNWAY FRICTION ESTIMATION BASED ON AIRPLANE ONBOARD DATA	April 2015
	6. Performing Organization Code
7. Author(s)	8. Performing Organization Report No.
Gerard W.H. van Es[1], Peter J. van der Geest[1], Andrew Cheng[2], and Don Stimson[3]	
9. Performing Organization Name and Address	10. Work Unit No. (TRAIS)
[1]National Aerospace Laboratory, NLR Anthony Fokkerweg 2, 1059 CM Amsterdam P.O. Box 90502, 1006 BM Amsterdam, The Netherlands [2]Federal Aviation Administration William J. Hughes Technical Center Aviation Research Division Atlantic City International Airport, NJ 08405 [3]Federal Aviation Administration Transport Airplane Directorate 1601 Lind Avenue SW Renton, WA 98057	
	11. Contract or Grant No.
12. Sponsoring Agency Name and Address	13. Type of Report and Period Covered
U.S. Department of Transportation Federal Aviation Administration Flight Technology and Procedure Division Washington, DC 20591	Final Report
	14. Sponsoring Agency Code
	Transport Airplane Directorate

15. Supplementary Notes

The Federal Aviation Administration William J. Hughes Technical Center Aviation Research Division COR was Andrew Cheng.

16. Abstract

Runway overrun accidents occurring during landings in slippery conditions continue to occur frequently worldwide. After a number of specific landing overrun accidents in the U.S., the National Transportation Safety Board (NTSB) issued a safety recommendation to investigate the technical and operational feasibility of outfitting transport category airplanes with equipment and procedures required to routinely calculate, record, and convey the airplane's braking ability.

In this context, this study developed an algorithm for real-time onboard runway friction estimation. The algorithm was demonstrated in a high-fidelity simulation test that applied data and knowledge of detailed aerodynamic and engine models to represent a specific regional jet. The primary objective was to evaluate the impact of measurement and modeling errors to the runway friction estimation obtained from the algorithm.

The simulation showed that onboard runway friction estimation can provide an accuracy of approximately ±5%; measuring errors based on realistic sensor noise and bias. However, to achieve such performance, a fairly precise estimate of instantaneous thrust, weight, and drag is required. It was noted that 1% of inaccuracy in these quantities translates directly into at least a 1% estimate error. A representative model of the ground effect is also critical to the estimation accuracy. Nevertheless, errors in the calculation of aerodynamic lift and pitching moment seemed to be negligible. The results of this study can be further used to define an operational concept in line with the recommendation of the NTSB.

17. Key Words	18. Distribution Statement
Runway condition, Friction, Real-time estimate, Algorithm, Simulation, Runway contamination, Safety	This document is available to the U.S. public through the National Technical Information Service (NTIS), Springfield, Virginia 22161. This document is also available from the Federal Aviation Administration William J. Hughes Technical Center at actlibrary.tc.faa.gov.

19. Security Classif. (of this report)	20. Security Classif. (of this page)	21. No. of Pages	22. Price
Unclassified	Unclassified	97	

Form DOT F 1700.7 (8-72) Reproduction of completed page authorized

TABLE OF CONTENTS

APPENDICES

LIST OF FIGURES

LIST OF TABLES

LIST OF ABBREVIATIONS AND ACRONYMS

kts	Knots
ADC	Air data computer
ARC	Aviation Rulemaking Committee
CG	Center of Gravity
FAA	Federal Aviation Administration
IRS	Inertial Reference System
ISA	International Standard Atmosphere
LVDT	Linear variable differential transducer
MAC	Mean aerodynamic chord
NTSB	National Transportation Safety Board
RA	Radio altimeter
RVDT	Rotary Variable Differential Transducer
T/R	Thrust reverser

EXECUTIVE SUMMARY

Runway overrun accidents occurring during landings in slippery conditions continue to occur frequently worldwide. A significant contributing factor is the lack of timely, accurate information about runway friction conditions that could help pilots assess landing distance safety margins when landing airplanes in adverse weather. After a number of specific landing overrun accidents in the United States, the National Transportation Safety Board issued a series of safety recommendations, from as early as 1974, on the subject of runway friction determination under slippery runway conditions. A particular recommendation to the Federal Aviation Administration was to investigate the technical and operational feasibility of outfitting transport-category airplanes with equipment and procedures required to routinely calculate, record, and convey the airplane's braking ability. In that context, this study developed an algorithm to estimate real-time runway friction levels by using information from onboard sensor systems during the landing roll. The algorithm was demonstrated in a high-fidelity simulation test that applied data and knowledge of detailed aerodynamic and engine models to represent a specific regional jet.

The main objective of the study was to demonstrate the accuracy and limitation of a real-time runway friction estimation algorithm. The simulation study evaluated the accuracy of the estimate by considering realistic sensor characteristics and possible measurement and modeling errors. A high-fidelity simulator representing a specific regional jet was used to generate data during landings on different contaminated runways. The study compared the estimate that resulted from the algorithm, including maximum achievable friction under friction-limited braking, to the actual runway friction coefficient that was used to generate the simulation data to determine the accuracy of the algorithm. The evaluation of the algorithm included an assessment of the impacts of realistic noise and biases on the onboard measurements, and modeling errors in the calculation of thrust, drag, lift, pitching moment, and ground effect.

The simulation study showed that, theoretically (based on noise-free measurements), the runway friction coefficient can be estimated with an error margin of approximately ±5%. Taking realistic sensor characteristics into account would slightly increase the noise level of the friction estimate without significantly affecting the average error. Nevertheless, the friction estimation is sensitive to errors in the assumed aircraft weight. A 1% error in aircraft weight was found to result in an approximately 1.2% error in the estimated friction. Errors in computed drag and net engine thrust would also easily impact the estimate of the friction coefficient. The drag and engine thrust must be calculated within a limited error margin to get reliable results. Inaccuracies in the assumed center-of-gravity (CG) location seemed to be less sensitive. Only a 0.4% estimation error was noted with 1% of inaccuracy in CG. The estimate accuracy was not very sensitive to modeling errors in computed aerodynamic lift and pitching moment, either. The contribution of the pitching moment is almost negligible and, therefore, the algorithm can be simplified by omitting the pitching moment equations without significant effect on the accuracy of the estimated friction coefficient. Overall, it is concluded that, in principle, the onboard runway friction calculation is feasible, given that the aircraft weight, thrust, and drag can be computed with sufficient accuracy.

Given the potential feasibility demonstrated in the simulation, various operational concepts of using such estimations can be likely developed to reduce landing overrun risk and therefore

increase safety. The operational concept should also address human factor aspects and the relationships and responsibilities of flight crew and air traffic control. It is recommended that the follow-up studies investigate when and how to use the onboard friction estimation, determine the performance requirements, and specify the required accuracy and integrity of the friction-estimation system.

1. INTRODUCTION

1.1 BACKGROUND

Runway overrun accidents continue to occur in slippery conditions during landing. The most recent Boeing Statistical Summary of Commercial Jet Airplane Accidents shows that runway excursions, abnormal contact, and undershoot/overshoot remain the third-leading cause of fatalities in the worldwide commercial jet fleet [1]. A significant contributing factor is the lack of timely, accurate information regarding runway friction conditions for pilots to assess landing distance safety margins when landing airplanes in adverse weather. The National Transportation Safety Board (NTSB) has issued a number of safety recommendations since 1974 on the subject of runway friction determination in slippery runway conditions. Recent examples include the Southwest Airlines Boeing 737-700 accident at Chicago Midway Airport on December 8, 2005; the Shuttle America Embraer 170 accident at Cleveland Hopkins International Airport on February 18, 2007; and the Pinnacle Airlines Bombardier/Canadair Regional Jet accident at Cherry Capital Airport, Traverse City, Michigan, on April 12, 2007. As a result of the Southwest Airlines landing overrun, the NTSB recommended that the Federal Aviation Administration (FAA) should:

> Demonstrate the technical and operational feasibility of outfitting transport-category airplanes with equipment and procedures required to routinely calculate, record, and convey the airplane braking ability required and/or available to slow or stop the airplane during the landing roll. If feasible, require operators of transport-category airplanes to incorporate use of such equipment and related procedures into their operations [2].

The FAA chartered a Takeoff and Landing Performance Assessment Aviation Rulemaking Committee (ARC) to make recommendations to the FAA regarding, among other things, standards for runway surface-condition reporting. The ARC recommended the FAA consider sponsoring research to develop an onboard aircraft system to assess braking-system performance and display it to the pilot in real time. The ARC felt that the development of a system would significantly improve runway safety.

1.2 SCOPE OF WORK

The objective of this study is to investigate the accuracy and limitation of using onboard data from landing airplanes to identify and report real-time runway slipperiness conditions to controllers and flight crews of subsequent arriving airplanes. The ultimate goal is to improve runway safety by reducing the number of overruns on slippery runways by providing technological advances and information systems that can be used to anticipate changing runway friction conditions and predict the required stopping distance on slippery runway surfaces. In this report, a proof of concept study is presented that evaluates methods for using onboard recorded data to determine the instantaneous runway friction level or runway slipperiness condition. The study is limited to civil transport aircraft that are certified under Code of Federal Regulations Part 25 or equivalent regulations.

1.3 GENERAL DESCRIPTION AND APPROACH

This study aims to assess the conceptual feasibility of systems that use airplane onboard data to identify runway friction conditions. This means that the input data set is not limited to that recorded on the quick-access recorders or flight data recorders (which would be the case when the algorithm would be intended for post-processing), but that, in principle, all data within the aircraft systems and distributed by the aircraft data buses are available for the intended system, with corresponding accuracy and sampling rate. Therefore, all data from the Inertial Reference System (IRS), Air Data Computer (ADC), Flight Management System, Global Positioning System receiver, radio altimeter (RA), and engine parameters are potential valid input data to the friction-estimation system.

It is worth noting that an aircraft experiences maximum friction when applying full braking to the friction limits. However, full braking on slippery runways does not often occur during day-to-day landings. This means that the onboard friction estimation system will identify instantaneous friction levels that will mostly be significantly less than the maximum friction achievable. Therefore, even though the instantaneous friction coefficient can be identified, it may not be very useful to transmit such information unless the aircraft encounters a situation close to friction-limited braking. This leads to further questions regarding when to report, to whom to report, and what to do with the reported information. However, these issues are outside the scope of this study, which focuses only on technical feasibility.

Another issue to address is the type of test data available to evaluate a prototype runway friction determination algorithm. Although it could be best to collect the required onboard flight parameters during full braking on slippery runways through actual flight tests, this approach is expensive and, therefore, not feasible within the scope and budget of this study. The engineering simulation provides an adequate alternative to generating the required onboard data relating to landing and braking during landings on contaminated runways. An advantage of using simulations is that real values of runway braking can be controlled and used as truth values to be compared with the results of the runway friction algorithm. These simulations will be further described in section 2.

2. GENERATION OF ONBOARD TEST DATA

The Dutch National Aerospace Laboratory Air Transport Safety Institute has several 6-degrees of freedom, nonlinear simulation models of different transport aircraft. The most extensive model available is the regional (100-seat) jet model. This engineering model is fully validated against flight test data and is used in level D training flight simulators. The model accounts for ground effect using data on lift, drag, pitching moment, trim, and power in ground effect. Furthermore, the model calculates ground reaction dynamics resulting from strut deflections, tire friction, side forces, weight, speed, and autobrake settings and configuration. Because this model incorporates representative brake and tire dynamics (including antiskid), it is capable of simulating braked landings on slippery runways.

Although developing realistic engineering models to simulate aircraft ground maneuvers is usually difficult [3], the Dutch National Aerospace Laboratory's regional jet model has been validated on slippery runway operations by using flight test data and demonstrated acceptable correlation between the model results and the test data. Therefore, this engineering model should provide satisfactory simulation data to study the aircraft performance during landing roll.

The baseline simulations have been selected to cover a wide range of conditions. The following parameters have been varied:

- Runway conditions—Dry, wet, icy. The respective maximum available runway friction coefficients used in the model are as follows: dry: 0.65, wet: 0.28, and icy: 0.15. The actual, instantaneous, runway braking coefficient depends on groundspeed and slip ratio, as shown in figure 1.

- Weather conditions—International Standard Atmosphere (ISA) (in combination with dry/wet) and ISA-15 degrees (with icy runway).

- Wind and turbulence—No wind/no turbulence and 15 knots (kts) crosswind with corresponding turbulence.

- Braking action—Auto (controlled to 0.15g deceleration), 50% (half brake), 100% (full brake).

- Thrust reverser (T/R)—Idle, full.

These variations resulted in 25 total individual simulation runs. A survey of all conducted simulations is given in table 1. All simulations were carried for the selected regional jet model with a mass of 34,000 kg (75,000 lb). The CG location was approximately 30% mean aerodynamic chord (MAC). The aircraft was initialized at approximately 10 ft above the runway. The landing, touchdown, and rollout under given conditions were simulated. The simulation was terminated when the aircraft reached a full stop. A total of 100 parameters of interest were stored. A survey of these parameters is provided in appendix A.

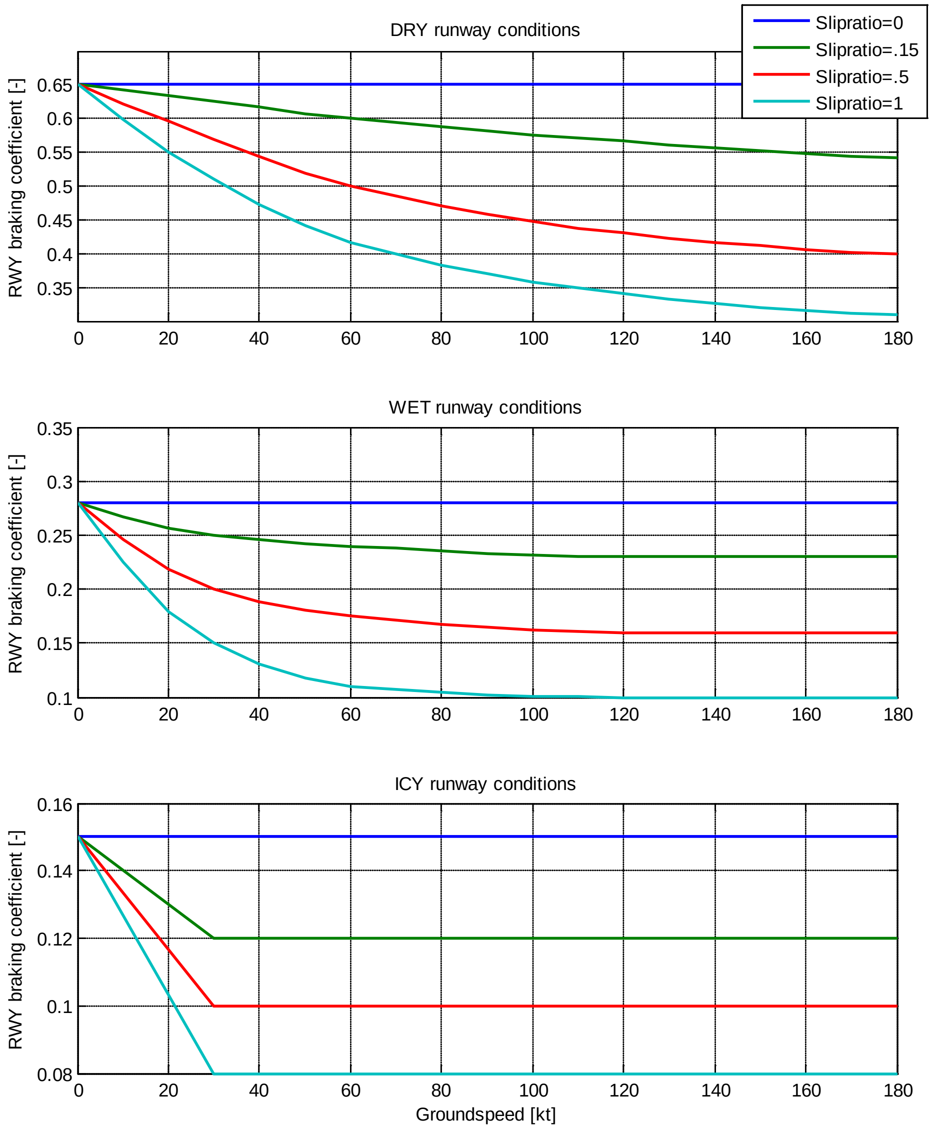

Figure 1. Maximum Runway Braking Coefficient Used in the Simulation Model

Table 1. Summary of Conducted Simulation Runs

Case	Designator	Runway Condition	Weather	X-wind	Turb	Brake	Reverse
1	dat_dry_0.15g	dry	ISA	no	no	auto	no
2	dat_dry_0.15g_wnd	dry	ISA	15 kt	yes	auto	no
3	dat_dry_hlfbrk_idlrev	dry	ISA	no	no	50%	idle
4	dat_dry_hlfbrk_idlrev_wnd	dry	ISA	15 kt	yes	50%	idle
5	dat_dry_hlfbrk_mxrev	dry	ISA	no	no	50%	full
6	dat_dry_hlfbrk_mxrev_wnd	dry	ISA	15 kt	yes	50%	full
7	dat_dry_mxbrk_idlrev	dry	ISA	no	no	100%	idle
8	dat_dry_mxbrk_idlrev_wnd	dry	ISA	15 kt	yes	100%	idle
9	dat_dry_mxbrk_mxrev	dry	ISA	no	no	100%	full
10	dat_dry_mxbrk_mxrev_wnd	dry	ISA	15 kt	yes	100%	full
11	dat_icy_0.15g	icy	ISA-15	no	no	auto	no
12	dat_icy_hlfbrk_idlrev	icy	ISA-15	no	no	50%	idle
13	dat_icy_hlfbrk_mxrev	icy	ISA-15	no	no	50%	full
14	dat_icy_mxbrk_idlrev	icy	ISA-15	no	no	100%	idle
15	dat_icy_mxbrk_mxrev	icy	ISA-15	no	no	100%	full
16	dat_wet_0.15g	wet	ISA	no	no	auto	no
17	dat_wet_0.15g_wnd	wet	ISA	15 kt	yes	auto	no
18	dat_wet_hlfbrk_idlrev	wet	ISA	no	no	50%	idle
19	dat_wet_hlfbrk_idlrev_wnd	wet	ISA	15 kt	yes	50%	idle
20	dat_wet_hlfbrk_mxrev	wet	ISA	no	no	50%	full
21	dat_wet_hlfbrk_mxrev_wnd	wet	ISA	15 kt	yes	50%	full
22	dat_wet_mxbrk_idlrev	wet	ISA	no	no	100%	idle
23	dat_wet_mxbrk_idlrev_wnd	wet	ISA	15 kt	yes	100%	idle
24	dat_wet_mxbrk_mxrev	wet	ISA	no	no	100%	full
25	dat_wet_mxbrk_mxrev_wnd	wet	ISA	15 kt	yes	100%	full

3. DEVELOPMENT OF THE ALGORITHM

The runway friction algorithm has been based on the equilibrium of accelerations and forces acting on the airframe (Newton's second law). A total of four force components can be discerned: aerodynamic, engine, ground reaction (gear), and gravity forces. This results in the following vector equation for linear acceleration:

$$\overrightarrow{F_{aero}} + \overrightarrow{F_{engine}} + \overrightarrow{F_{gear}} + \overrightarrow{F_{gravity}} = M\vec{a} \quad (1)$$

Note that it is assumed that angular rotations are negligible because the airframe is supposed to move along a straight line over the runway[1].

Because of the assumption of rectilinear motion, it is also assumed that moments acting on the airframe are in equilibrium:

$$\overrightarrow{M_{aero}} + \overrightarrow{M_{engine}} + \overrightarrow{M_{gear}} = 0 \tag{2}$$

By estimating the aerodynamic forces ($\overrightarrow{F_{aero}}$) and the engine forces ($\overrightarrow{F_{engine}}$), and measuring the gravity forces ($\overrightarrow{F_{gravity}}$) and the linear accelerations, the above-mentioned equation can be solved to find the ground reaction forces ($\overrightarrow{F_{gear}}$).

It is imperative that the ground reaction forces acting on the main gear and the nose gear be considered individually. These forces can be calculated respectively by satisfying equation 2 for an equilibrium state of aerodynamic, engine, and undercarriage moments. The aerodynamic and engine forces are calculated based on the available aerodynamic and engine engineering model using the onboard measured input parameters of the models.

Once the vertical force component of the nose gear is known, the rolling friction force component of the nose gear[2] can be estimated using the method described in ESDU 05011 [4]. When the rolling friction of the nose gear is known, it can be subtracted from the total *x*-component (longitudinal) of the total ground reaction force to get the instantaneous *x*-component of the main gear reaction force.

By definition, the ratio of the *x*-component and the *z*-component (vertical) of the main gear reaction forces is the friction coefficient as experienced by the main gear. This parameter will be the output of the runway friction algorithm (designated as μ_estimated). Please note that this parameter is merely the instantaneously achieved friction braking coefficient under the given conditions and the actual braking pressure applied, and is not necessarily the maximum runway braking friction coefficient achievable on the particular runway. It should also be noted that in the current algorithm, lateral forces (*y*-component) and moments (around the top axis) are neglected.

The calculations as described above have been implemented in MATLAB®/Simulink®. The top-level diagram of this implementation is shown in figure 2.

The algorithm has been defined as only using parameters from onboard systems, such as the IRS, ADC, and RA, and linear and rotary data pick-ups (linear variable differential transducers [LVDTs] and rotary variable differential transducers [RVDTs]), the flight management system, and the engine.

[1] Otherwise a term $M\vec{\omega} \times \vec{v}$ should be added to the left hand side of Equation (1).
[2] The nose gear is unbraked.

The output of the friction estimation algorithm is the estimate of the instantaneous runway friction coefficient (μ_estimated). Because this friction coefficient usually does not represent the maximum friction coefficient achievable, a second output is defined to indicate the friction coefficient when the applied braking leads to near-friction-limited braking. For simplicity, the simulation assumed that the friction-limited braking occurs when the slip ratio exceeds 17% (i.e., the aircraft ground speed exceeds the wheel circumference speed by more than 17%). In such cases, the calculation provides a second output, μ_reported, as an annunciation to indicate the braking coefficient when the braking limited condition has occurred.

The second-level diagram, zooming in on the components of the friction estimator block, is given in figure 3. It is composed of three basic components:

- The aerodynamic model
- The engine model
- The friction calculation, based on equations 1 and 2

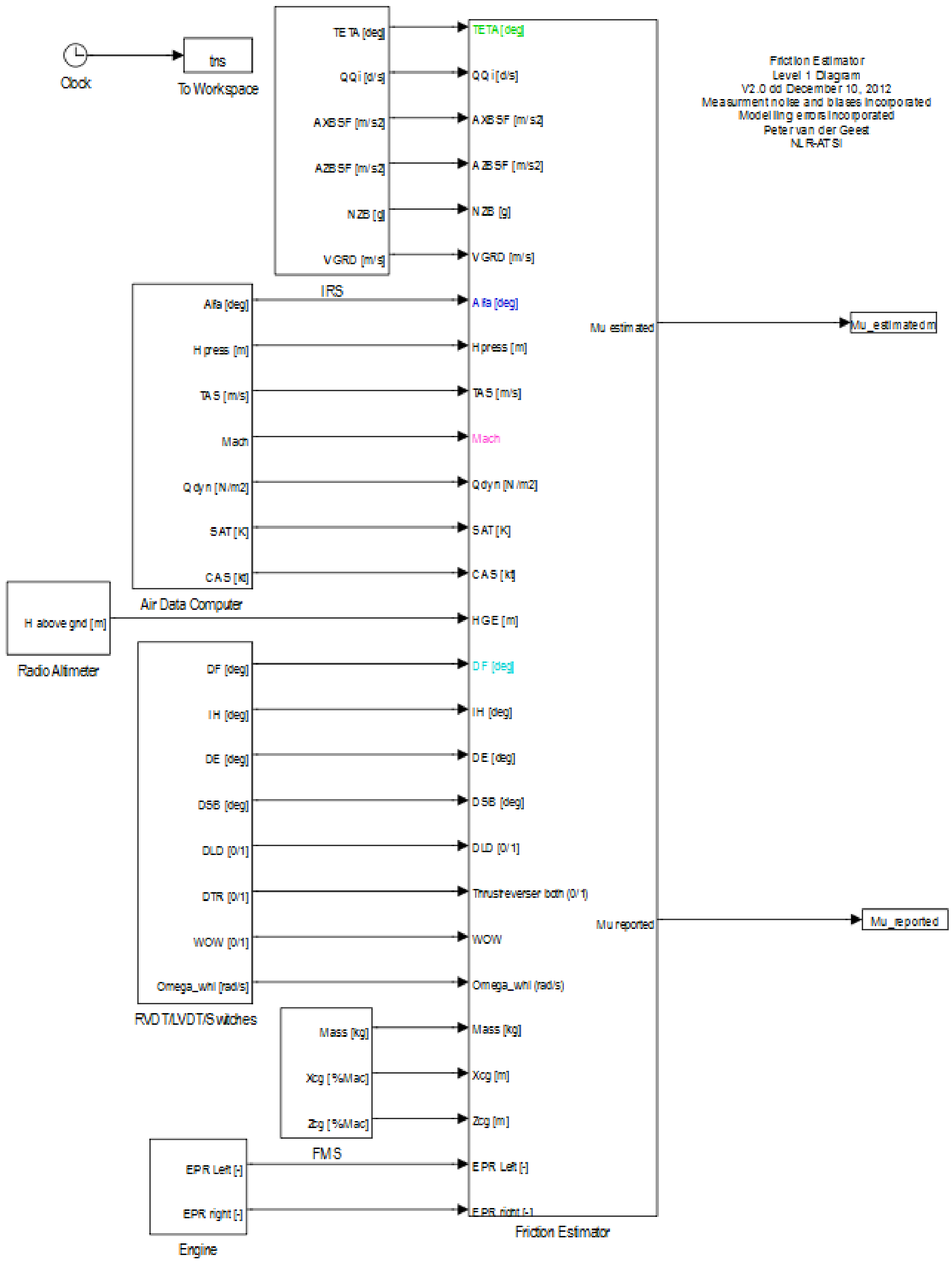

Figure 2. Top-Level Simulation Block of the Friction Estimation Algorithm

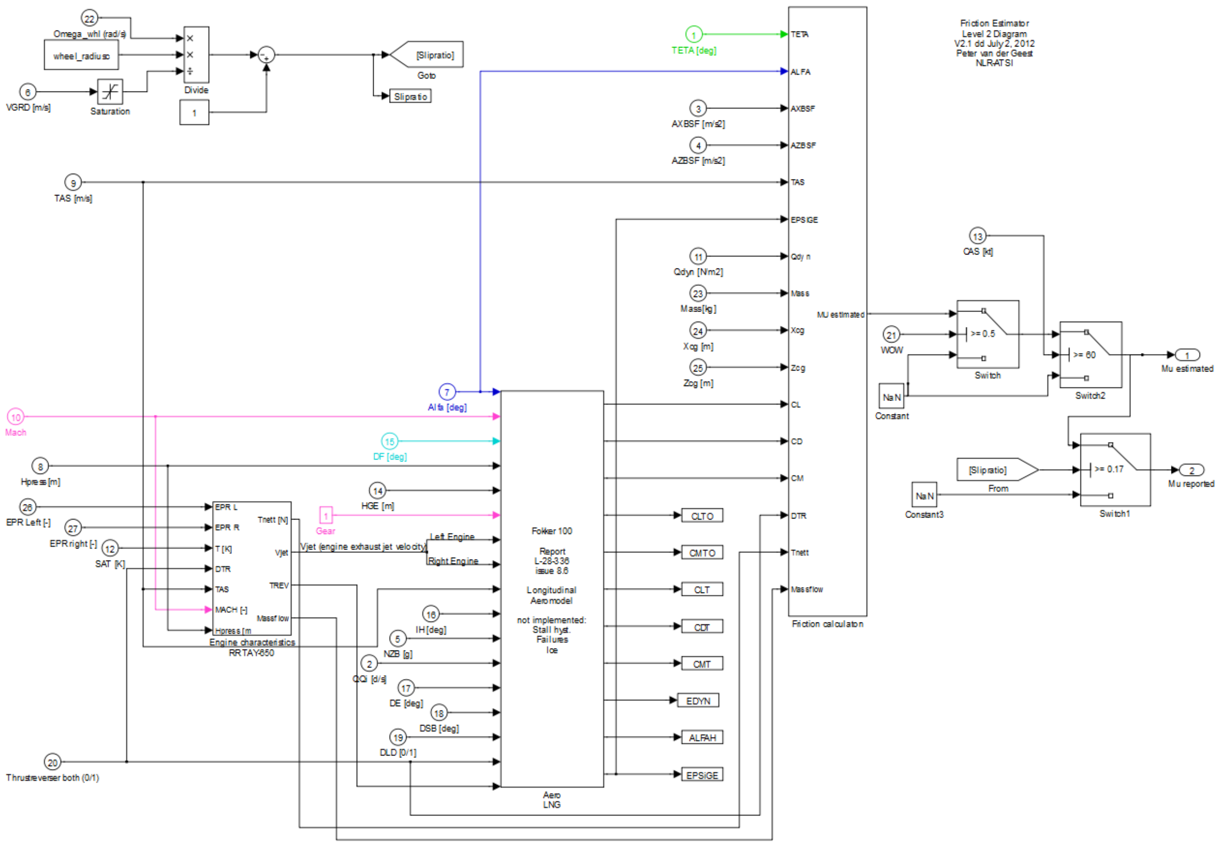

Figure 3. Level 2 Diagram of the Friction Estimation Simulation Block

3.1 AERODYNAMIC MODEL

The aerodynamic model has been based on the full (level D) aerodynamic model of the selected regional jet, as described in the corresponding aerodynamic database [5]. Because this is a proprietary model, no further details are given here. Some simplifications were introduced to limit the model to the low-speed region only and to discard special features, such as ice accumulation, failures, and stall hysteresis. Therefore, the model was tailored to the flight regime near or at the ground under normal (low-speed) conditions. It may be assumed that the level of detail of this model is similar to the engineering simulation models available to any aircraft manufacturer as part of an aircraft-development process. Therefore, it may also be assumed—despite the model still being fairly extensive—that any aircraft manufacturer will have the capability to design a similar algorithm based on existing aerodynamic models.

As shown in figure 3, the aerodynamic model requires 17 input parameters, which are measured onboard or can be derived from onboard measurements, to calculate the aerodynamic lift, drag, and pitching moment coefficients. These coefficients are input to the friction calculation to compute the aerodynamic forces and moments on the airframe.

3.2 ENGINE MODEL

The engine model has been based on available knowledge of the specific Rolls Royce engine type, which is a proprietary model. As part of the design process, this type of information will be available to any aircraft or engine manufacturer. A rather simplified model has been used that relates the net engine thrust to the engine pressure ratio, given a certain true airspeed and static air temperature. Also, the amount of reverse thrust is calculated in case the T/Rs are engaged.

It is worth noting that the actual engine-related forces and moments components will not only depend on the generated thrust, but also on local flow characteristics. To adequately take account of the effects of local flow dynamics, the input for the friction estimation model should include gross thrust and intake drag in addition to the net thrust so that the downwash at the engine and the interaction with reverse thrust will be computed. The engine model (shown in figure 3) provides only the net thrust. The engine/aerodynamic interference effects and the required axes transformations are computed in the friction estimator block.

3.3 FRICTION CALCULATION

In the friction calculation block, the actual estimation of the instantaneous main gear wheel braking coefficient is carried out. It basically solves equations 1 and 2 by using the required inputs from the engine and aerodynamic model plus a number of additional required parameters. All required axes transformations are performed in this block. All forces and moments are transformed to the intermediate axes system. The origin of the intermediate axes system is at the CG location. The *x*-axis is pointed forward in the symmetry plane aligned with the velocity vector relative to the air. The velocity vector is assumed to always be parallel with the runway surface when the aircraft is on the ground. The *y*-axis is perpendicular to the right, and the *z*-axis is perpendicular downward. The selection of this axes frame simplifies the calculations. Within the aerodynamic model, all aerodynamic forces and moments are given in this axes frame. Another advantage is that runway friction components of the undercarriage are always aligned along the *x*-axis in this axes frame, independent of the gear compression of the main and nose gear. This facilitates the calculation of the ground reaction pitching moment.

4. EVALUATION OF THE ALGORITHM

4.1 EVALUATION APPROACH

Three evaluation steps have been defined to evaluate the performance of the friction estimation algorithm, as introduced in the previous sections:

- Evaluation of fault-free performance
- Evaluation of performance with realistic sensor properties
- Evaluation of performance with modeling errors

The first step evaluates the theoretical performance of the algorithm. In this case, it is assumed that all required input measurements have no measurement errors, along with infinite resolution and small sampling intervals (0.03 sec). The objective of this first step is to ascertain how accurately, under ideal conditions, the algorithm is able to estimate the instantaneous friction. Results of the first step are presented in section 4.2.

The second step is to investigate the sensitivity of the algorithm for real sensor characteristics and measurement imperfections. Results of the first step are presented in section 4.3.

The third step investigates the sensitivity of the algorithm for modeling errors. The algorithm is based on knowledge of the aerodynamic and engine model. However, the same aerodynamic and engine model is also used in the aircraft simulation program to generate the measurement data. Therefore, if the same modeling errors were to exist in both models, they would not affect the results of the friction-estimating algorithm. However, in reality, it must be assumed that aerodynamic and engine models, despite the efforts of aircraft manufacturers to develop the most accurate models, still may contain some modeling errors, particularly in the challenging area of near-ground and in-ground effects. The impact of the modeling errors is presented in section 4.4.

4.2 FAULT-FREE PERFORMANCE

For the 25 baseline simulation cases presented in section 2, the runway friction has been estimated using the algorithm described in the previous section. The results of all cases are shown in appendix B. The time histories are related to the landing run from touchdown (weight on wheels) to 25 kt ground speed. It is assumed that the estimation algorithm itself cannot provide accurate results below approximately 60 kt computed airspeed because, in general, measurements from the Air Data System at speeds lower than 60 kt become unreliable. Therefore, estimated and reported friction coefficients are shown only for the period when the airspeeds are above 60 kt.

Based on these results, it can be concluded that the estimated friction coefficient in general matches fairly well with the true friction coefficients of the right and left main gear (right_µ_true and left_µ_true). In cases of crosswind, it is shown that reaction forces on the left and right main gear are somewhat different, leading to a difference between the left and right main gear friction coefficient. Generally, the estimated friction coefficient in these cases is close to the average friction coefficient. Therefore, it is concluded that neglecting the lateral dynamics in the calculations does not lead to significant errors in the estimated friction coefficient.

The results are summarized in table 2, which shows, for each case, the maximum actual (true) friction coefficient calculated by the simulation program during the landing run. The actual friction coefficient is determined by the average of the right and left gear (true) friction coefficient (left_µ_true + right_µ_true) /2). The mean estimation error is calculated as the difference between the estimated braking coefficient and the mean of the right and left gear (true) friction coefficient (mean(µ_estimated - (left_µ_true + right_µ_true) /2) averaged over the time period from touchdown until reaching 60 kt groundspeed. Generally, this covers a period of approximately 8–10 seconds (see appendices) and, therefore, approximately 240–300 samples are used to calculate the mean estimation error and standard deviation.

A number of observations were made:

- The deceleration is controlled to a constant value in case of auto braking. When no T/R is used, it leads to a constant value of the friction coefficient, independent of runway condition (dry or wet), unless the available maximum friction is insufficient to achieve the required deceleration (icy).

- Under icy conditions, the available friction always leads to friction-limited braking. Therefore, the calculated friction coefficient is usually constant (~0.13), independent of the braking action (auto, half, or max) and amount of reverse thrust applied.

- Under wet conditions, the maximum runway friction coefficient is approximately 0.28, which is also the approximate value calculated under maximum braking action.

- Generally, the calculated friction coefficient slightly overestimates the true friction coefficient. On average, this leads to a bias of 1%.

- The standard deviation of the error in the estimated friction coefficient is strongly dependent on the presence of wind and turbulence. Under no wind conditions, the standard deviation of the error is, on average, approximately 2%. In the presence of wind and turbulence, the standard deviation increases to approximately 10%.

Table 2. Fault Free Performance Results

Case	Runway Condition	Brake	Reverse	Max. μ Actual	Mean error %	Standard deviation %
1	dry	auto	idle	0.177	0.48	0.48
2	dry	auto	idle	0.178	-2.08	11.63
3	dry	50%	idle	0.174	0.01	3.53
4	dry	50%	idle	0.177	-8.32	11.94
5	dry	50%	full	0.174	1.77	1.54
6	dry	50%	full	0.176	0.33	10.16
7	dry	100%	idle	0.335	1.96	2.15
8	dry	100%	idle	0.337	-4.71	6.86
9	dry	100%	full	0.334	2.96	0.84
10	dry	100%	full	0.337	-4.66	7.23
11	icy	auto	idle	0.126	-0.36	0.54
12	icy	50%	idle	0.126	-0.90	3.47
13	icy	50%	full	0.126	0.88	1.91
14	icy	100%	idle	0.126	0.90	3.47
15	icy	100%	full	0.126	0.88	1.91
16	wet	auto	idle	0.172	2.94	0.43
17	wet	auto	idle	0.173	-2.22	15.3
18	wet	50%	idle	0.203	3.20	2.56
19	wet	50%	idle	0.206	4.91	11.78
20	wet	50%	full	0.204	4.21	0.97
21	wet	50%	full	0.209	1.22	13.55
22	wet	100%	idle	0.284	4.24	1.89
23	wet	100%	idle	0.284	3.47	9.34
24	wet	100%	full	0.284	4.90	0.78
25	wet	100%	full	0.284	7.37	5.55

4.3 EFFECT OF MEASUREMENT NOISE AND BIASES

Results concerning runway friction estimation from simulated flight data were presented in section 4.2. It was shown that using available aircraft and engine engineering data can yield rather accurate estimate of instantaneous runway friction experienced by the aircraft if all measurements are perfectly recorded and the exact CG location and aircraft mass are known. The average estimation error is only a few percent. For real-world applications, it is crucial to know to what extent the estimation would be affected when the required input signals are not perfect. In Section 4.3 we will discuss the accuracy assessment of the friction estimation in the presence of imperfect measurements. Realistic measuring errors have been introduced to all the required input signals to access the impact to the accuracy of the friction estimation algorithm. The characteristics—in terms of accuracy, bandwidth, resolution, etc.—of the measuring errors follow the specifications listed in ARINC 738A-1 [6] for the air data and IRS. In addition, a sensitivity analysis was performed to establish how the friction estimation accuracy is affected by biases in the assumed aircraft mass and CG location.

4.3.1 Measurement Errors

The applied error characteristics for the air data and inertial reference data are summarized in table 3, as derived from ARINC 738A-1 [6]. This document specifies the accuracy of air data and inertial measurement signals, referring to an error band that contains 95% of the measurements. This is close to a 2σ standard deviation, assuming a Gaussian error distribution.

In addition to the parameters previously mentioned, the friction estimation algorithm requires the position of a number of aerodynamic surfaces (such as elevator, lift dumpers, speed brakes, etc.). The positions of these surfaces are usually measured with LVDTs or RVDTs. It is assumed that the resolution of such signals is 0.05 degrees, with accuracy of 0.5 degrees. Based on this error model, all the input signals for the estimation algorithm have been perturbed with the applicable measurement noise using the appropriate sampling rate and resolution. This has been achieved by adding random Gaussian noise (with zero mean and standard deviation equaling accuracy/2) to the relevant simulation signals. In case it is needed, the resulting signal has been resampled to a lower sampling frequency, with a zero-order hold for intermediate samples (see table 3). Finally, for each perturbed signal, the internal machine resolution is reduced to the required resolution to resemble the real measurement signal. In all cases, the perturbed signals were free of biases. The combined effect of adding the error model to all relevant signals is discussed in section 4.3.2.

The simulation results for all cases are shown in appendix C. The layout of these time histories is similar to that in appendix B, except that the charts in appendix C include the "friction annunciation" (μ-reported) in the fourth graph. It is worth noting that friction-limited braking occurred in the simulation of all icy cases and two wet cases so that the algorithm provided a friction annunciation to the pilot. The annunciation of the friction coefficient occurred over a time period of approximately 10 seconds. It is expected that this time period would be sufficient for the pilot to take appropriate action and report the critical runway value to the air traffic controller if required.

The impact of adding measurement noise on the computed friction coefficient is evident from the time histories. The numeric results are given in table 4, which shows that the mean error in the estimated friction coefficient is hardly affected by the incorporation of measurement noise. There are small random differences with the fault-free cases. However, in general, the mean error remains within the same range. Furthermore, as expected, the standard deviation of the friction estimation error increases because of the measurement noise. Without measurement noise, the average standard deviation of the error is approximately 5%; however, with measurement noise, the standard deviation of the error increases to an average of approximately 10%. As shown in table 4, cases that are also subject to wind and turbulence generally lead to the largest errors. However, it is expected that appropriate filtering could be introduced to suppress the dynamic errors.

Table 3. Simulated Sensor Characteristics

Parameter	Resolution	Accuracy	Units	Sample Frequency (Hz)
Pitch Angle	0.011	0.1	deg	32
True Airspeed	0.0625	4.0	kt	8
Angle of Attack	0.05	0.25	deg	16
Mach	0.0000625	0.015	-	8
Pressure Altitude	2.7	6.75	ft	32
Radio Altitude	0.125	5.0	ft	32
Load Factor	0.001	0.01	g	32
Pitch Rate	0.015	0.1	deg	32
Ground Speed	0.01	1.0	kt	16
Impact Pressure	0.03125	1.0	mb	8

Deg = degrees; kt = knots; ft = feet; g = gravity; mb = minibar

Table 4. Friction Estimation Performance With Realistic Sensor Characteristics

Case	Runway Cond.	Brake	Reverser	Max. µ Actual	Mean Error %		Std. Dev %	
					w/o noise	w/ noise	w/o noise	w/ noise
1	dry	auto	idle	0.177	0.48	-0.21	0.48	7.62
2	dry	auto	idle	0.178	-2.08	0.59	11.63	14.4
3	dry	50%	idle	0.174	0.01	-1.37	3.53	9.47
4	dry	50%	idle	0.177	-8.32	-8.72	11.94	14.3
5	dry	50%	full	0.174	1.77	-0.30	1.54	9.55
6	dry	50%	full	0.176	0.33	-0.31	10.16	13.7
7	dry	100%	idle	0.335	1.96	0.74	2.15	5.60
8	dry	100%	idle	0.337	-4.71	-6.30	6.86	8.62
9	dry	100%	full	0.334	2.96	2.06	0.84	5.47
10	dry	100%	full	0.337	-4.66	-6.75	7.23	8.97
11	icy	auto	idle	0.126	-0.36	-0.95	0.54	8.53
12	icy	50%	idle	0.126	-0.90	-0.68	3.47	8.69
13	icy	50%	full	0.126	0.88	-0.88	1.91	8.87
14	icy	100%	idle	0.126	0.90	-0.05	3.47	7.92
15	icy	100%	full	0.126	0.88	-1.48	1.91	10.2
16	wet	auto	idle	0.172	2.94	2.18	0.43	7.00
17	wet	auto	idle	0.173	-2.22	-3.03	15.3	16.8
18	wet	50%	idle	0.203	3.2	1.71	2.56	7.10
19	wet	50%	idle	0.206	4.91	4.54	11.78	13.1
20	wet	50%	full	0.204	4.21	2.04	0.97	7.60
21	wet	50%	full	0.209	1.22	-0.95	13.55	15.4
22	wet	100%	idle	0.284	4.24	2.76	1.89	4.93
23	wet	100%	idle	0.284	3.47	1.61	9.34	10.6
24	wet	100%	full	0.284	4.90	2.61	0.78	4.80
25	wet	100%	full	0.284	7.37	5.66	5.55	7.28

4.3.2 Errors in CG and Aircraft Weight Estimation

The results presented in table 4 do not include errors in the estimation of the CG and aircraft weight. In general, these parameters are not directly measured onboard the aircraft, but are calculated during the flight based on initial values from the load sheet and fuel used during the flight. Therefore, actual values during the landing can deviate from true values because of errors in the initial values and inaccuracies in the onboard calculation of the consumed fuel during the flight. These errors will express themselves as potential bias errors, so the sensitivity of the friction-estimation error for biases in the established mass and CG location has been assessed as well as the effects of measurement noise. For all test cases, a bias error of ±10% in aircraft mass and ±15% MAC in CG location have been applied. This is expected to represent a worst-case range of bias errors for CG and aircraft under normal operating conditions. The mentioned biases in aircraft mass and CG have been applied separately.

Table 5 shows the sensitivity analysis results and the relative error (in percent) of the estimated friction coefficient due the given (separate) variation in aircraft mass and CG. With respect to the effect of biases in the CG location, it appears that the mentioned variation results consistently in a bias of approximately ±6% in the mean error in the friction estimate. A positive bias leads to a negative bias (underestimate) in the friction estimate. There appears to be no significant effect resulting from runway condition and braking application on the resulting bias error. The same conclusion cannot be drawn in the case of a bias in the aircraft mass. Table 5 shows a clear variation in the effect of such a bias on the resulting error in the friction estimate, depending on runway condition and the amount of braking applied. The results are strongly correlated with the amount of reverse thrust applied. It can be roughly stated that the relative error doubles when full reverse is applied as compared with idle reverse.

The smallest effect of aircraft mass bias occurs for cases with autobraking and idle reverse (approximately 5%). However, in cases for which the amount of braking increases by applying full reverse or manual braking, the error in the estimated friction can increase substantially (in the worst case, up to 22%). This effect can be explained from the longitudinal equilibrium of forces and acceleration ($F = Ma$, see equation 1). Because of a positive error in the aircraft mass (M), the resulting deceleration (a) due to aerodynamic/engine forces would be underestimated ($a = F/M$). To achieve the actual measured acceleration, the forces on the gear must increase. As a consequence, the runway friction is overestimated. Therefore, the larger the aerodynamic forces (in terms of reverse thrust), the bigger the error in the estimated friction coefficient.

A second effect is that the estimation of the friction coefficient is dependent on the amount of manual braking (lower values of manual braking lead to higher errors in the estimated friction coefficient). The absolute value of the error is approximately constant, but the relative error increases when the absolute value of deceleration decreases. For this reason, cases with 50% braking (in particular on dry runways) show a higher relative error than cases with 100% braking.

Based on these observations, it is concluded that it is important to have an accurate aircraft weight estimate. Each percent of error in the weight estimate (i.e., in this case 340 kg) could lead to an error in the order of 2% in the estimated friction coefficient.

Table 5. Simulated Sensor Characteristics

Case	Runway Condition	Brake	Reverse	Variation in µ_estimated % due to +10% variation in Mass	Variation in µ_estimated % due to +15% MAC variation in CG
1	dry	auto	idle	4.22	-6.46
2	dry	auto	idle	4.94	-5.11
3	dry	50%	idle	11.50	-5.60
4	dry	50%	idle	10.26	-5.26
5	dry	50%	full	21.23	-6.72
6	dry	50%	full	21.16	-5.78
7	dry	100%	idle	6.40	-6.77
8	dry	100%	idle	6.36	-5.91
9	dry	100%	full	12.24	-7.07
10	dry	100%	full	11.60	-6.19
11	icy	auto	idle	4.89	-5.58
12	icy	50%	idle	10.63	-5.71
13	icy	50%	full	22.05	-6.50
14	icy	100%	idle	11.11	-5.14
15	icy	100%	full	22.04	-5.73
16	wet	auto	idle	4.79	-6.38
17	wet	auto	idle	4.21	-5.61
18	wet	50%	idle	8.42	-5.85
19	wet	50%	idle	8.90	-5.91
20	wet	50%	full	16.51	-6.51
21	wet	50%	full	17.43	-5.81
22	wet	100%	idle	5.83	-6.64
23	wet	100%	idle	2.58	-7.05
24	wet	100%	full	9.89	-7.06
25	wet	100%	full	10.46	-6.19

4.3.3 Conclusions

The analysis provided in this section leads to the following conclusions:

- The basic accuracy of the runway friction algorithm is not significantly affected by the incorporation of sensor measurement noise. The average error remains at approximately 1% (mean error).

- The spread of the friction estimate slightly increases when considering realistic measurement noise. The average standard deviation of the friction estimate increases from approximately 5% in the noise-free case to roughly 10% with measurement noise incorporated.

- The mean error of the friction estimate increases to approximately 2% per 1% bias in the aircraft mass (i.e., per 340 kg in this case).

- The mean error of the friction estimate increases by approximately 0.4% per 1% MAC bias in the aircraft CG location.

4.4 EFFECT OF MODELING ERRORS

This study investigates a friction estimation algorithm that is based on high-fidelity aircraft aerodynamic and engine models to resemble a regional jet aircraft. The basic assumption is that aerodynamic and engine models produced by the aircraft/engine manufacturers are in general validated to provide aerodynamic and thrust coefficients with high accuracy. However, even such models will inherently contain some inaccuracies and modeling errors. In particular, the complexities of aerodynamic modeling in ground effect and of highly nonlinear aerodynamic effects, such as those due to T/R application, are well-known. It must therefore be assumed that any aerodynamic and engine model to be applied in the friction-estimating algorithm inherently will include some modeling errors that may result in errors in the computed aerodynamic coefficients (pertaining to lift, drag, and pitching moment) and computed net thrust.

To assess the sensitivity of the algorithm for such modeling errors, specific modeling errors have been included in the algorithm. The modeling errors have been implemented as bias and proportional errors on each of the main aerodynamic coefficients and the engine net thrust coefficient. Moreover, the ground effect as implemented in the aerodynamic model can be reduced to evaluate the impact of inaccurate ground effect on the estimated friction coefficient.

4.4.1 Errors in Computed Thrust

Bias and proportional errors in the computed thrust will lead to errors in the estimated friction coefficient. It can be expected that when thrust is overestimated, it will lead to overestimation of the friction coefficient as well. The excess thrust will have to be compensated for by a higher friction coefficient to match the measured deceleration.

To get an impression of the sensitivity of the friction coefficient for errors in the computed thrust, all 25 cases have been simulated with a proportional error of 10% in the computed thrust and (separately) with a bias error of 500 lbf. The results are presented in table 6.

Table 6. Sensitivity of the Friction Estimation for Proportional and Bias Errors in Engine Thrust Calculation

Case	Runway Condition	Brake	Reverse	Error in μ_estimated % due to +10% proportional error in computed thrust	Error in μ_estimated % due to +500 lbf bias error in computed thrust
1	dry	auto	idle	0.69	7.19
2	dry	auto	idle	1.09	7.02
3	dry	50%	idle	-3.19	7.45
4	dry	50%	idle	-2.61	7.51
5	dry	50%	full	-12.16	7.80
6	dry	50%	full	-11.17	8.48
7	dry	100%	idle	-0.98	5.02
8	dry	100%	idle	-1.50	4.44
9	dry	100%	full	-6.82	5.47
10	dry	100%	full	-6.13	5.19
11	icy	auto	idle	1.15	7.44
12	icy	50%	idle	-2.39	6.39
13	icy	50%	full	-12.22	8.20
14	icy	100%	idle	-2.42	6.76
15	icy	100%	full	-12.20	7.11
16	wet	auto	idle	1.04	6.59
17	wet	auto	idle	1.21	7.16
18	wet	50%	idle	-2.29	6.17
19	wet	50%	idle	-2.15	6.73
20	wet	50%	full	-10.10	7.01
21	wet	50%	full	-8.99	6.32
22	wet	100%	idle	-1.77	4.24
23	wet	100%	idle	0.55	3.84
24	wet	100%	full	-4.97	4.75
25	wet	100%	full	-5.61	4.13

The application of the proportional error shows a large variation in the effect on the friction coefficient, partly because the effect was only marginal (in the order of 1%) when the T/Rs were not used. This can be explained by the fact that when no T/Rs are applied, idle thrust will be commanded, which results in low values of thrust. Therefore, a proportional error in computed thrust at low thrust situations will not significantly impact the accuracy of the friction coefficient estimates. However, in cases for which full reverse thrust is applied, a significant error in computed negative thrust will occur. This leads also to a significant under-estimation of the friction coefficient—specifically, up to a -13% error. An example of such a case is given in appendix D.

It must be noted here that the existence of a pure bias error in the computed thrust is not very realistic because it would be independent of the application of forward or reverse thrust. It has been presented here for the purpose of completeness.

4.4.2 Errors in Computed Aerodynamic Coefficients

The current aerodynamic model provides lift, drag, and pitching-moment coefficients to the friction estimation algorithm. It is expected that the accuracy of the friction estimation is most sensitive to the accuracy of the computed drag coefficient because the difference between thrust and drag determines how much runway friction is required to achieve the actual aircraft deceleration. The impact of lift and pitching moment coefficients has a rather indirect impact on the estimated friction because they primarily play a role in the determination of the normal forces on the undercarriage and distribution of the normal forces over the nose and main gear.

To get an impression of the sensitivity of the friction coefficient for errors in the computed drag coefficient, all 25 cases have been simulated with a proportional error of 10% in the computed drag coefficient and (separately) bias error of 0.01 (100 counts).

As shown in table 7, the results indicate:

- A 10% proportional error in computed drag coefficient leads to an approximate 7.5% error in estimated friction coefficient. There is a negative correlation: a positive error in the drag coefficient leads to underestimating the friction coefficient. The largest errors occur in cases of full reverse thrust (up to approximately 11%).

- A 100-drag-count bias in computed drag coefficient leads to an approximate 3.5% error in estimated friction coefficient. There is a negative correlation: a positive bias in the drag coefficient leads to underestimating the friction coefficient.

Table 7. Sensitivity of the Friction Estimation for Errors in Aircraft Proportional and Bias Errors in the Computed Aircraft Drag

Case	Runway Condition	Brake	Reverse	Error in μ_estimated % due to +10% proportional error in computed drag	Error in μ_estimated % due to + 0.01 bias error in computed drag
1	dry	auto	idle	-6.18	-4.44
2	dry	auto	idle	-6.48	-4.70
3	dry	50%	idle	-10.02	-3.92
4	dry	50%	idle	-9.19	-3.99
5	dry	50%	full	-11.24	-3.28
6	dry	50%	full	-10.69	-4.80
7	dry	100%	idle	-5.75	-2.55
8	dry	100%	idle	-5.81	-2.19
9	dry	100%	full	-5.87	-2.35
10	dry	100%	full	-6.74	-2.51
11	icy	auto	idle	-7.26	-4.08
12	icy	50%	idle	-8.99	-3.71
13	icy	50%	full	-9.92	-3.32
14	icy	100%	idle	-9.14	-3.50
15	icy	100%	full	-10.81	-2.79
16	wet	auto	idle	-6.08	-3.84
17	wet	auto	idle	-6.48	-4.10
18	wet	50%	idle	-7.51	-2.88
19	wet	50%	idle	-8.30	-3.38
20	wet	50%	full	-9.63	-2.81
21	wet	50%	full	-8.83	-4.04
22	wet	100%	idle	-4.84	-1.95
23	wet	100%	idle	-4.22	-2.33
24	wet	100%	full	-6.00	-2.62
25	wet	100%	full	-4.97	-1.95

4.4.3 Errors in the Computed Lift Coefficient

The nominal lift coefficient of the aircraft during approach is approximately 1.4. After touchdown, the lift coefficient quickly reduces to approximately 0.25 because of a reduction in the angle of attack and activation of the ground spoilers. Because the lift becomes even smaller as the speed decreases during roll out, it is likely that the normal force on the gear is predominately determined by the aircraft weight. In other words, the correlation between the estimated friction coefficient and the computed lift coefficient may be negligible. To evaluate the effect of the computed lift coefficient on the overall result, the friction estimation has been performed while completely discarding the generated lift on the airframe.

The results listed in table 8 indicate that discarding the lift equation in the friction estimation algorithm causes a significant error to occur (approximately 11%) in the estimation of the friction coefficient. Discarding the lift equation leads consistently to underestimation of the friction coefficient. It is therefore concluded that the calculation of the lift coefficient in the algorithm cannot be neglected. However, the aerodynamic equations for the computation of the lift coefficient can probably be simplified without a significant effect on the end result. If modeling errors in the lift coefficient can be contained within ±10% of margin of the real lift coefficient, this can be tolerated in the computational model without significant errors in the calculated friction coefficient

4.4.4 Errors in the Computed Pitching Moment Coefficient

As long as the aircraft is in stable flight, the overall pitching moment acting on the aircraft is very small because of aerodynamic equilibrium. Because aerodynamic equilibrium is not required after touchdown, the aerodynamic pitching moment could affect how the loads are distributed over the main and nose gear. However, simulations show that the resulting aerodynamic pitching moment coefficient remains rather small during ground movement—within a range of ±0.2. Once the aircraft is decelerating, the overall pitching moment reduces. Based on these considerations, it can be expected that contribution of pitching moment to the accuracy of the friction estimation is rather small.

For verification, all 25 cases were investigated by ignoring the computation of pitching moment. The results presented in table 8 show that there was no significant impact on the estimated friction coefficient by setting the aerodynamic pitching moment to zero. The resulting error is only a few percent, which is within the inherent noise level of the computation. On average (with respect to all 25 cases), the absolute error is less than 1%. Based on these observations, it is concluded that an accurate calculation of the pitching moment is not a prerequisite for accurate estimation of the friction coefficient. The underlying aerodynamic model could be simplified by omitting the pitch moment equations without significantly degrading the accuracy of the algorithm.

4.4.5 Errors in the Ground Effect

The ground effect is related to the change of the aircraft aerodynamic characteristics when the airframe is close to the ground. The ground effect generally becomes noticeable when the proximity of the ground is less than one wingspan. The impact of the ground effect is generally increased lift, reduced drag, and a nose-down pitching moment. The ground effect is a complex aerodynamic phenomenon that is usually highly nonlinear as a function of altitude. Therefore, accurate aerodynamic modeling of the ground effect is a complex task. However, with respect to aircraft that have been subject to autoland certification, it can be expected that the ground effect is modeled quite accurately to achieve the required autoland simulation reliability. Nevertheless, modeling errors still may be present in the aerodynamic model, particularly for cases in which the aircraft is on the ground. For that reason, it is interesting to investigate the impact that modeling errors can have on the accuracy of the friction estimation.

To evaluate the effect of the ground effect, the study attempted to reprocess the μ_estimated for all 25 cases without considering the ground effect. Table 8 shows that this leads to significant errors in the estimated friction coefficient. On average, the friction coefficient appears to be underestimated by approximately 11% when the ground effect is totally neglected. An example is given in appendix D. Based on this result, it is concluded that it is important for the aerodynamic model to incorporate a fairly accurate ground effect model. To contain the inaccuracy caused by modeling errors in the ground effect within a 1% error range of the friction estimate, the modeling errors in the ground effect should be less than approximately 10%.

Another error source for the ground effect is related to the accuracy of the RA. The measured height above the ground by the RA is the main input for determining the magnitude of the ground effect. Therefore, the accuracy of the RA is an important factor for the accuracy of the friction estimation. In general, the bias in the RA signal is small.

The maximum error in the RA is 3 meters [7]. Based on this information, it has been investigated how the friction estimation is affected by a maximum error of 3 meter radio height. Results from the 25 test cases show that the impact of such error is very small, on average less than 1%. Therefore, it appears that the accuracy of the RA is not a dominant factor in the friction-estimation process. In contrast, modeling errors in the ground effect could have a significant impact.

Table 8. Impact of Neglecting the Lift Equation, Pitching-Moment Equation, and Ground-Effect Equation in the Friction-Estimation Algorithm

Case	Runway Condition	Brake	Reverse	Error in μ_estimated % due to neglecting the lift equation	Error in μ_estimated % due to neglecting the moment equation	Error in μ_estimated % due to neglecting the ground effect equation
1	Dry	auto	idle	-10.14	0.77	-11.32
2	Dry	auto	idle	-11.55	0.64	-12.41
3	Dry	50%	idle	-9.56	-0.01	-11.67
4	Dry	50%	idle	-7.03	0.89	-8.46
5	Dry	50%	full	-12.61	-0.43	-11.66
6	Dry	50%	full	-12.63	-1.43	-11.69
7	Dry	100%	idle	-9.37	0.08	-8.68
8	Dry	100%	idle	-6.40	-0.32	-7.71
9	dry	100%	full	-13.73	-0.49	-10.76
10	dry	100%	full	-11.07	-0.70	-8.58
11	icy	auto	idle	-9.82	0.77	-10.77
12	icy	50%	idle	-10.27	-1.11	-12.51
13	icy	50%	full	-13.75	-0.67	-11.81
14	icy	100%	idle	-9.01	-1.05	-10.84
15	icy	100%	full	-15.18	-1.89	-12.96
16	wet	auto	idle	-10.37	0.73	-11.00
17	wet	auto	idle	-9.28	0.09	-10.71
18	wet	50%	idle	-10.24	-0.37	-10.19
19	wet	50%	idle	-10.64	0.14	-10.48
20	wet	50%	full	-13.96	-1.43	-10.53
21	wet	50%	full	-12.84	-1.47	-10.84
22	wet	100%	idle	-9.07	-0.51	-8.64
23	wet	100%	idle	-10.00	0.34	-9.69
24	wet	100%	full	-13.07	-2.04	-9.56
25	wet	100%	full	-13.65	-0.96	-9.02

4.4.6 Conclusions

The results of this section are summarized as follows:

- Modeling errors in the computed thrust have a significant effect on the accuracy of the estimated friction coefficient. Accurate modeling of reverse thrust is particularly important. A 1% error in computed reverse thrust may lead to a slightly more than 1% error in the friction estimate.

- Modeling errors in the computed drag coefficient have a significant effect on the accuracy of the estimated friction coefficient. A 10% proportional error in computed drag coefficient leads, on average, to an approximately 7.5% error in estimated friction coefficient.

- Modeling errors in the computed lift coefficient are less significant for the accuracy of the friction estimate compared to the drag coefficient. However, the lift equations cannot be discarded from the estimation algorithm without introducing significant errors. It is possible that the estimation algorithm adapts a simplified lift model as long as errors in the computed lift coefficient remain within a 10% margin.

- Modeling error resulted by the pitching moment is almost irrelevant for the accuracy of the friction estimate. Therefore, the computation of the pitching moment coefficient can be neglected to simplify the friction model without significantly affecting the accuracy of the estimation.

- Modeling errors in the computed ground effect have a significant impact on the accuracy of the friction estimate. Removing the ground effect from the algorithm may lead to significant (in the order of 12%) under estimation of the estimated friction. Therefore, it is important that the algorithm includes a fairly accurate ground effect model. The accuracy of the RA is generally sufficient to provide an accurate ground effect calculation.

5. CONCLUSIONS AND RECOMMENDATIONS

The results presented in this report lead to the following conclusions:

- Onboard, real-time, runway braking friction computation is feasible in principle, with fair accuracy (roughly within a ±5% error margin).

- To achieve this accuracy, it is critical that weight, thrust (forward or reverse), and drag are computed with high accuracy. A 1% error in each of these components results directly into at least 1% inaccuracies in the estimated friction coefficient.

- The noise level of the friction estimate increases when realistic sensor characteristics are simulated. However, this noise level remains within reasonable bounds and can be further reduced by appropriate filtering for real applications.

- It is important for the friction-estimation algorithm to use an accurate model of the ground effect. Neglecting the ground effect can lead to significant errors (>10%) in the estimated friction coefficient.

- Modeling errors in the computed lift coefficient are less significant for the accuracy of the friction estimate as compared to the drag coefficient. It is possible to use a simplified lift model as long as errors in the computed lift coefficient remain within approximately a 10% margin.

- Modeling errors in the computed pitching moment coefficient are almost irrelevant for the accuracy of the friction estimation. It can be considered to simplify the algorithm by neglecting the pitching moment equations.

It is worth noting that the output of the onboard runway friction estimation system is the instantaneous runway friction coefficient, which is usually less than the maximum achievable or available friction. The maximum achievable friction can be measured only under friction-limited braking conditions. With this in mind, it is recommended that operational concepts be further developed to make best use of the onboard friction estimation, including addressing the human factors aspects and the relationships between, and responsibilities of, flight crew and air traffic control in the follow-up studies. The operational concept study should investigate under which condition the onboard friction estimation systems can be used, determine performance requirements, and specify the required accuracy and integrity of the friction-estimation system.

6. REFERENCES

1. “Statistical Summary of Commercial Jet Airplane Accidents, Worldwide Operations 1959–2011,” Boeing Commercial Airplanes, July 2012, http://www.boeing.com/news/techissues/pdf/statsum.pdf (accessed on 09/25/2014).

2. National Transportation Safety Board, Safety Recommendation A-07-58–A-07-64, Washington, DC, October 16, 2007.

3. AGARDograph 333. “Enhancement of Aircraft Ground Handling Simulation Capability.” http://ftp.rta.nato.int/public/PubFulltext/AGARD/AG/AGARD-AG-333/00FRONT.pdf (accessed on 09/25/2014).

4. “Comprehensive Method for Modeling Performance of Aircraft Tires Rolling or Braking Friction on Runways Contaminated With Water, Slush, Snow or Ice,” ESDU 05011, January 2009.

5. Anon, “Flight simulator data for the Fokker F28 Mk100,” Fokker Report L-28-336, issue 8.5, July 1992.

6. Air Data and the IRS, ARINC Characteristic 738A-1, July 31, 2001.

7. ICAO Doc 9274, “Manual on the Use of the Collision Risk Model (CRM) for ILS Operations,” 1980.

APPENDIX A—SIMULATED PARAMETERS

ID	***Name***	***Unit***	***Description***
YY(1)	T	sec	Time
YY(2)	MASS	kg	Aircraft mass
YY(3)	XCG2	%mac	cg position *x*-direction
YY(4)	YCG2	%span	cg position *y*-direction
YY(5)	ZCG2	%mac	cg position *z*-direction
YY(6)	DLTF	dg	flap deflection
YY(7)	UC	-	undercarriage position (0: in, 1:out)
YY(8)	DLTLD	-	lift dumper (0: in, 1: out)
YY(9)	DLTSB	dg	speed brake deflection
YY(10)	IH	dg	stab setting
YY(11)	PLADEM(1)	dg	power lever angle demanded (right)
YY(12)	PLADEM(2)	dg	power lever angle demanded (left)
YY(13)	PLA(1)	dg	power lever angle actual (right)
YY(14)	PLA(2)	dg	power lever angle actual (left)
YY(15)	DLTA	dg	aileron deflection
YY(16)	DLTE	dg	elevator deflection
YY(17)	DLTR	dg	rudder deflection
YY(18)	BRAKER	-	brake input right (0: none, 1: full)
YY(19)	BRAKEL	-	brake input left (0: none, 1: full)
YY(20)	VNGS	dg	nose wheel angle
YY(21)	NH(2)	rpm	N2 right
YY(22)	NH(1)	rpm	N2 left
YY(23)	ALT	ft	altitude
YY(24)	HW	ft	height of wheels
YY(25)	CAS	kts	calibrated airspeed
YY(26)	MACH	-	mach number
YY(27)	V/S	ft/min	vertical speed
YY(28)	NZW	g	normal load
YY(29)	RHO	kg/m3	air density
YY(30)	ALFA	dg	angle of attack
YY(31)	BETA	dg	side slip angle
YY(32)	TETA	dg	pitch angle
YY(33)	PSI	dg	heading
YY(34)	PHI	dg	roll angle
YY(35)	GAMF	dg	flight path angle
YY(36)	GAMFGRND	dg	flight path angle with respect to ground
YY(37)	TRACK	dg	track angle
YY(38)	DRIFT	dg	drift angle
YY(39)	CD	-	drag coefficient
YY(40)	CL	-	lift coefficient
YY(41)	CX	-	*cx* coefficient in body axes
YY(42)	CY	-	*cy* coefficient in body axes
YY(43)	CZ	-	*cz* coefficient in body axes

ID	*Name*	*Unit*	*Description*
YY(44)	CLROL	-	*clrol* coefficient in body axes
YY(45)	CM	-	*cm* coefficient in body axes
YY(46)	CN	-	*cn* coefficient in body axes
YY(47)	VWIND	kts	wind speed
YY(48)	GHIW	dg	wind direction
YY(49)	TAS	kts	true airspeed
YY(50)	VGRD	kts	ground speed
YY(51)	AXBSF	m/s2	specific force in *x*-body axes
YY(52)	AYBSF	m/s2	specific force in *y*-body axes
YY(53)	AZBSF	m/s2	specific force in *z*-body axes
YY(54)	UBDOT	m/s2	*ub* derivative in *x*-body axes
YY(55)	VBDOT	m/s2	*vb* derivative in *y*-body axes
YY(56)	HSLDT2	m/s2	-*wb* derivative in *z*-body axes
YY(57)	PB	dg/s	roll rate
YY(58)	QB	dg/s	pitch rate
YY(59)	RB	dg/s	yaw rate
YY(60)	THRUST_X	N	thrust component in *x*-body axes
YY(61)	THRUST_Y	N	thrust component in *y*-body axes
YY(62)	THRUST_Z	N	thrust component in *z*-body axes
YY(63)	FUELFLR	lb/hr	fuel flow right engine
YY(64)	MASSFLOWR	kg/s	mass flow right engine
YY(65)	P3R	N/m2/1000	P3 right engine
YY(66)	TGTINDR	dgC	ITT right engine
YY(67)	EPRR	-	EPR right engine
YY(68)	FXBGN	N	nose gear force in *x*-body axes
YY(69)	FXBGR	N	right main gear force in *x*-body axes
YY(70)	FXBGL	N	left main gear force in *x*-body axes
YY(71)	XRW	m	distance along runway
YY(72)	YRW	m	distance perpendicular to cl runway
YY(73)	IX	kgm2	inertial moment around *x*-body axis
YY(74)	IY	kgm2	inertial moment around *y*-body axis
YY(75)	IZ	kgm2	inertial moment around *z*-body axis
YY(76)	WOW	-	weight on wheels
YY(77)	OAT	dgC	static temp
YY(78)	TAT	dgC	total temp
YY(79)	HWNR	m	compression of right nose wheel tire
YY(80)	HWMRR	m	compression of outer wheel tire of right main gear
YY(81)	HWMLR	m	compression of outer wheel tire of left main gear
YY(82)	HWN1	m	compression of nose strut
YY(83)	HWMR1	m	compression of right main gear strut
YY(84)	HWML1	m	compression of left main gear strut
YY(85)	FGNDR	-	runway friction coefficient
YY(86)	FGND3R	-	runway braking friction coefficient

ID	*Name*	*Unit*	*Description*
YY(87)	SWUMR	-	cornering friction coefficient
YY(88)	FmuNR	-	friction coefficient of right nose wheel tire
YY(89)	FMURR	-	friction coefficient outer wheel tire of right main gear
YY(90)	FMULL	-	friction coefficient outer wheel tire of left main gear
YY(91)	SRNR	-	slip ratio of right nose wheel tire
YY(92)	SRRR	-	slip ratio outer wheel tire of right main gear
YY(93)	SRLL	-	slip ratio outer wheel tire of left main gear
YY(94)	VEQRR	kts	speed of outer wheel tire of right main gear
YY(95)	OMDTRR	dg/s2	angular acceleration of outer wheel tire of right main gear
YY(96)	OMRR	dg/s	angular speed of outer wheel tire of right main gear
YY(97)	FUARR	N	commanded brake force
YY(98)	FBLRR	N	limit brake force
YY(99)	RMBRRF	Nm	brake moment
YY(100)	RWHLRR	m	wheel radius

APPENDIX B—SIMULATION RESULTS OF FAULT-FREE PERFORMANCE

The following charts present the time histories of simulated landing runs in terms of velocity, deceleration, and aircraft configurations (power, brake, T/R), as well as the algorithm output of estimated μ and estimation error in μ, for the 25 cases outlined in table 1 of the main report from touchdown to 25 kt ground speed in a noise-free condition.

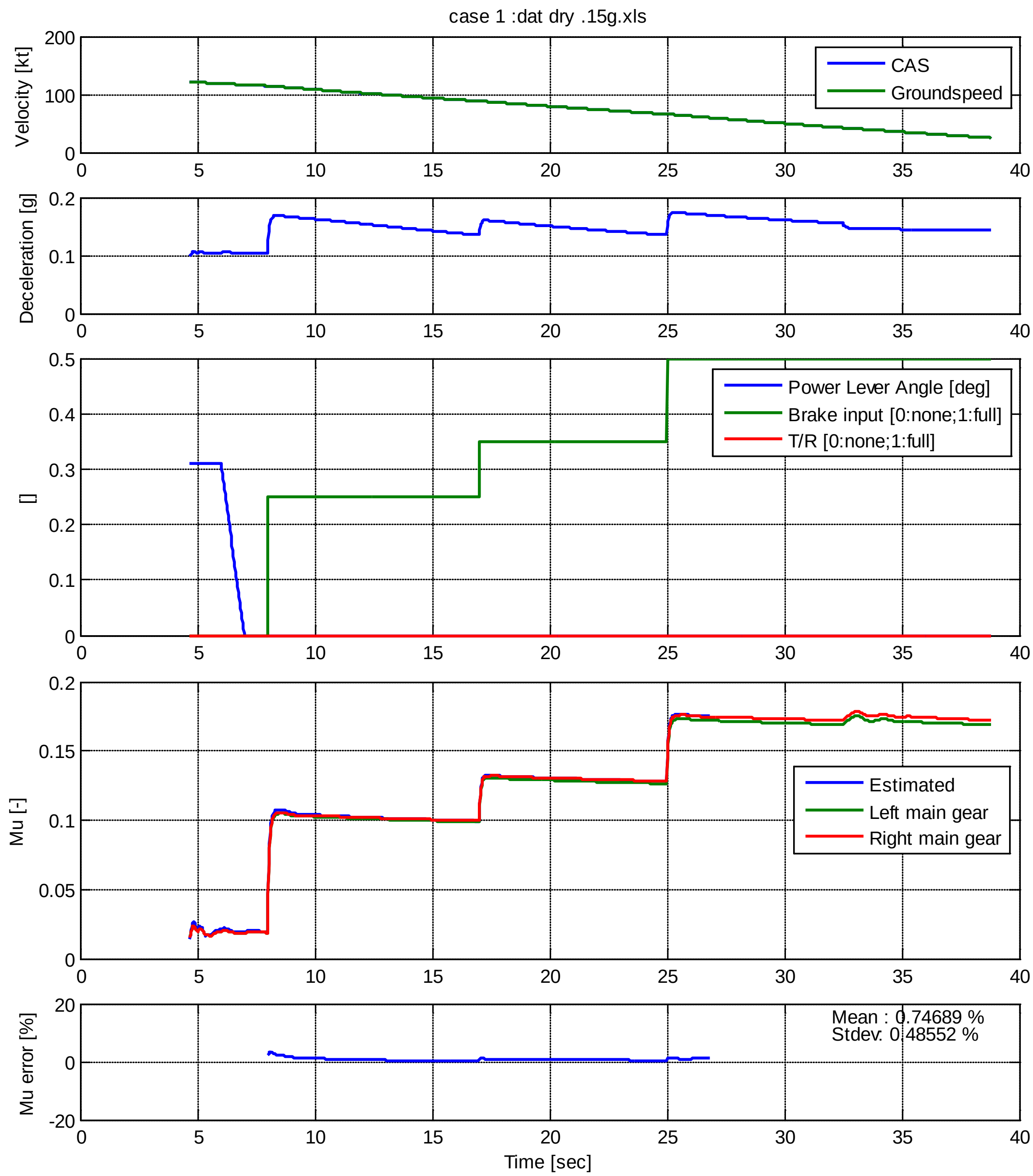

Figure B-1. Simulated Landing Run for Case 1

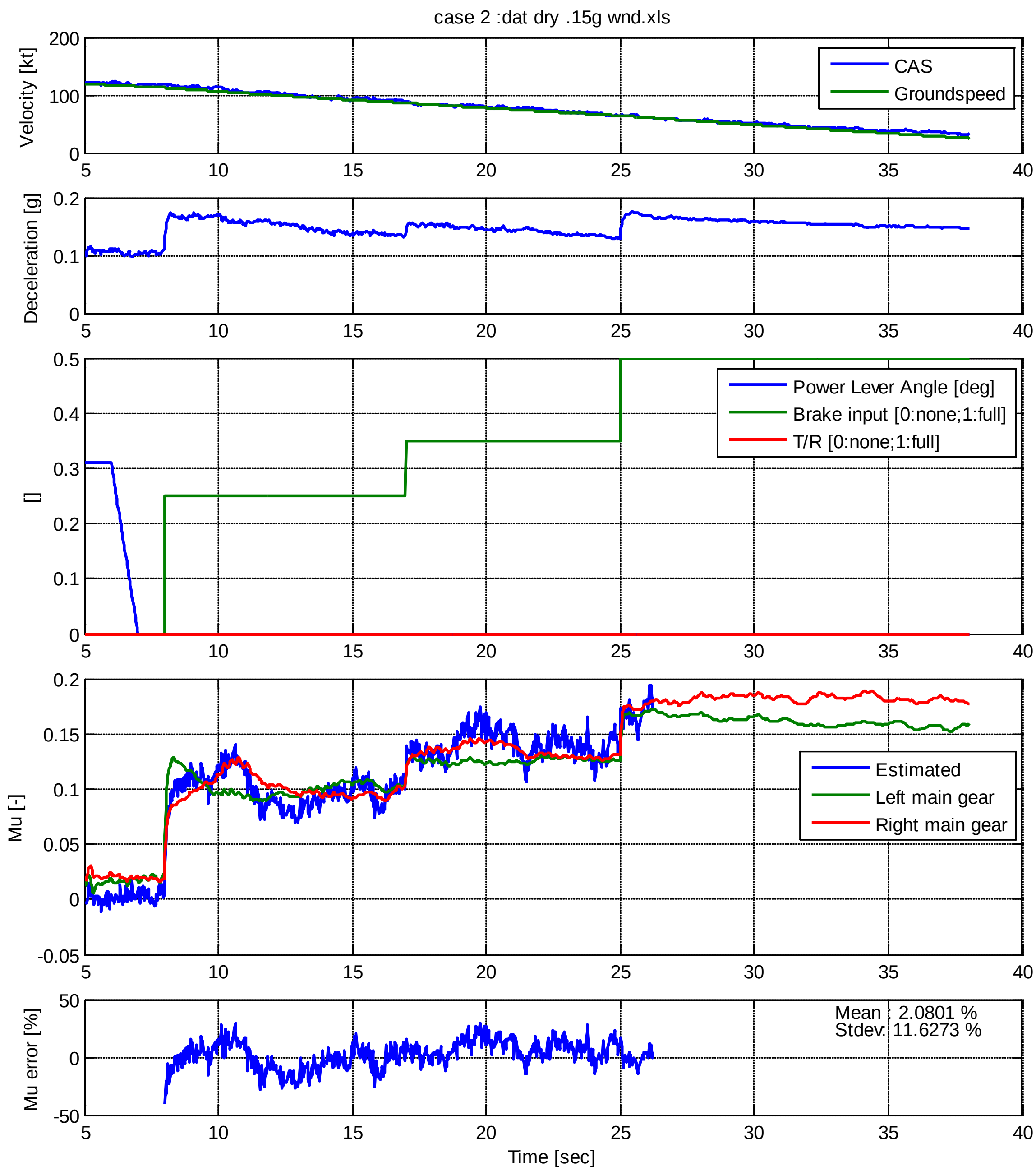

Figure B-2. Simulated Landing Run for Case 2

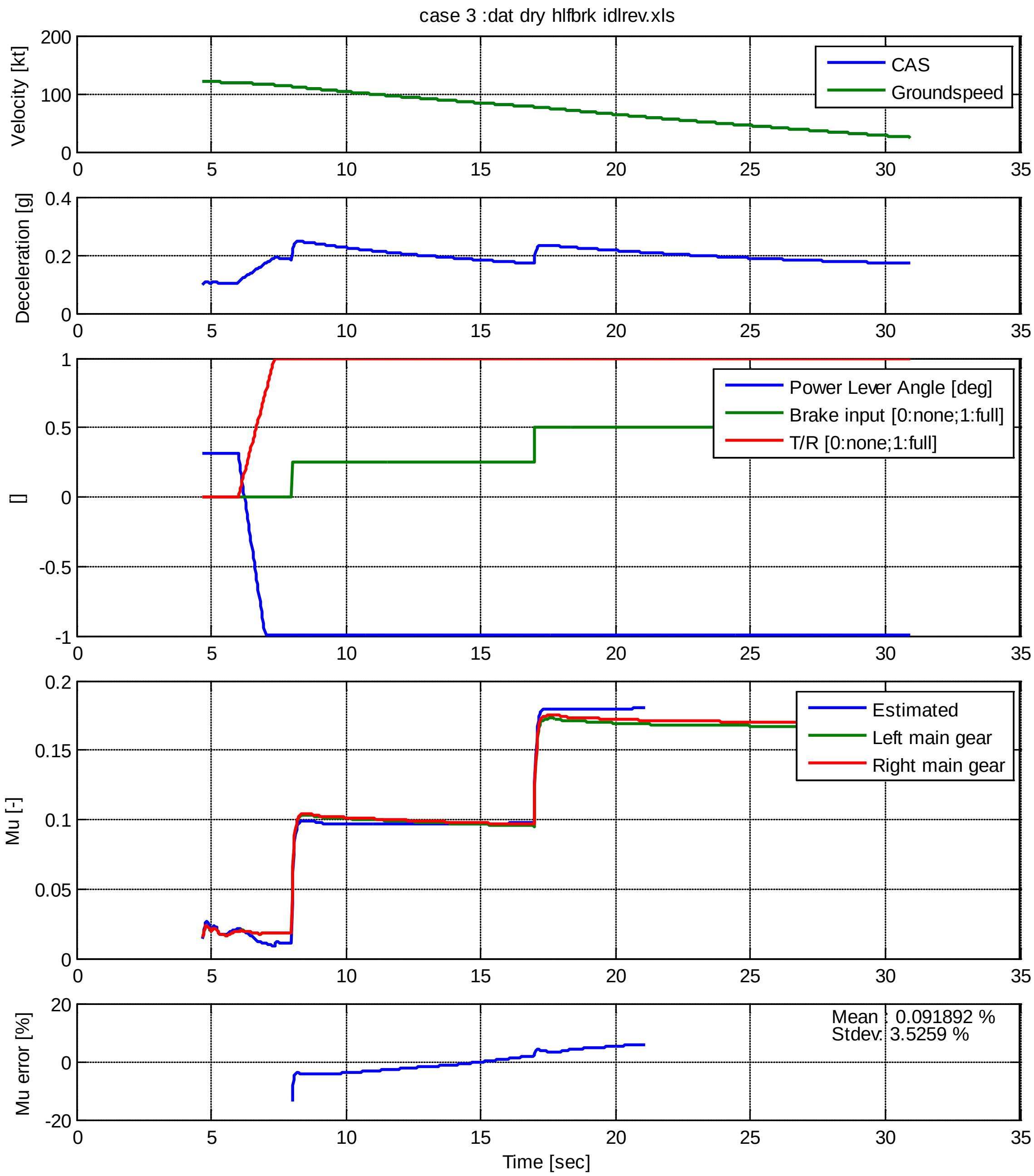

Figure B-3. Simulated Landing Run for Case 3

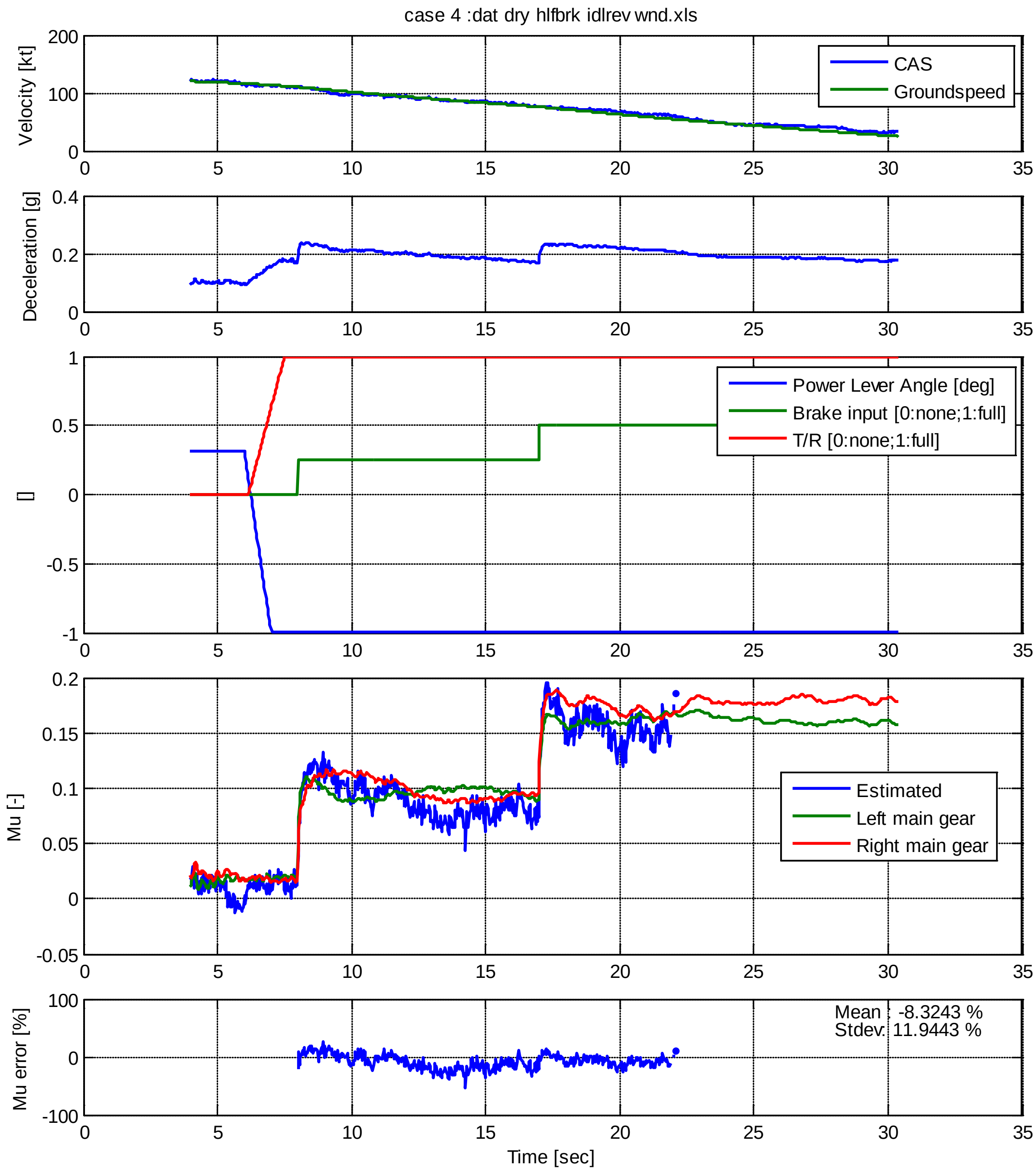

Figure B-4. Simulated Landing Run for Case 4

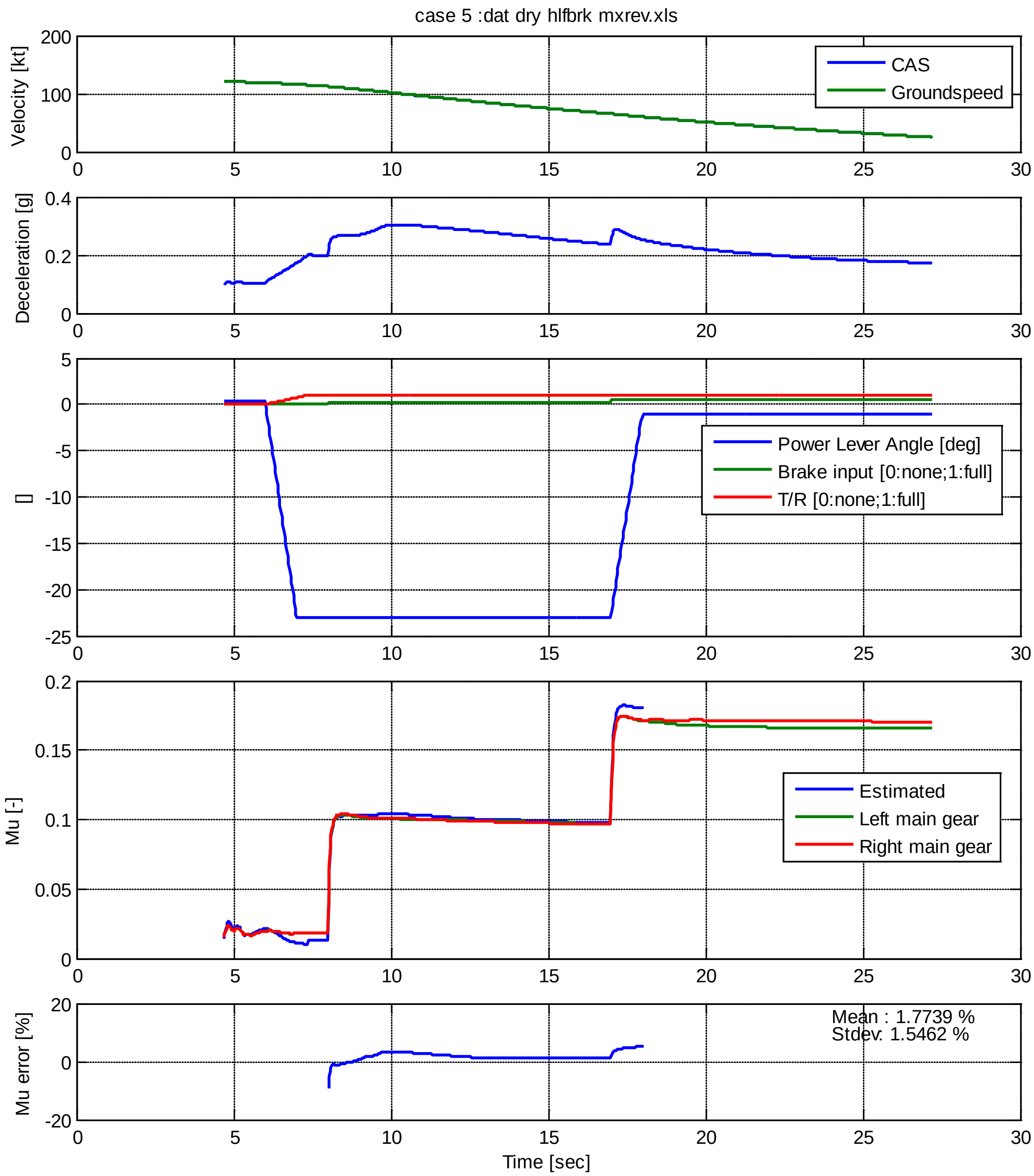

Figure B-5. Simulated Landing Run for Case 5

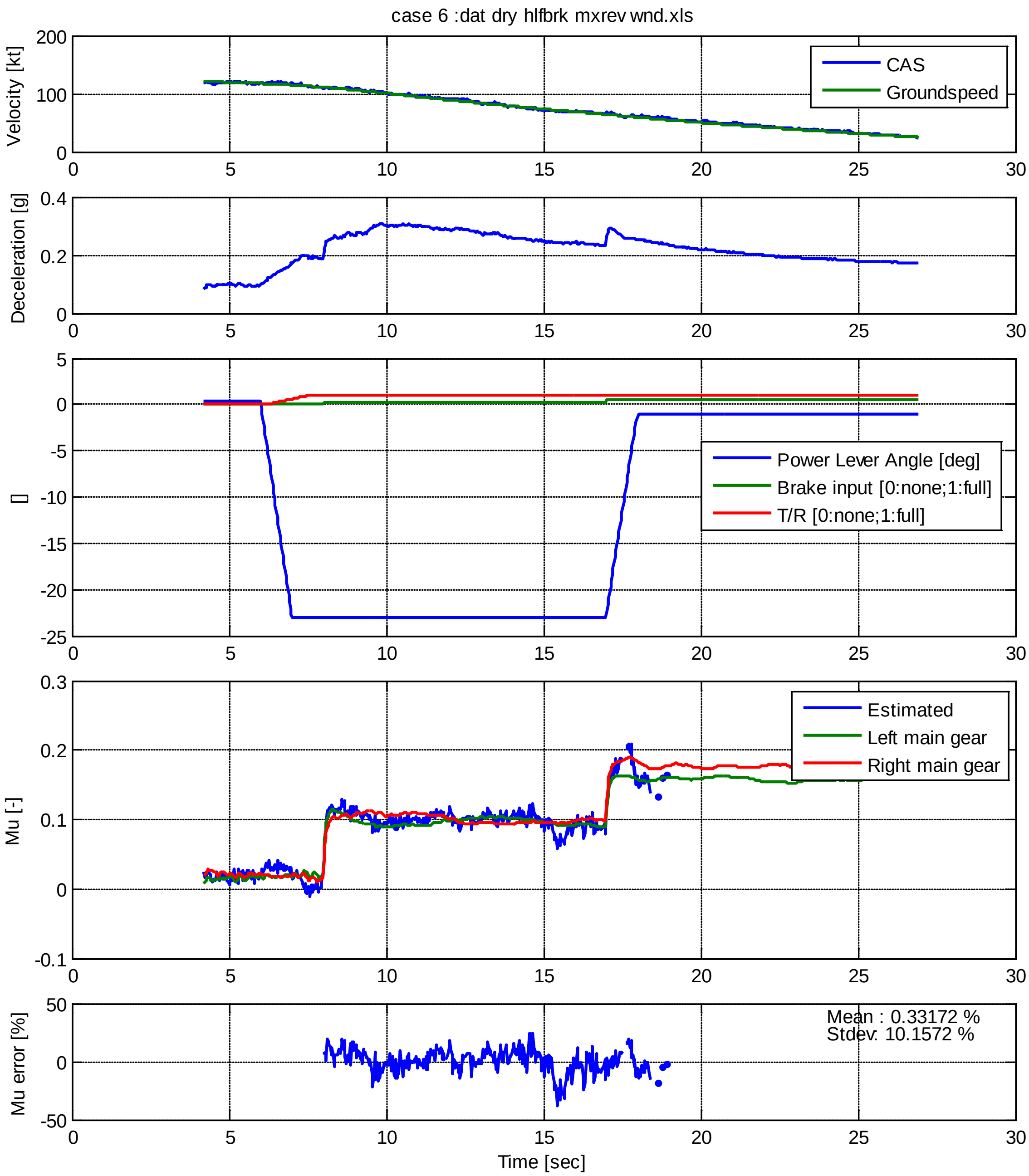

Figure B-6. Simulated Landing Run for Case 6

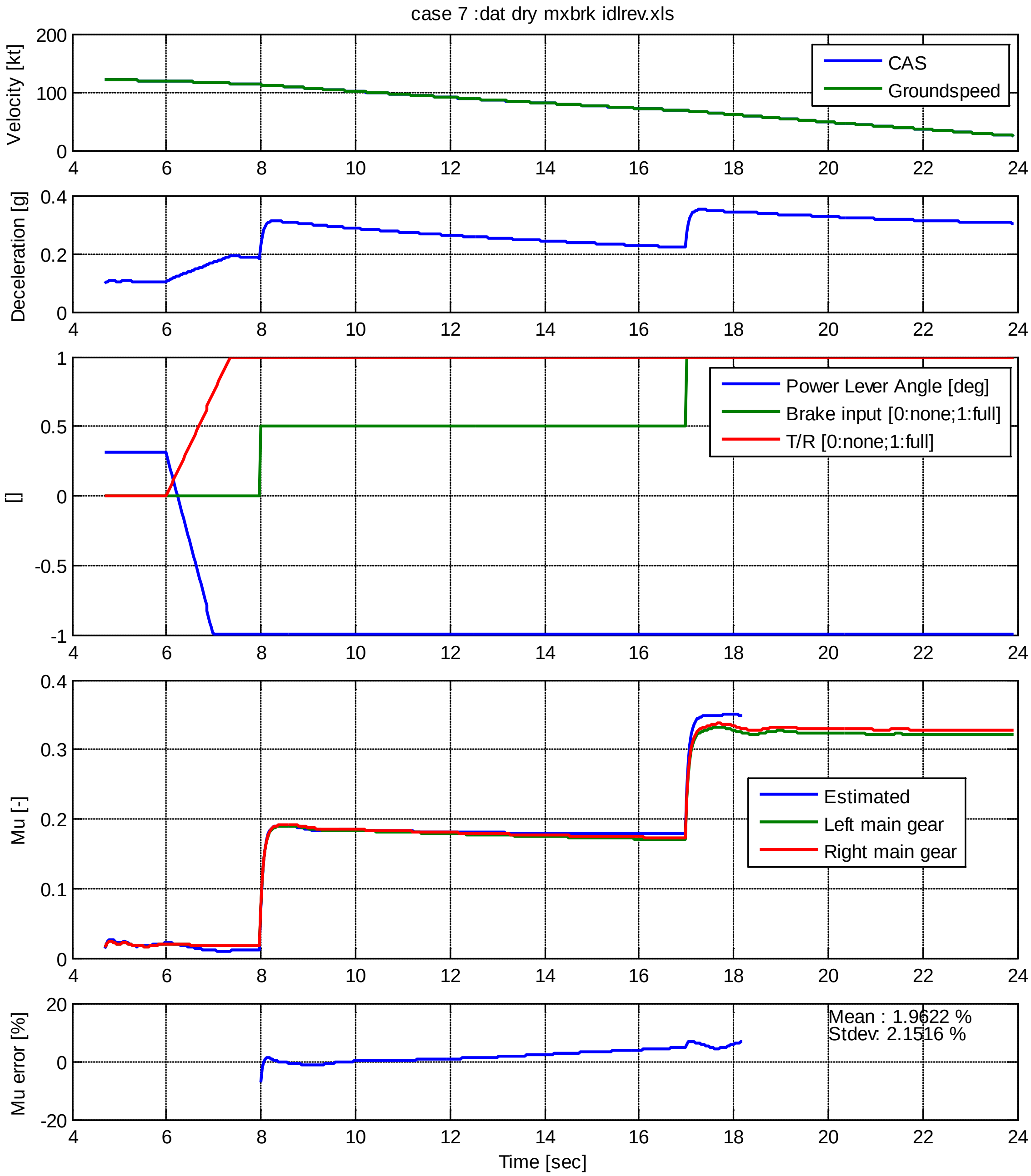

Figure B-7. Simulated Landing Run for Case 7

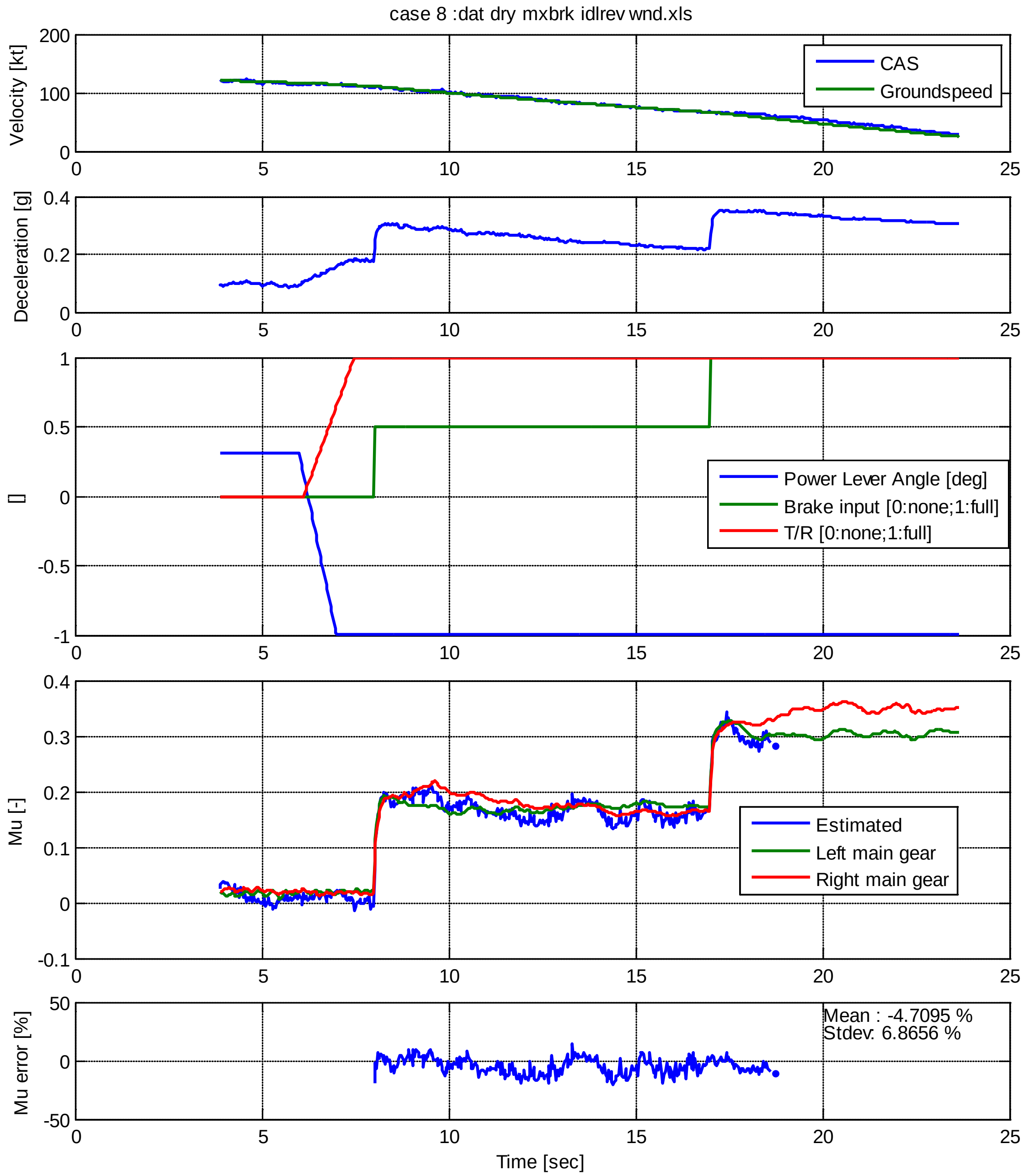

Figure B-8. Simulated Landing Run for Case 8

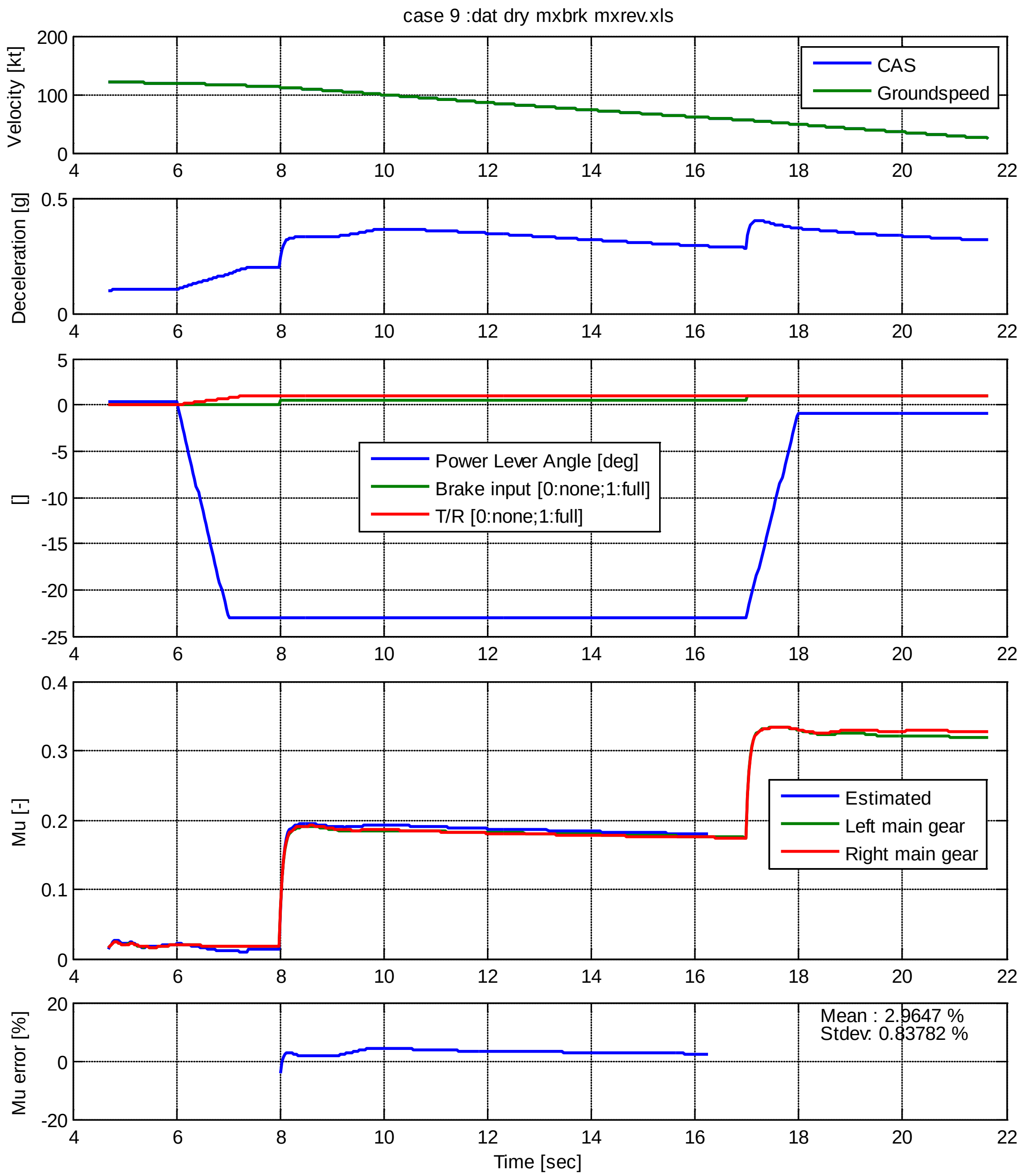

Figure B-9. Simulated Landing Run for Case 9

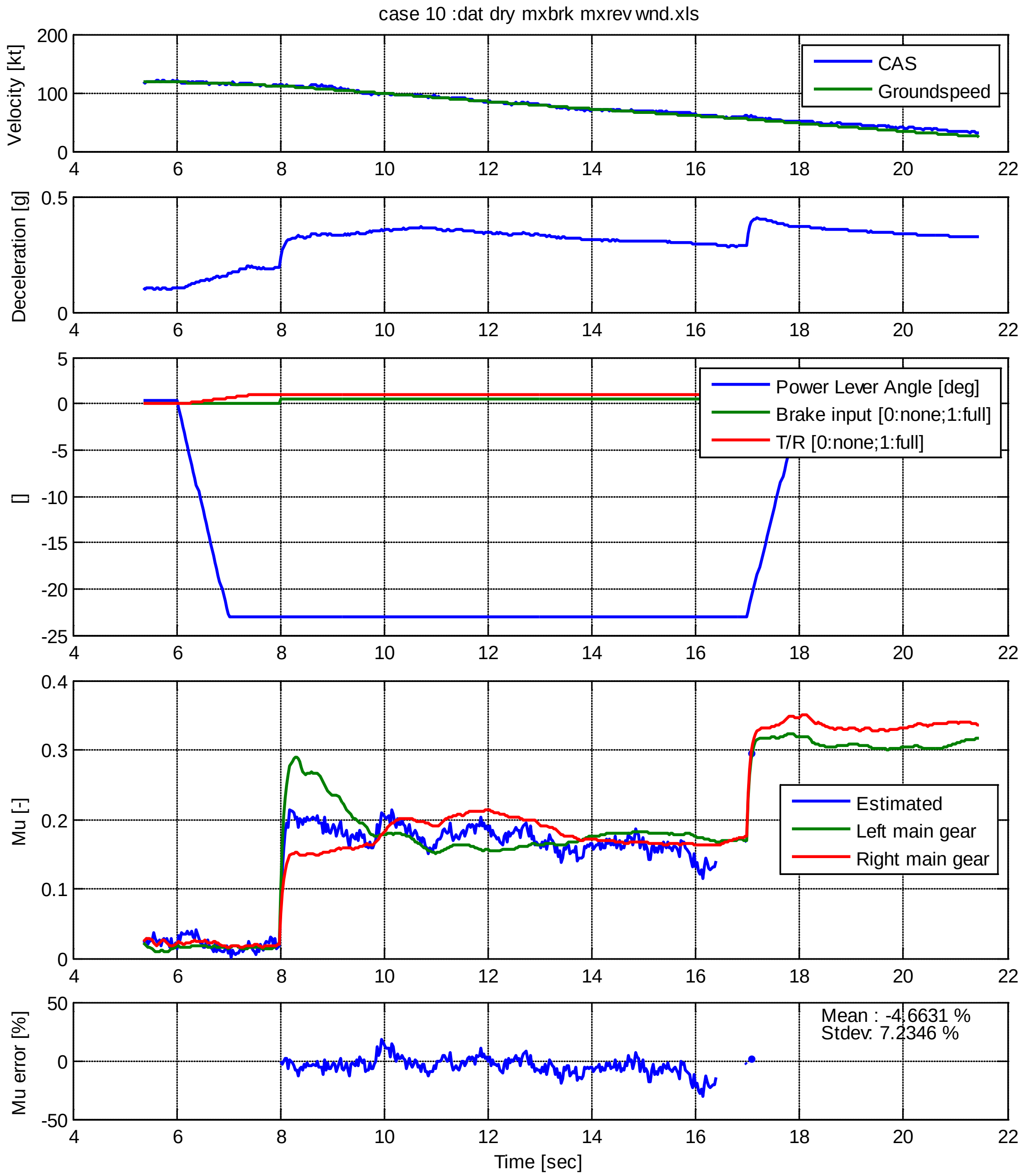

Figure B-10. Simulated Landing Run for Case 10

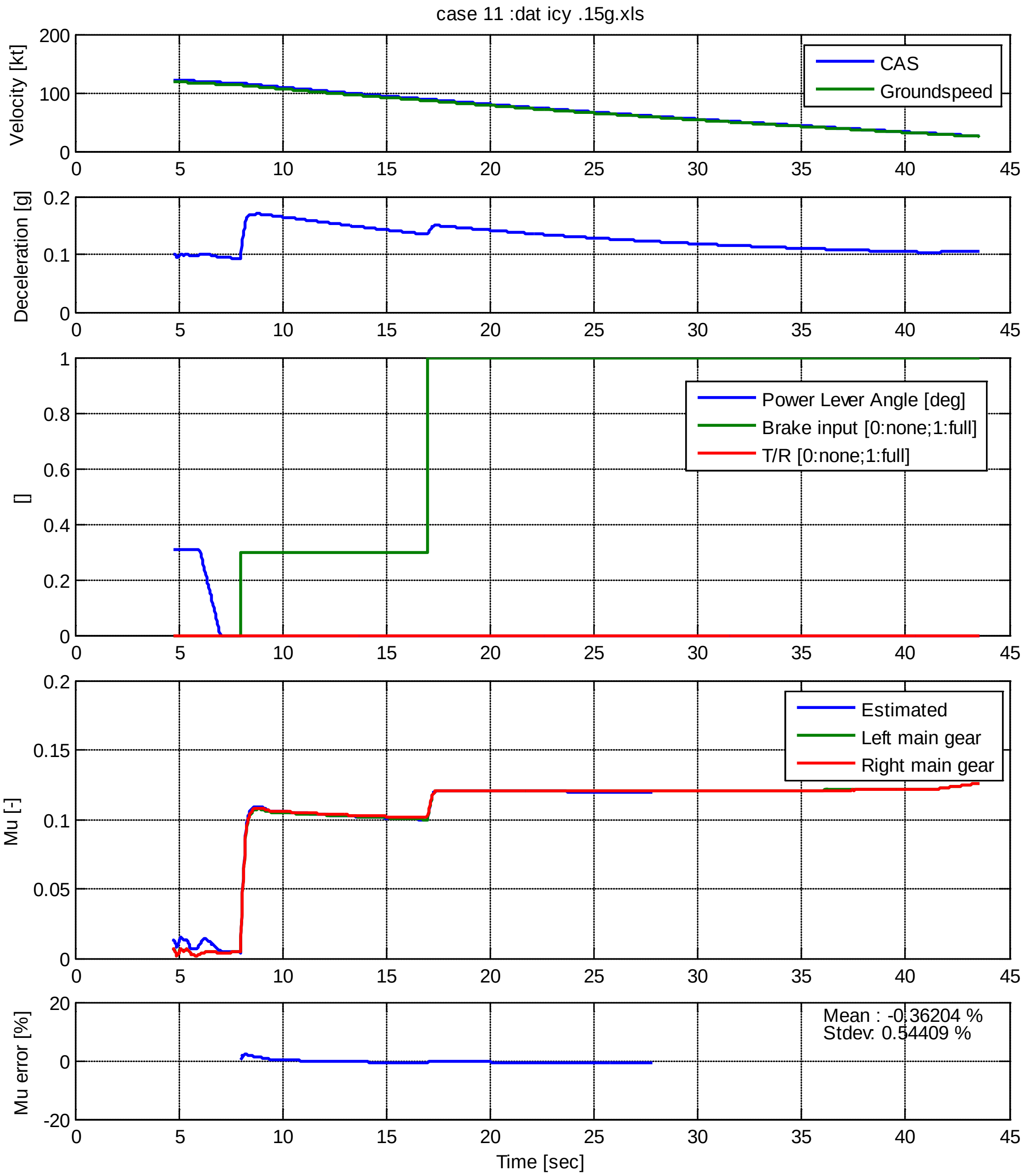

Figure B-11. Simulated Landing Run for Case 11

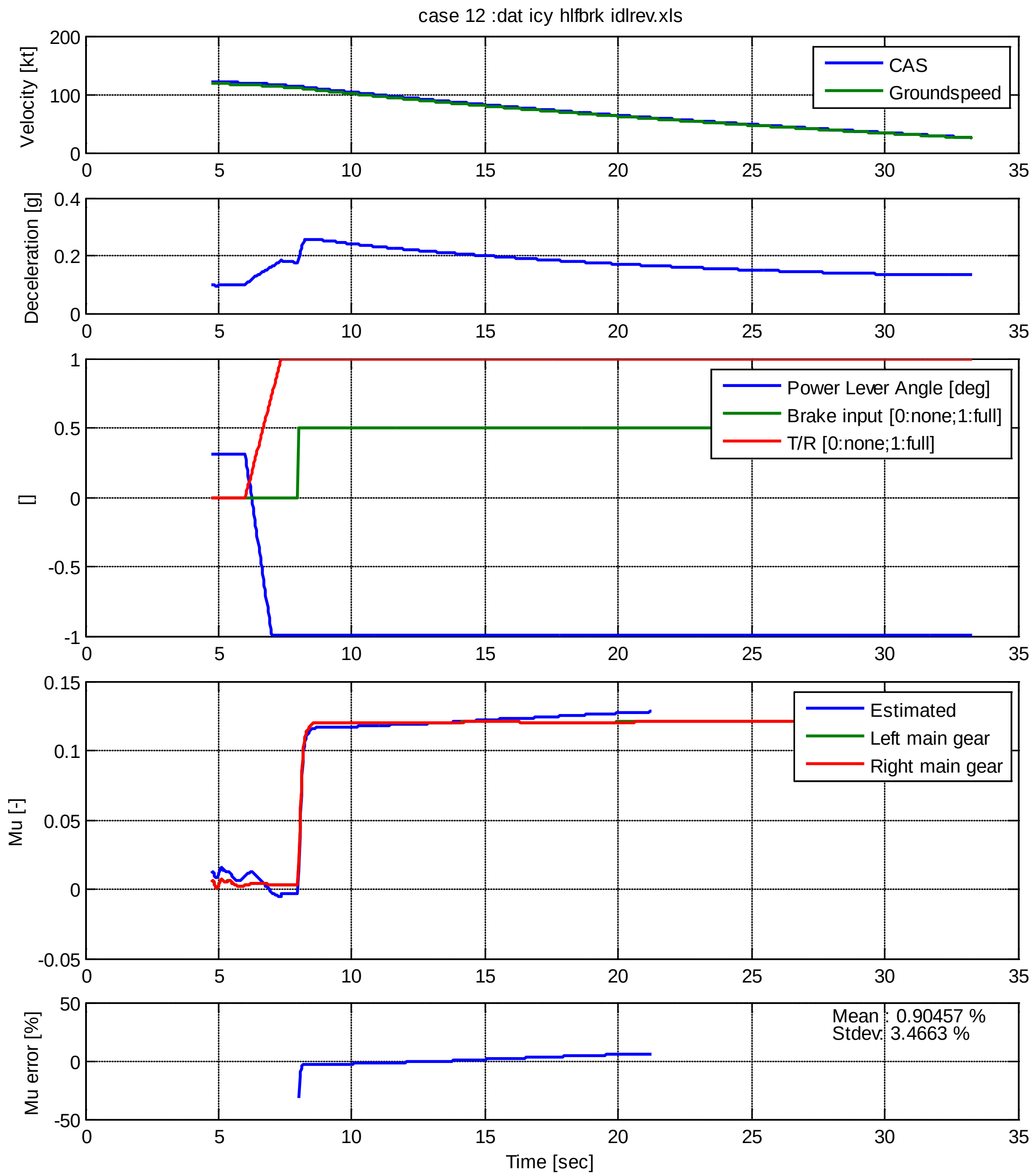

Figure B-12. Simulated Landing Run for Case 12

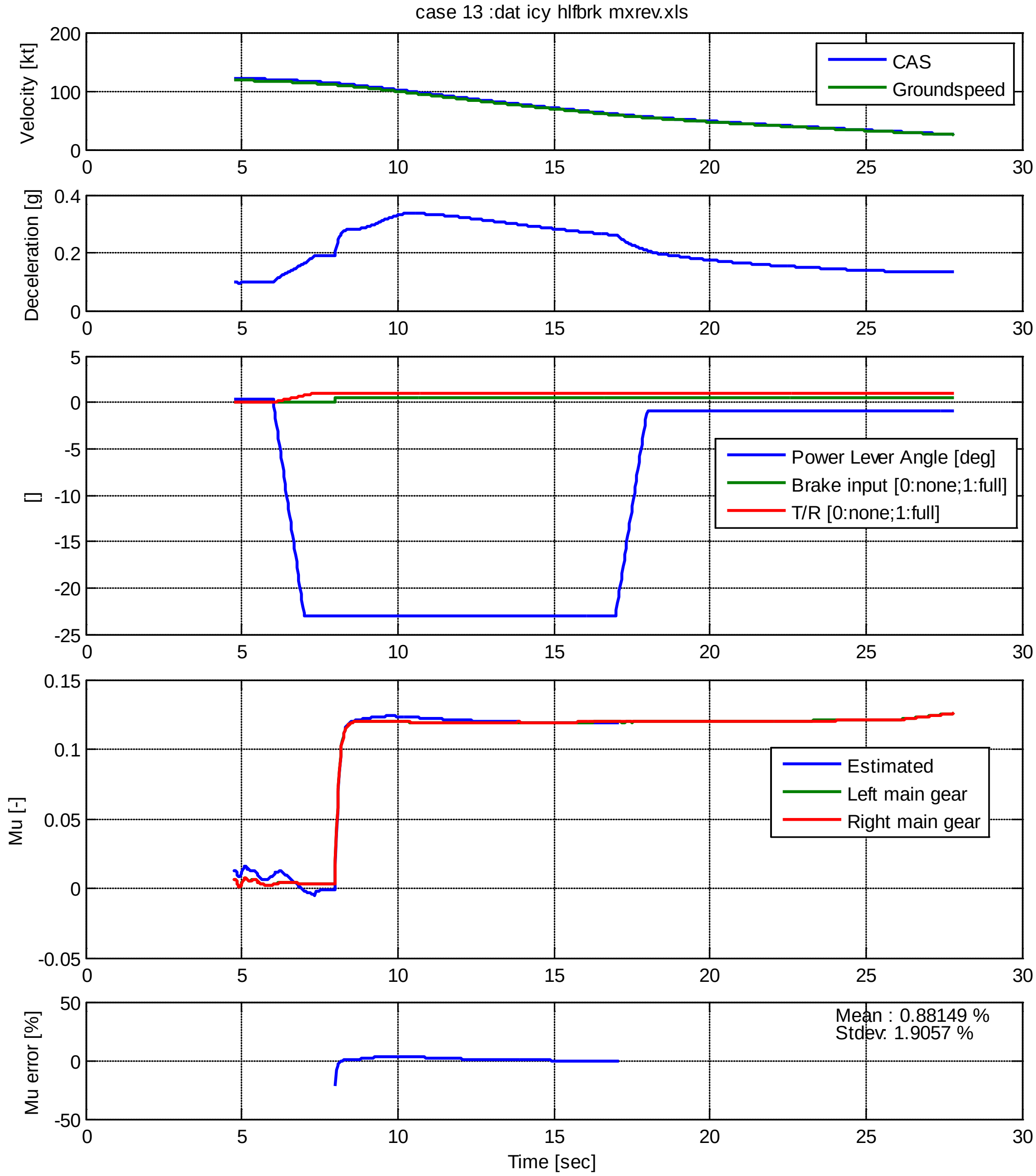

Figure B-13. Simulated Landing Run for Case 13

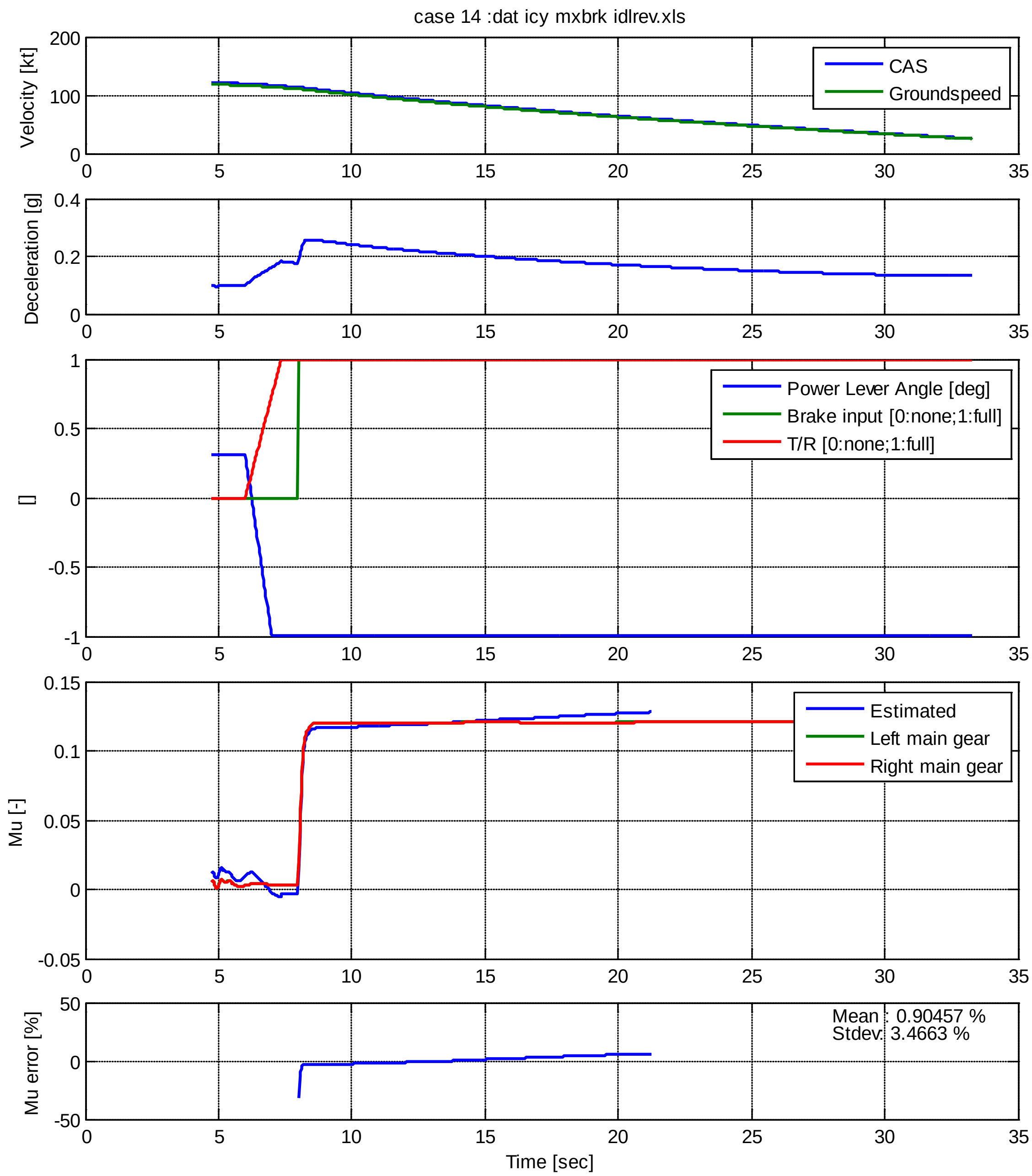

Figure B-14. Simulated Landing Run for Case 14

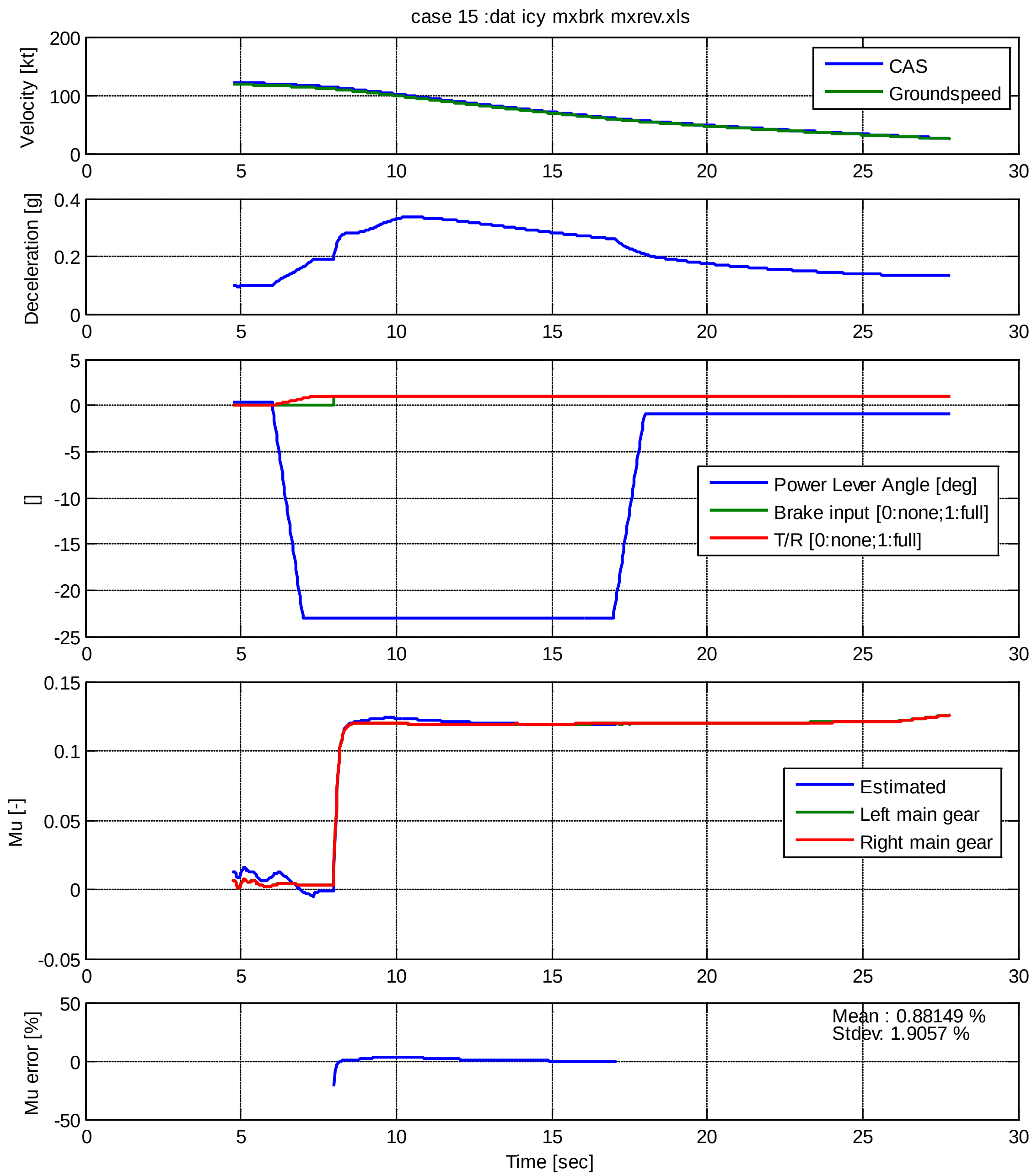

Figure B-15. Simulated Landing Run for Case 15

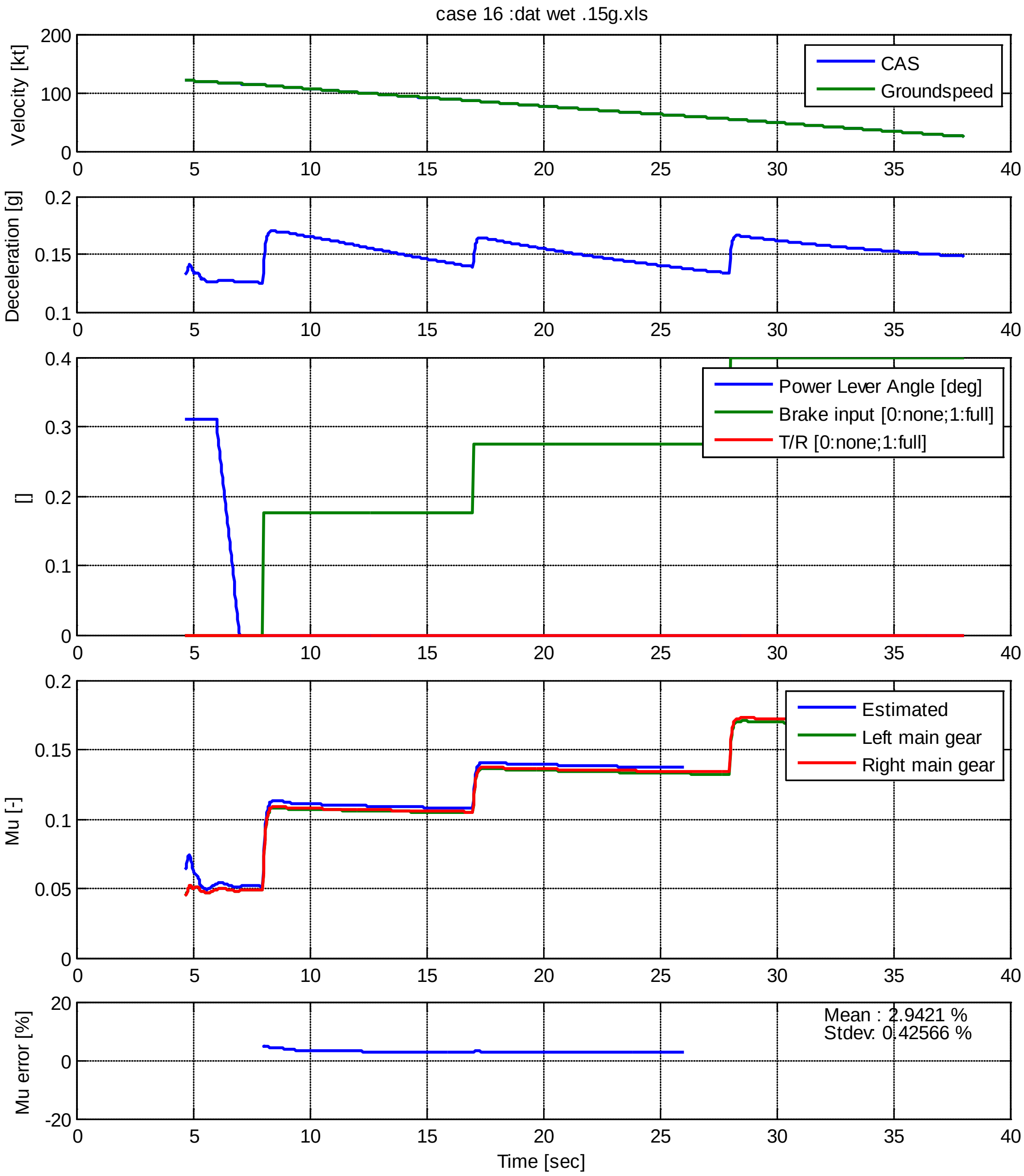

Figure B-16. Simulated Landing Run for Case 16

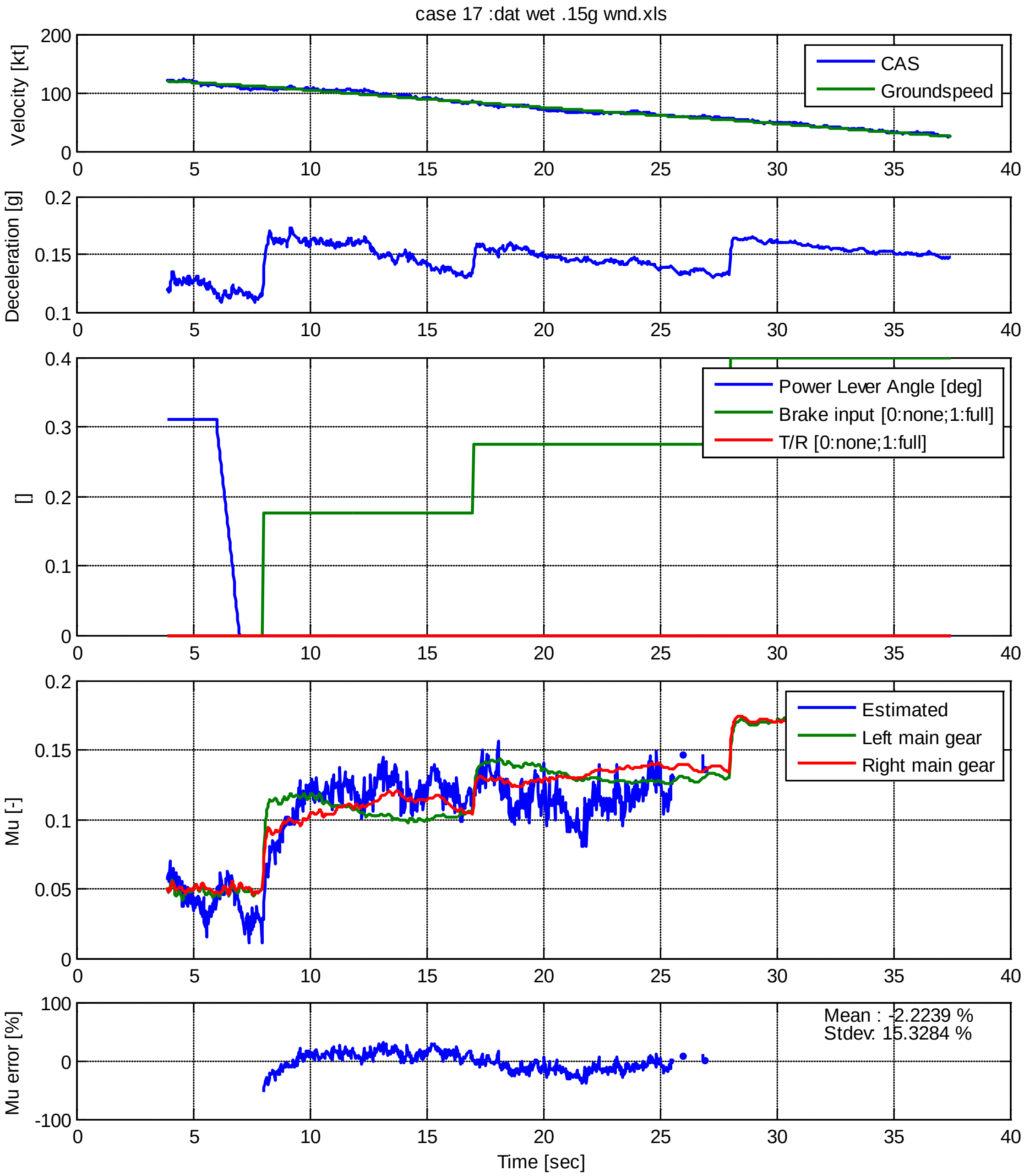

Figure B-17. Simulated Landing Run for Case 17

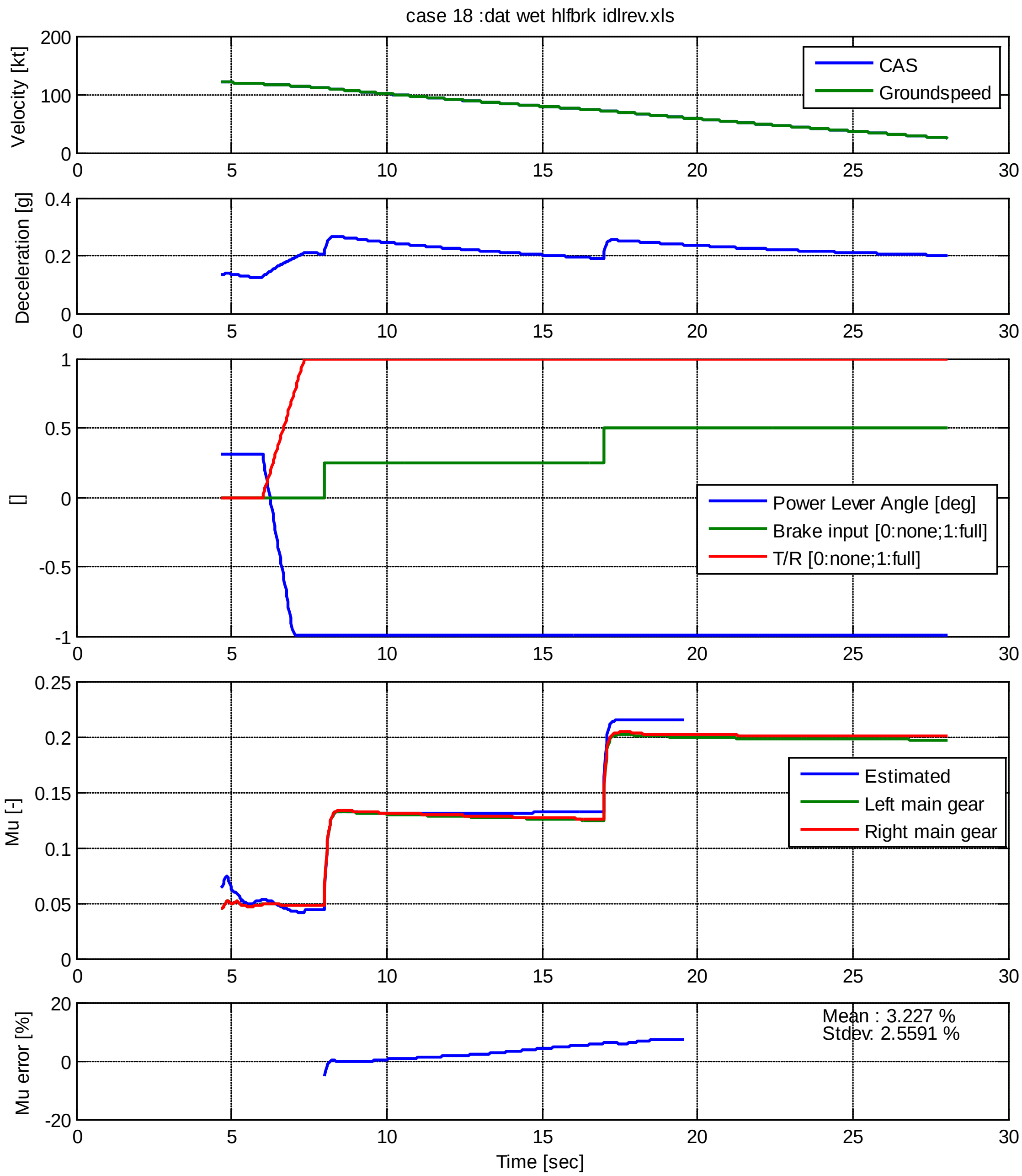

Figure B-18. Simulated Landing Run for Case 18

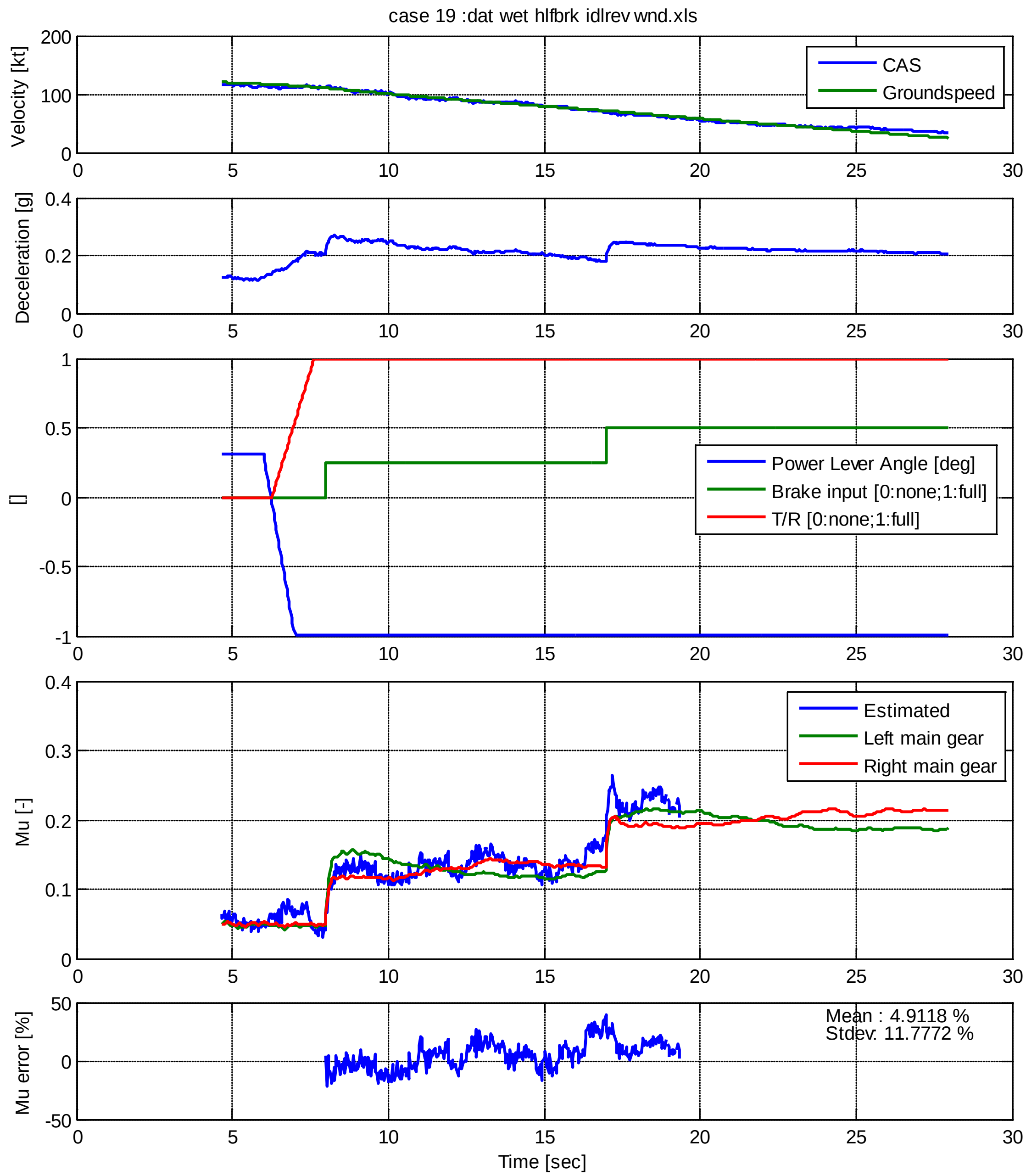

Figure B-19. Simulated Landing Run for Case 19

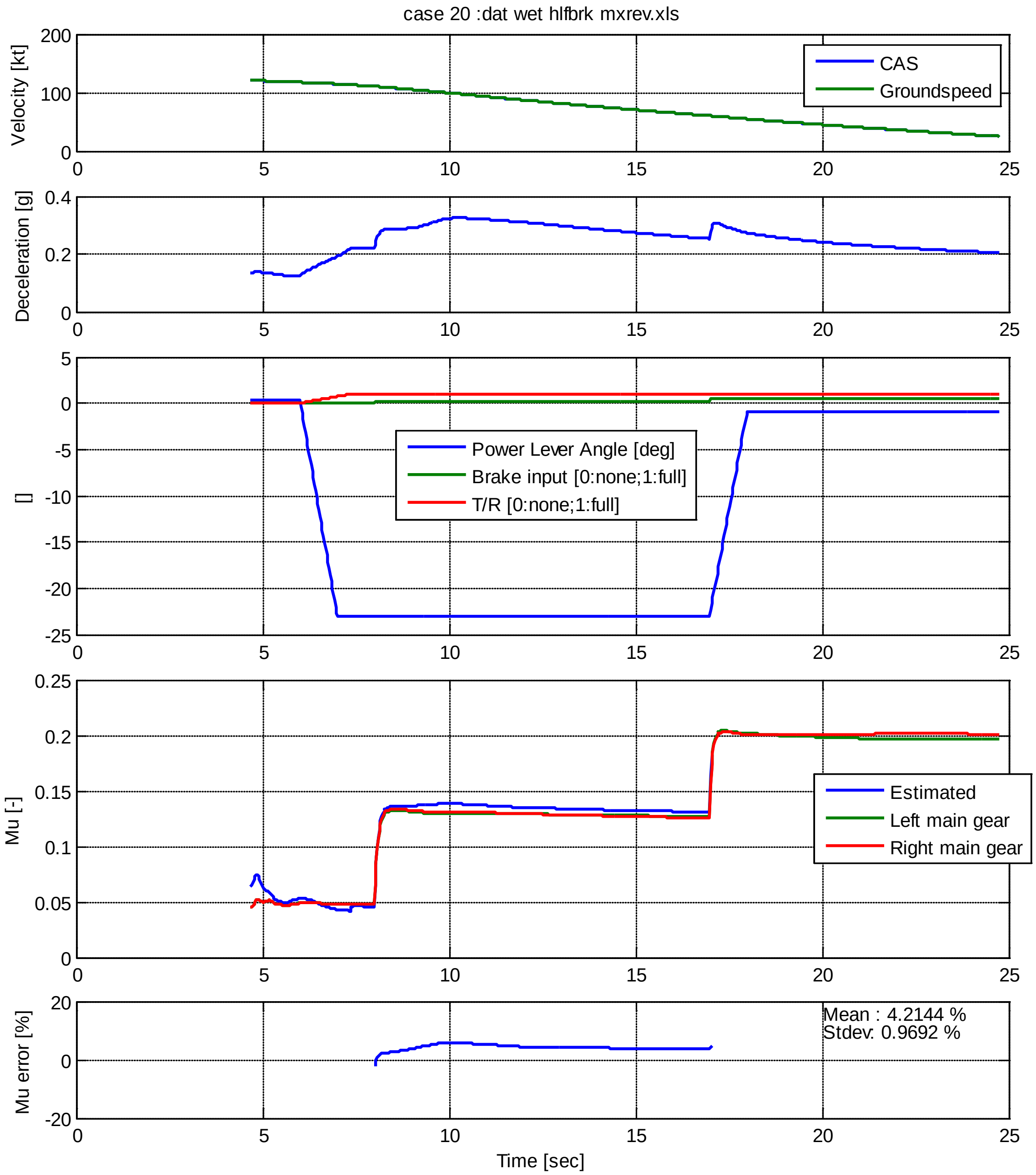

Figure B-20. Simulated Landing Run for Case 20

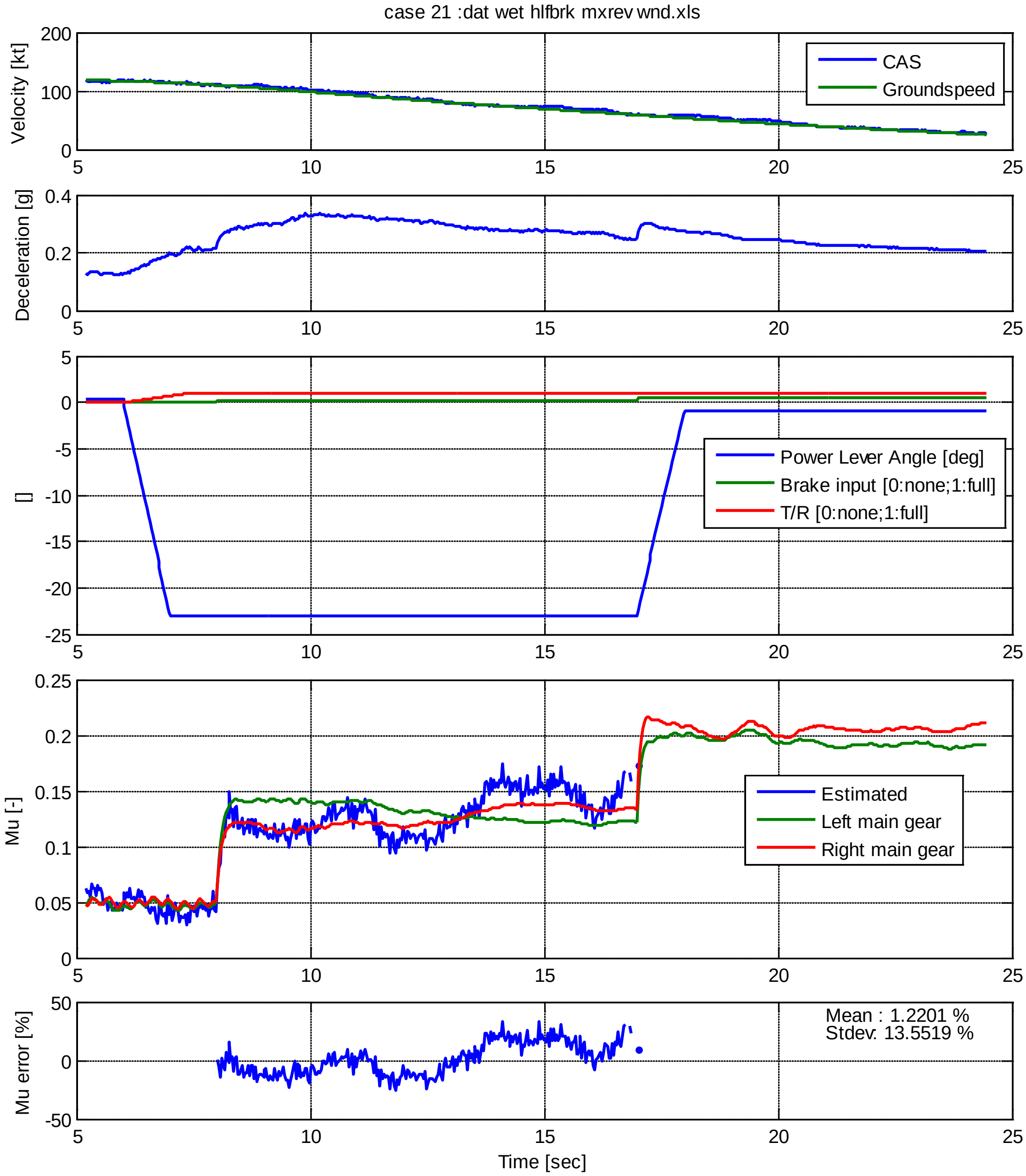

Figure B-21. Simulated Landing Run for Case 21

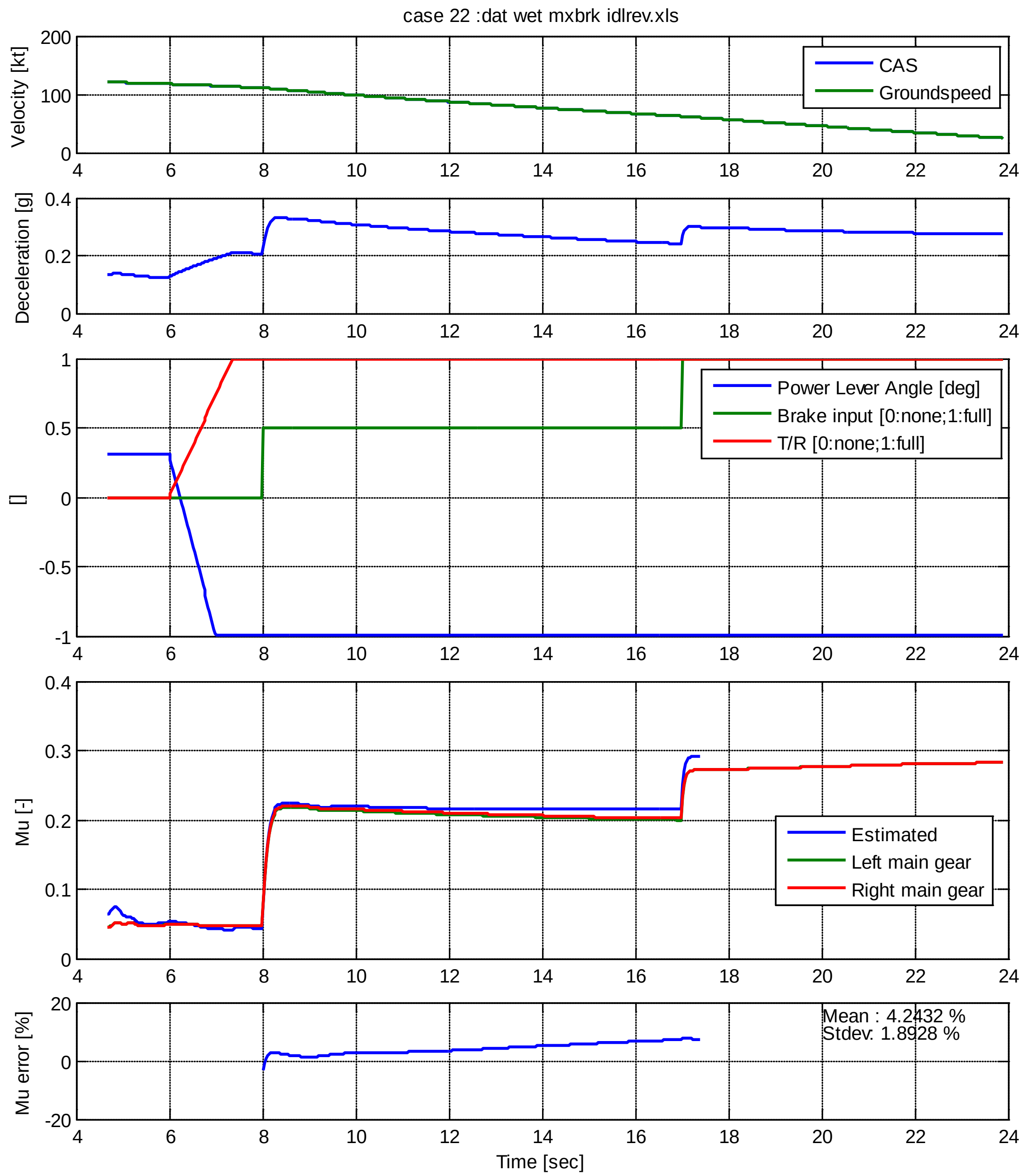

Figure B-22. Simulated Landing Run for Case 22

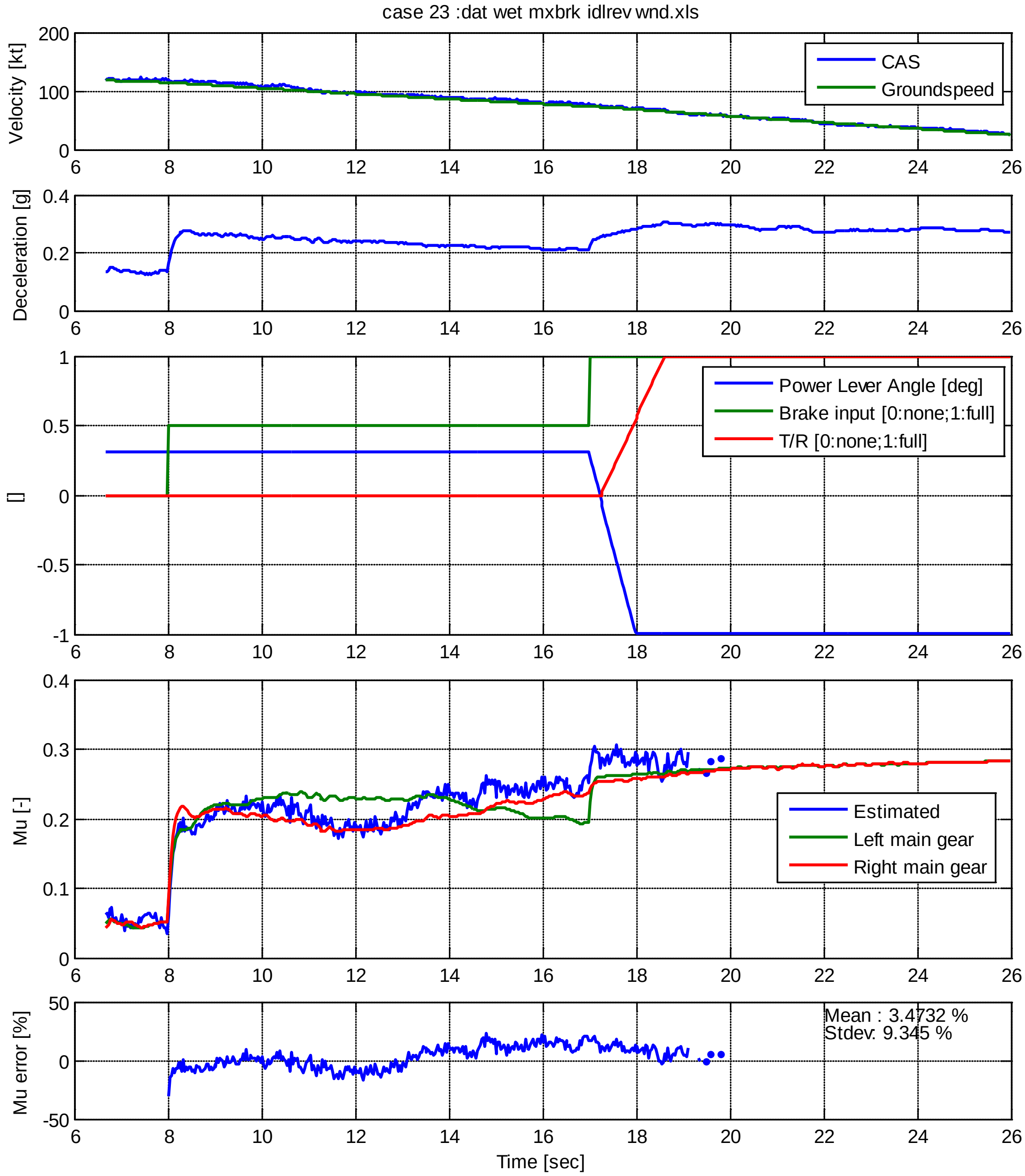

Figure B-23. Simulated Landing Run for Case 23

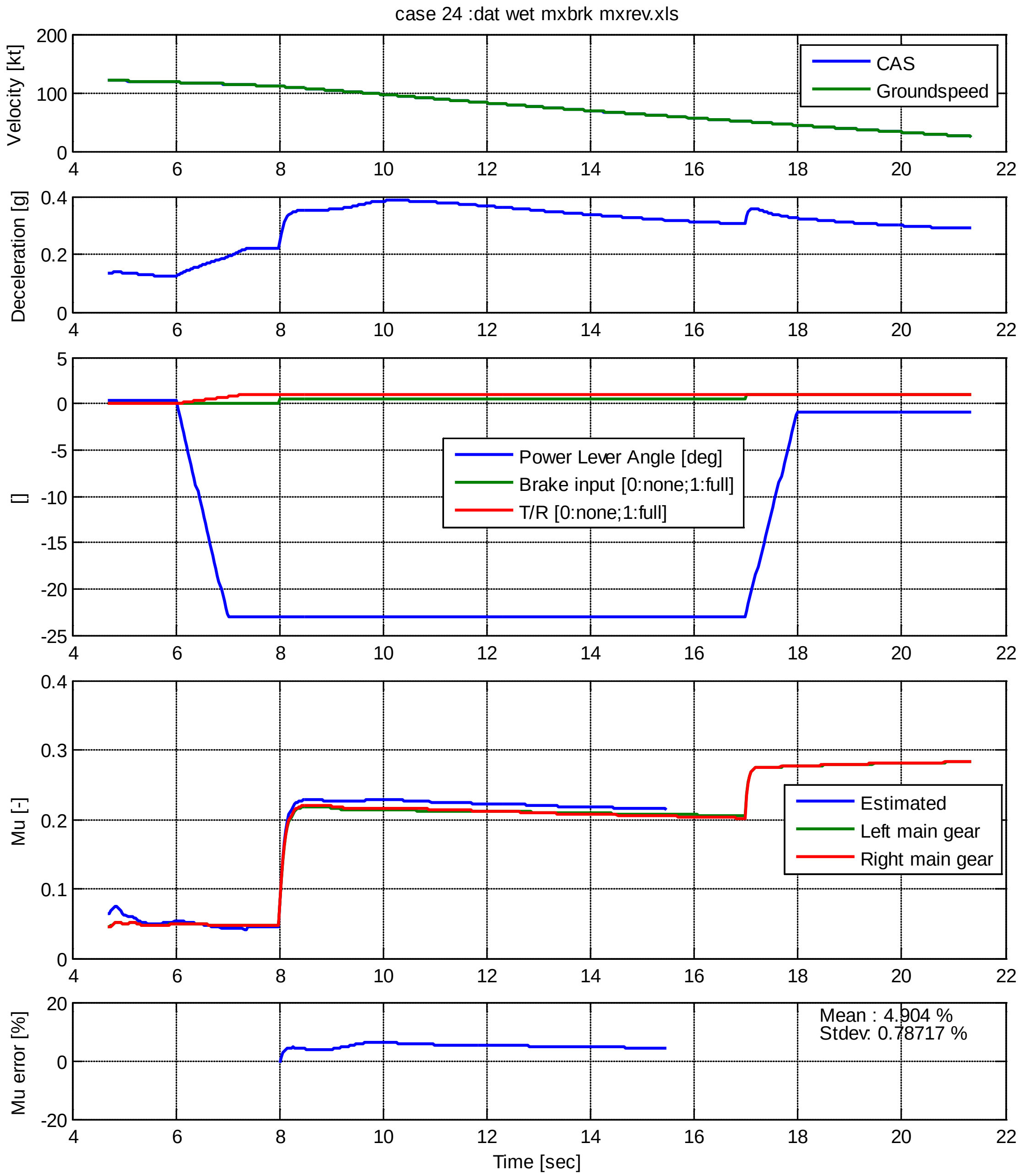

Figure B-24. Simulated Landing Run for Case 24

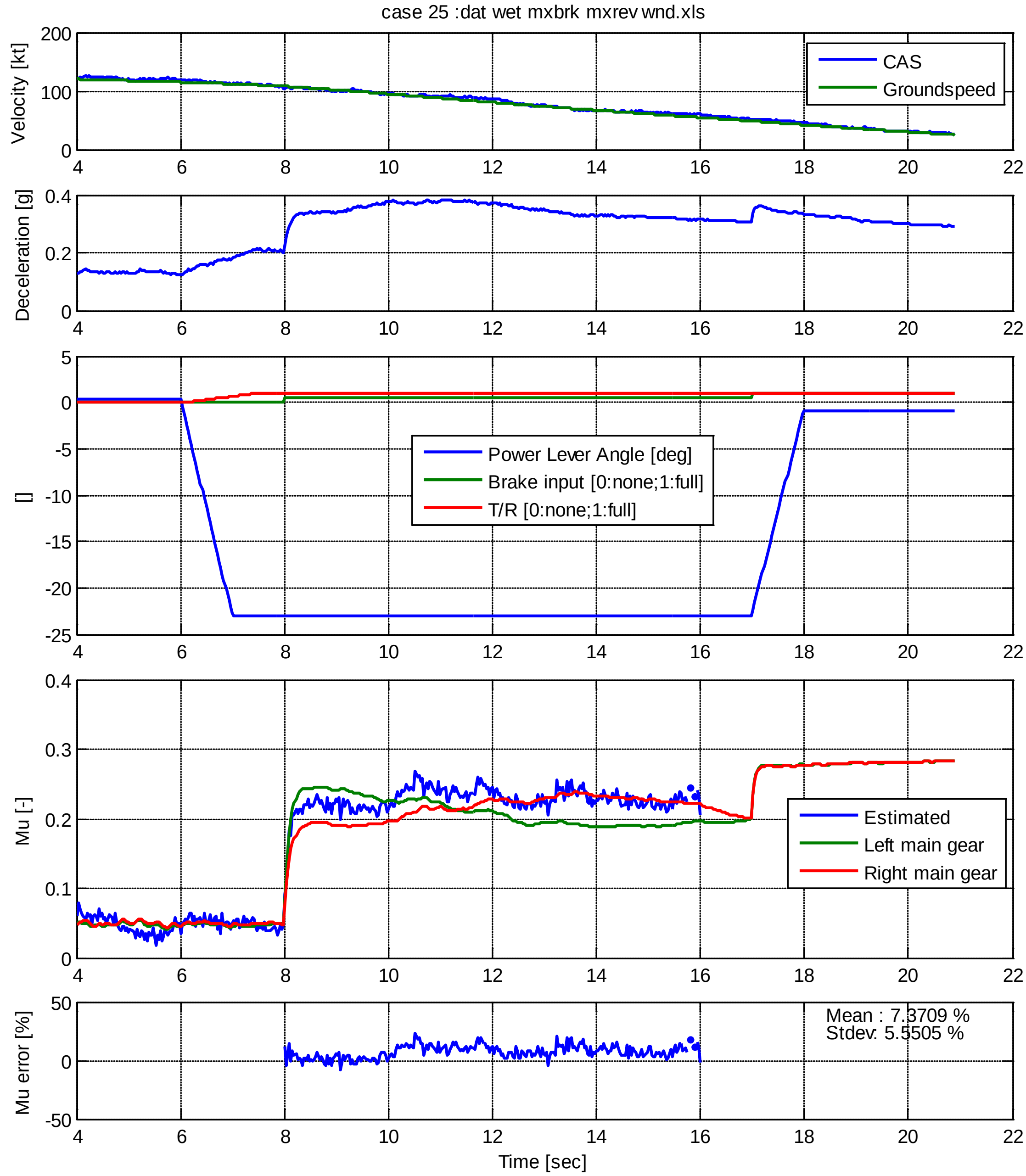

Figure B-25. Simulated Landing Run for Case 25

APPENDIX C—SIMULATION RESULTS WITH MEASUREMENT NOISES

The following charts present the time histories of simulated landing runs in terms of velocity, deceleration, and aircraft configurations (power, brake, T/R), as well as the algorithm outputs (estimated μ, left/right true μ, reported μ) and error in estimated μ, for the 25 cases outlined in table 1 of the main report from touchdown to 25 kt ground speed when the measuring errors are introduced.

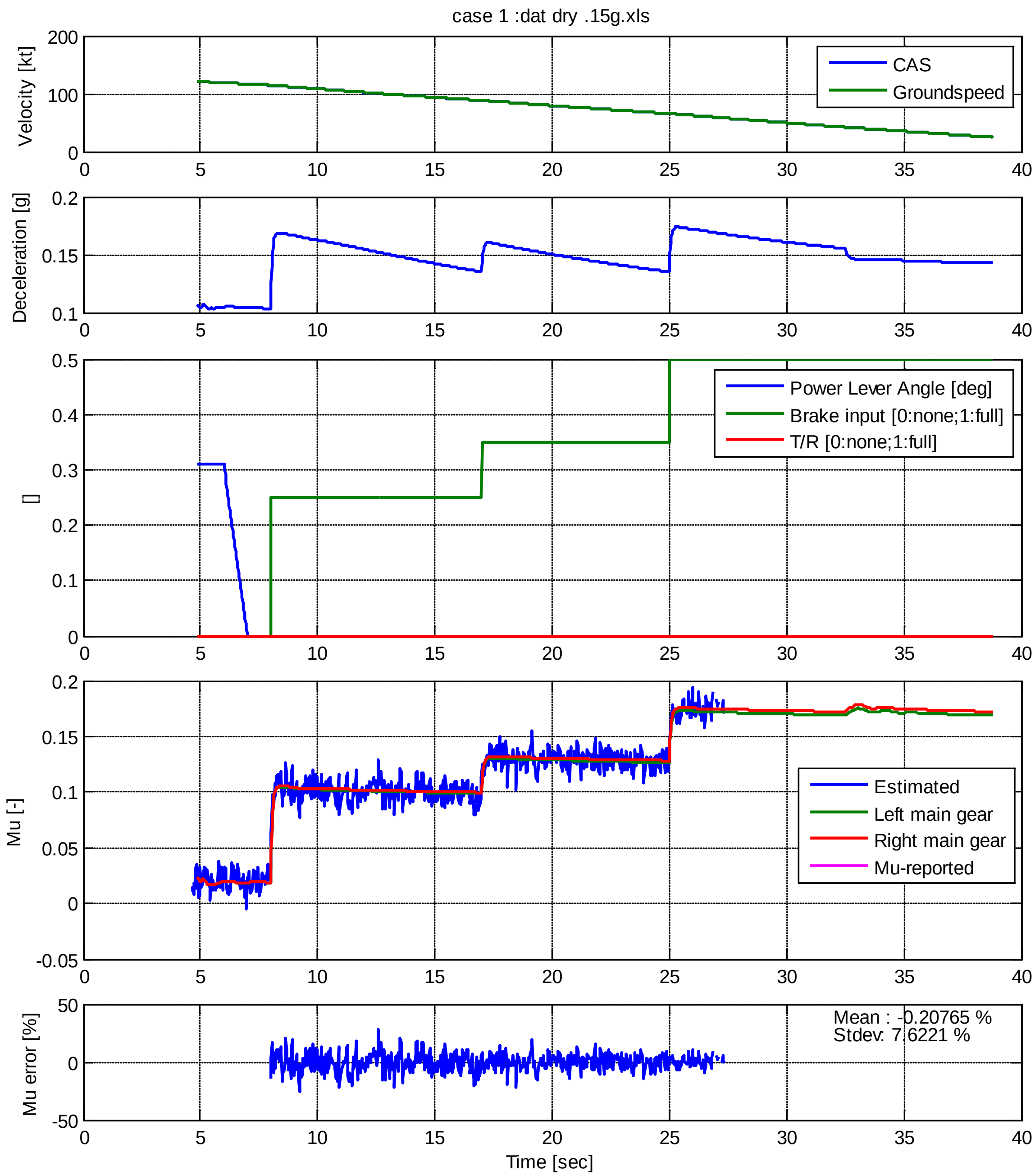

Figure C-1. Simulated Landing Run for Case 1

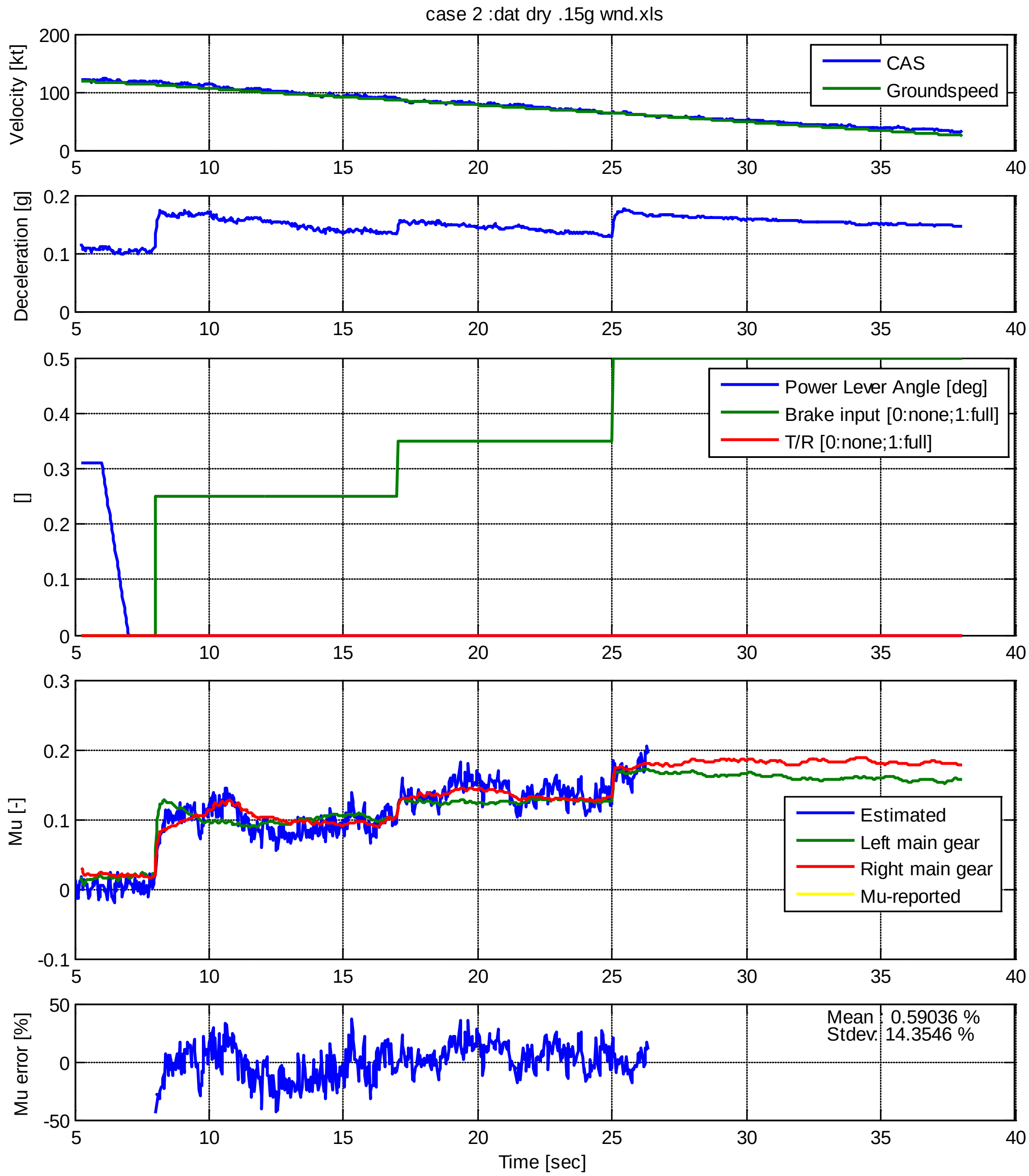

Figure C-2. Simulated Landing Run for Case 2

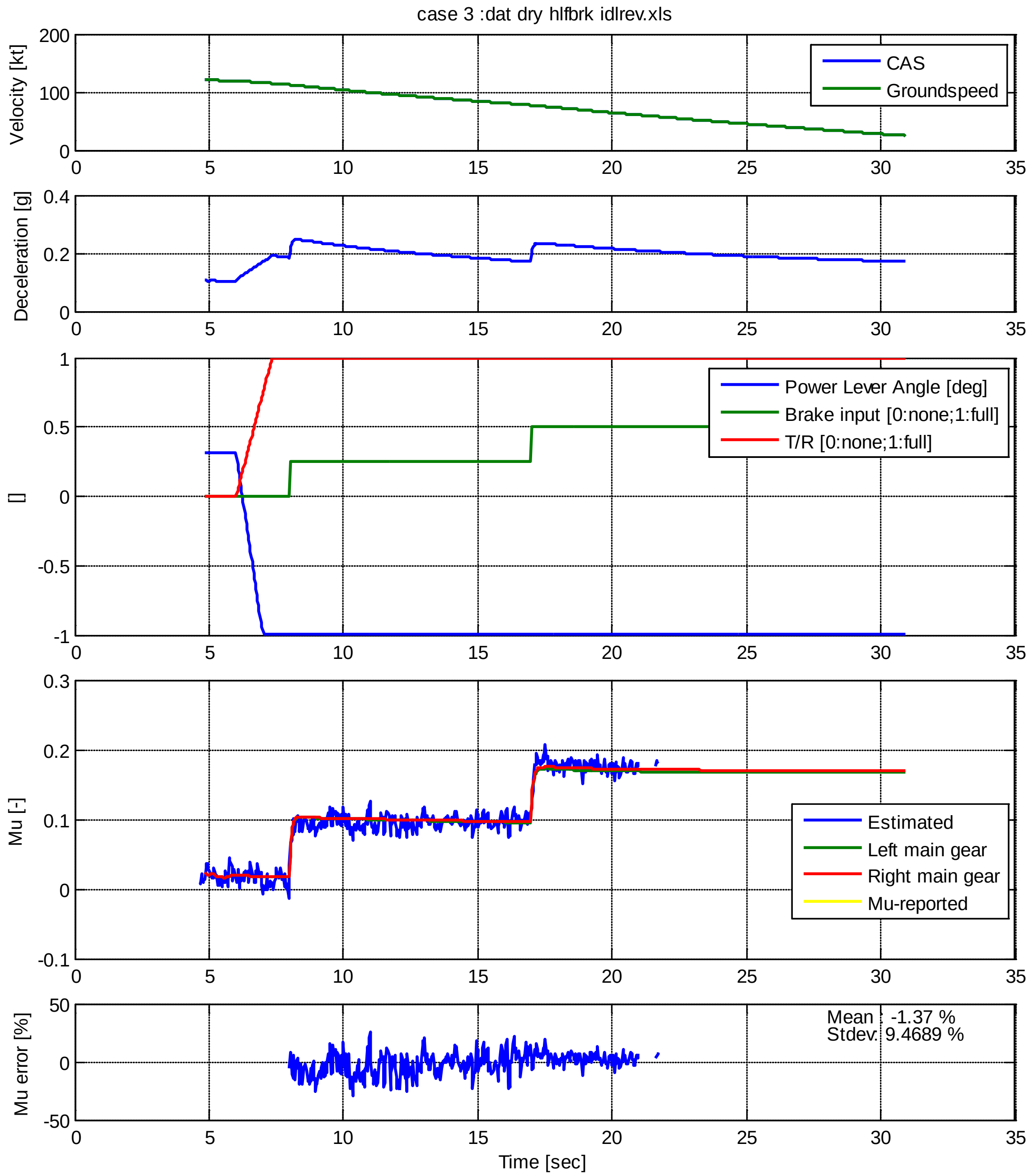

Figure C-3. Simulated Landing Run for Case 3

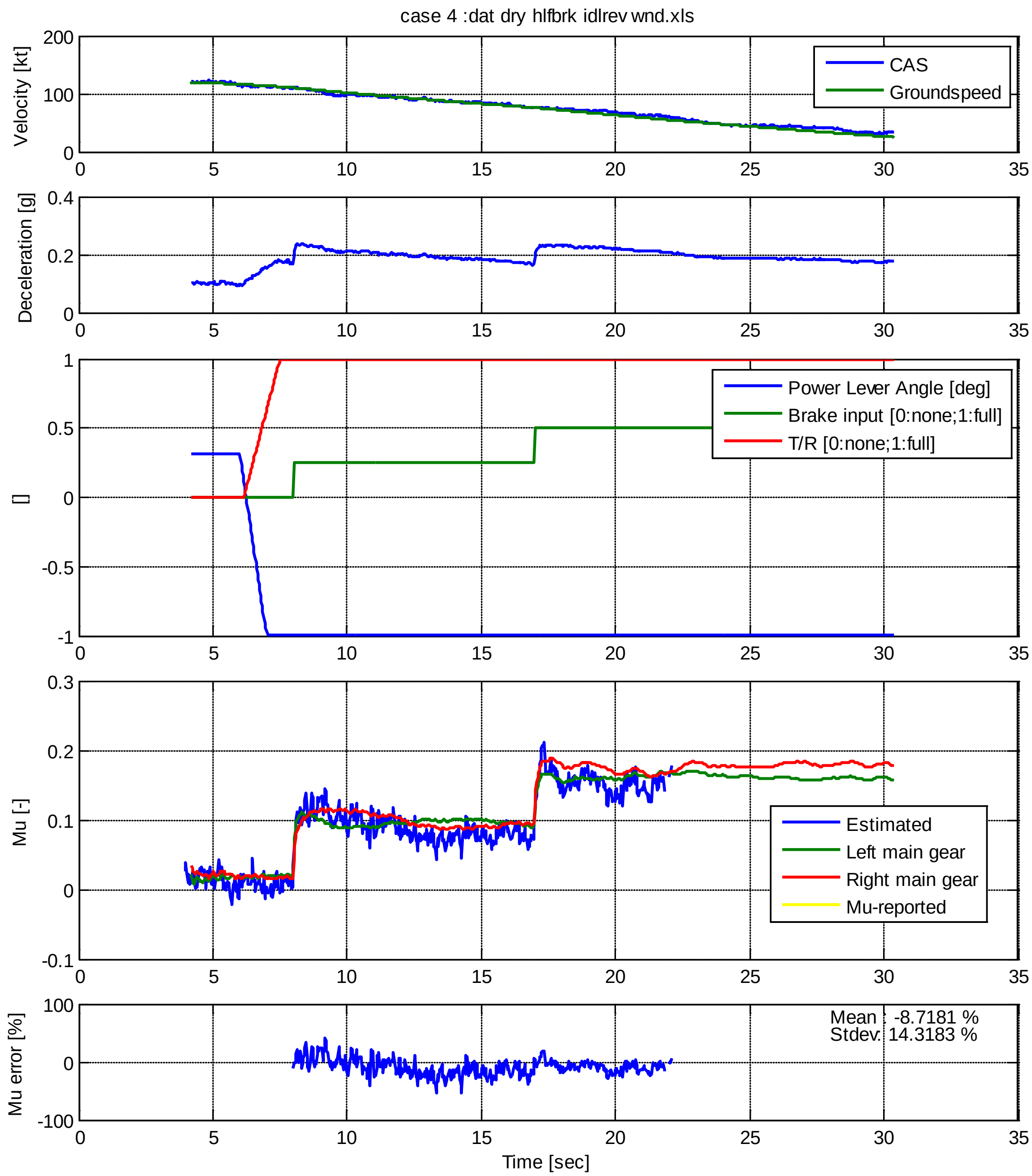

Figure C-4. Simulated Landing Run for Case 4

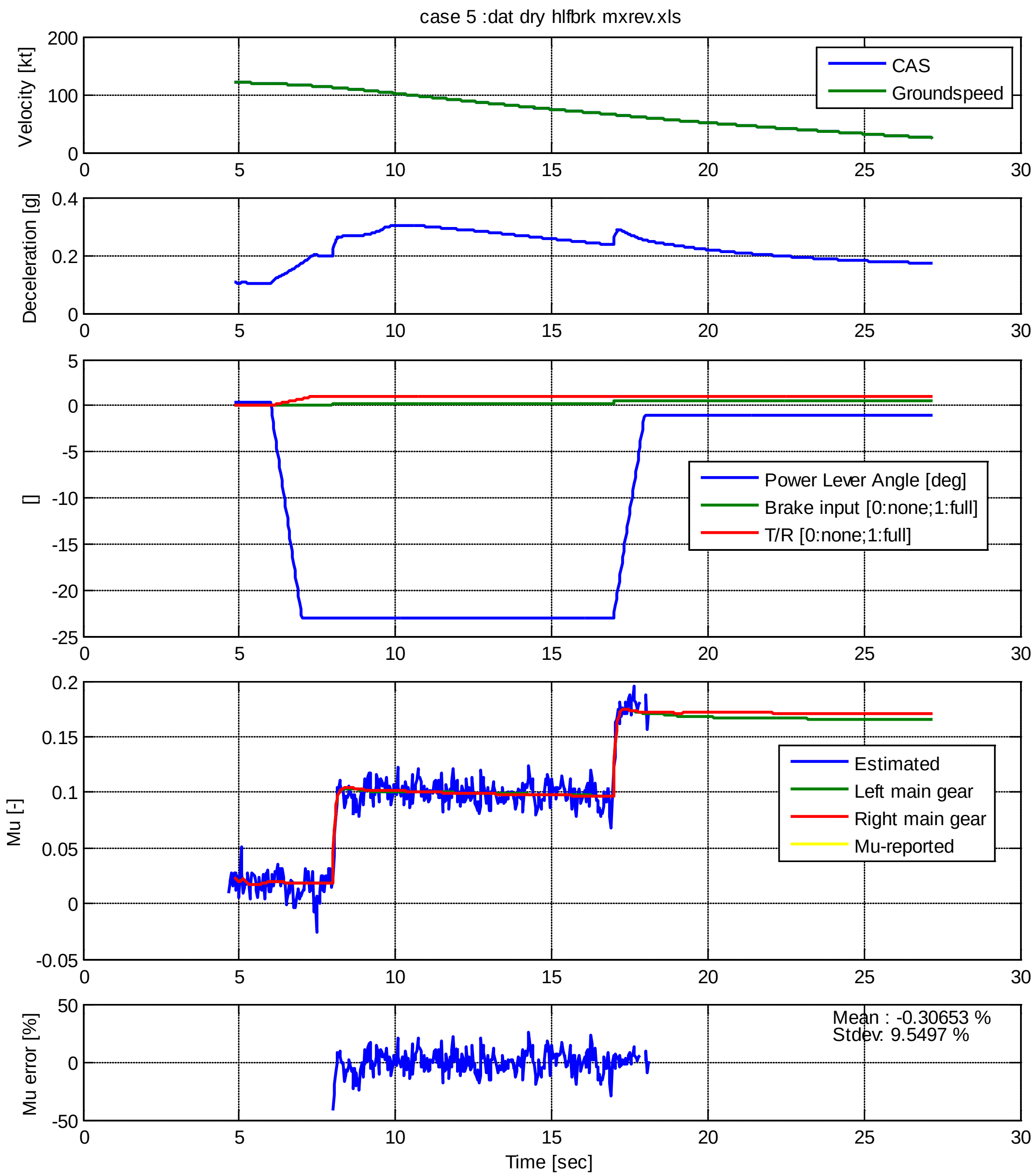

Figure C-5. Simulated Landing Run for Case 5

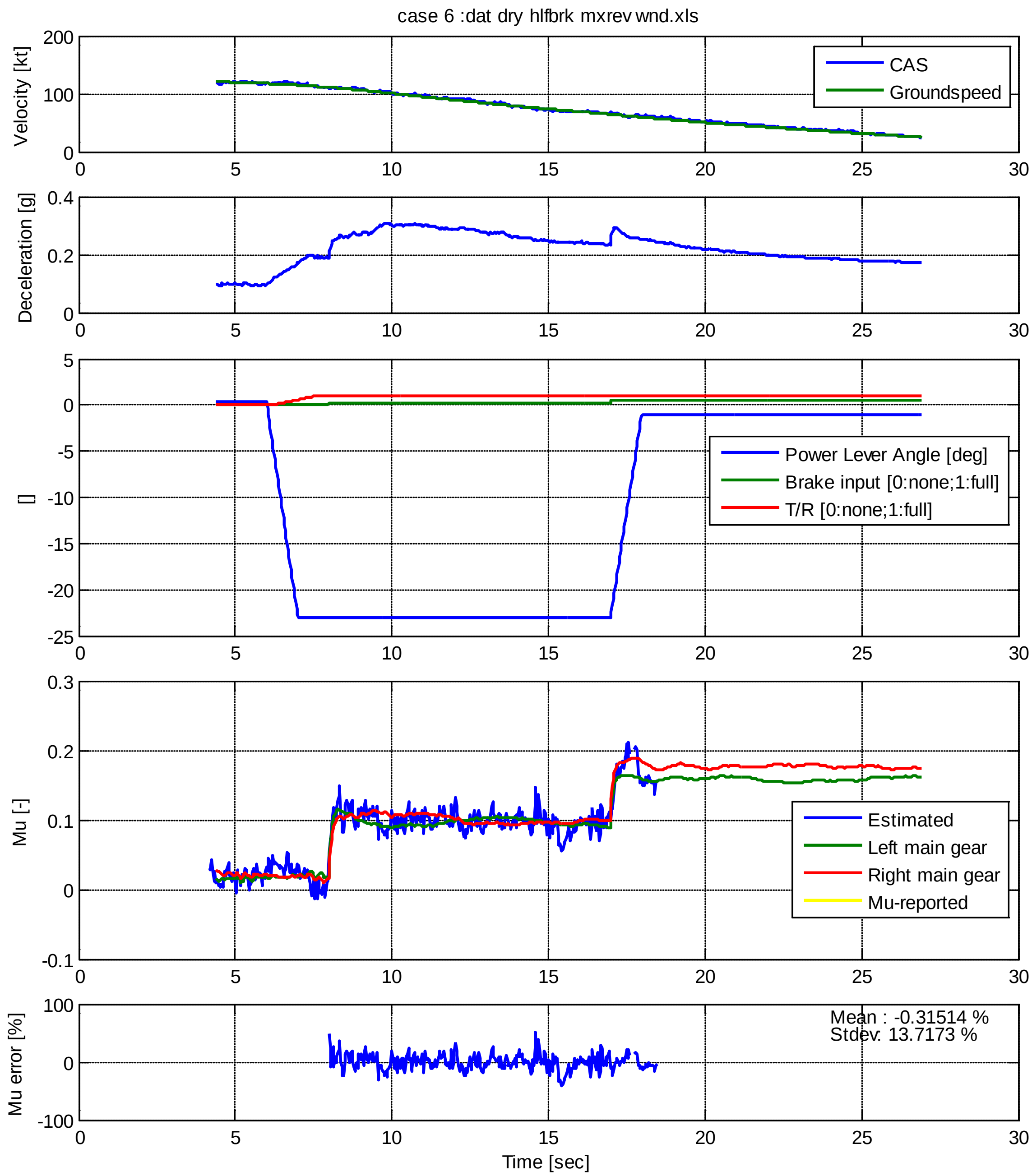

Figure C-6. Simulated Landing Run for Case 6

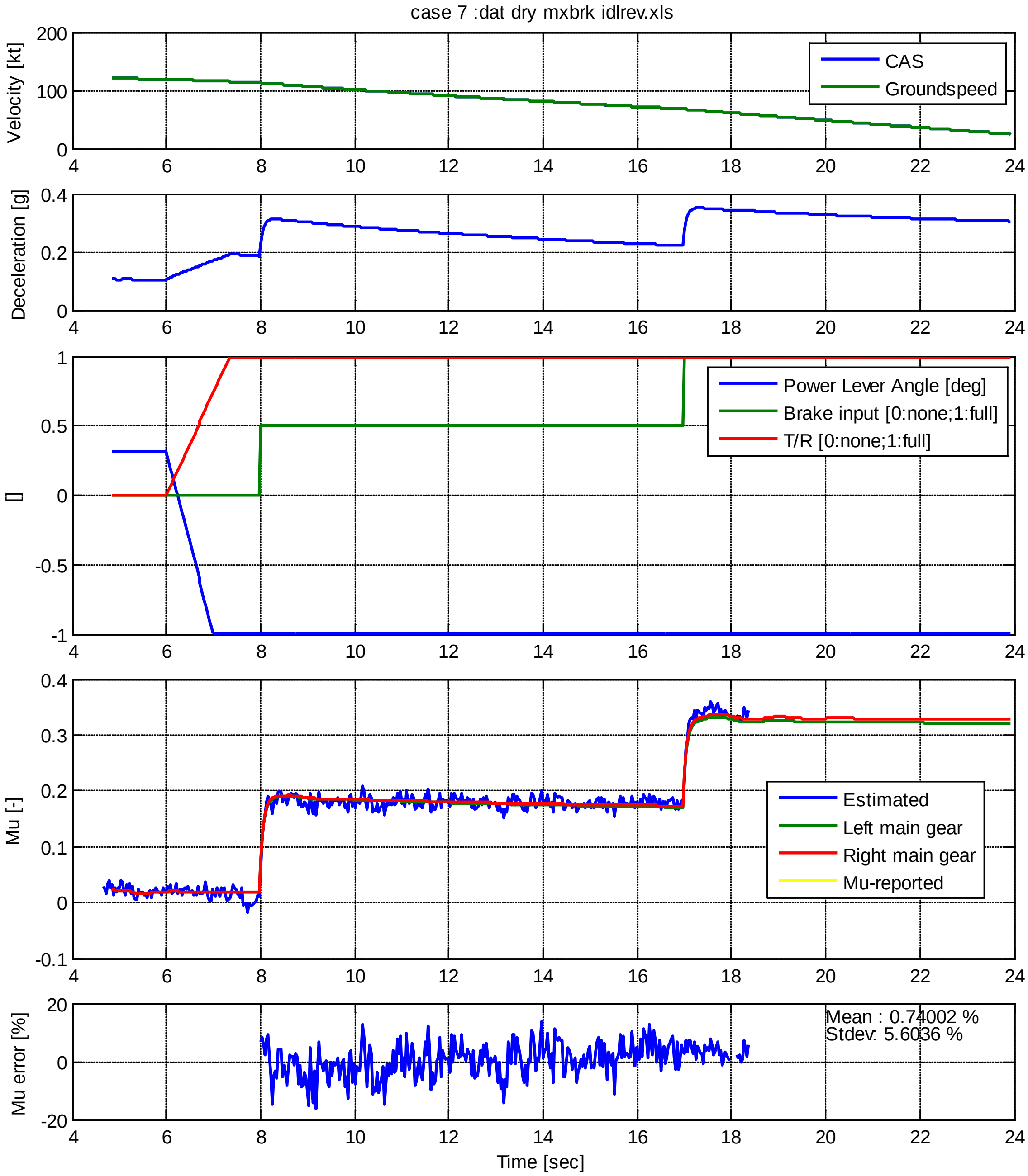

Figure C-7. Simulated Landing Run for Case 7

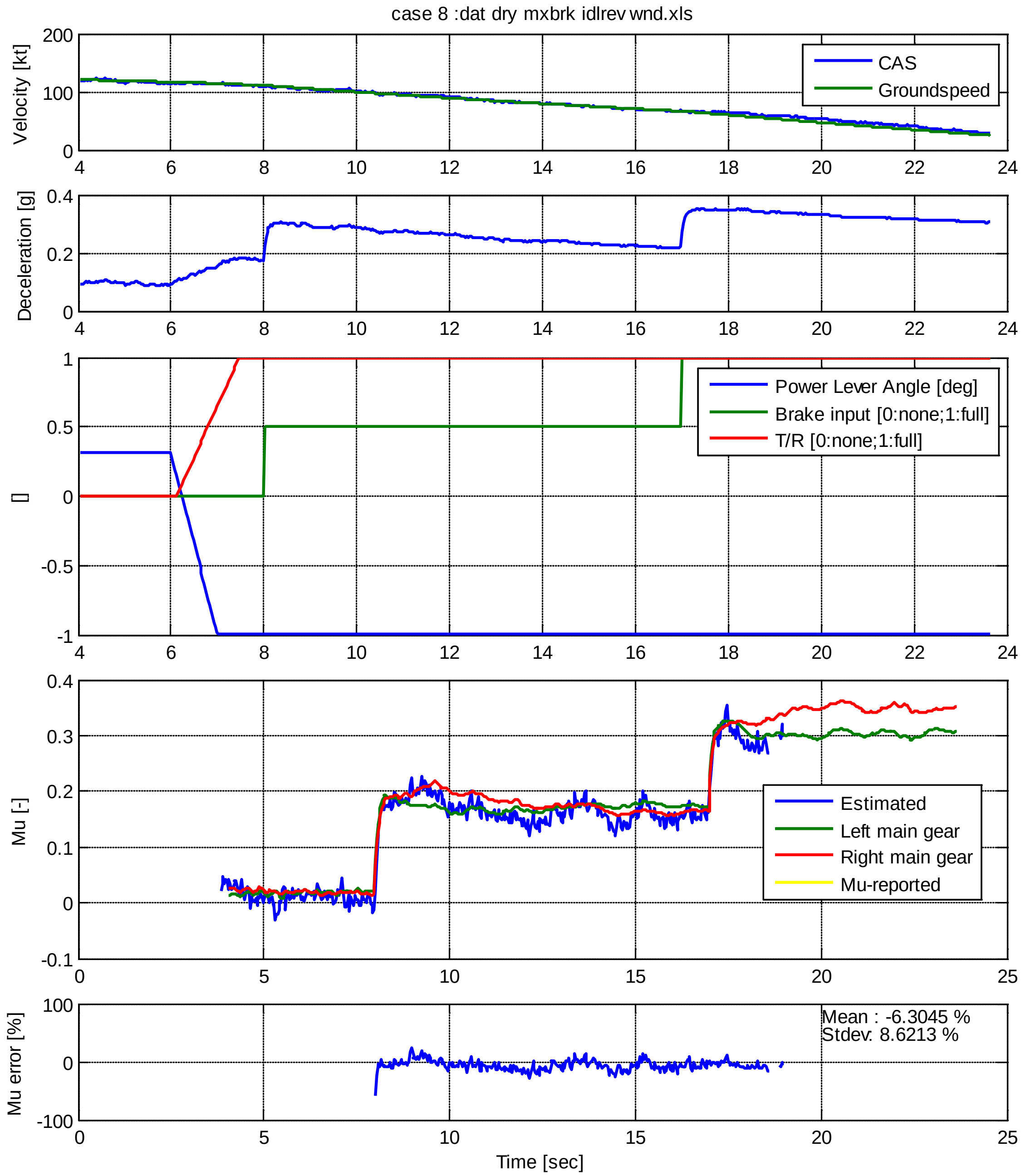

Figure C-8. Simulated Landing Run for Case 8

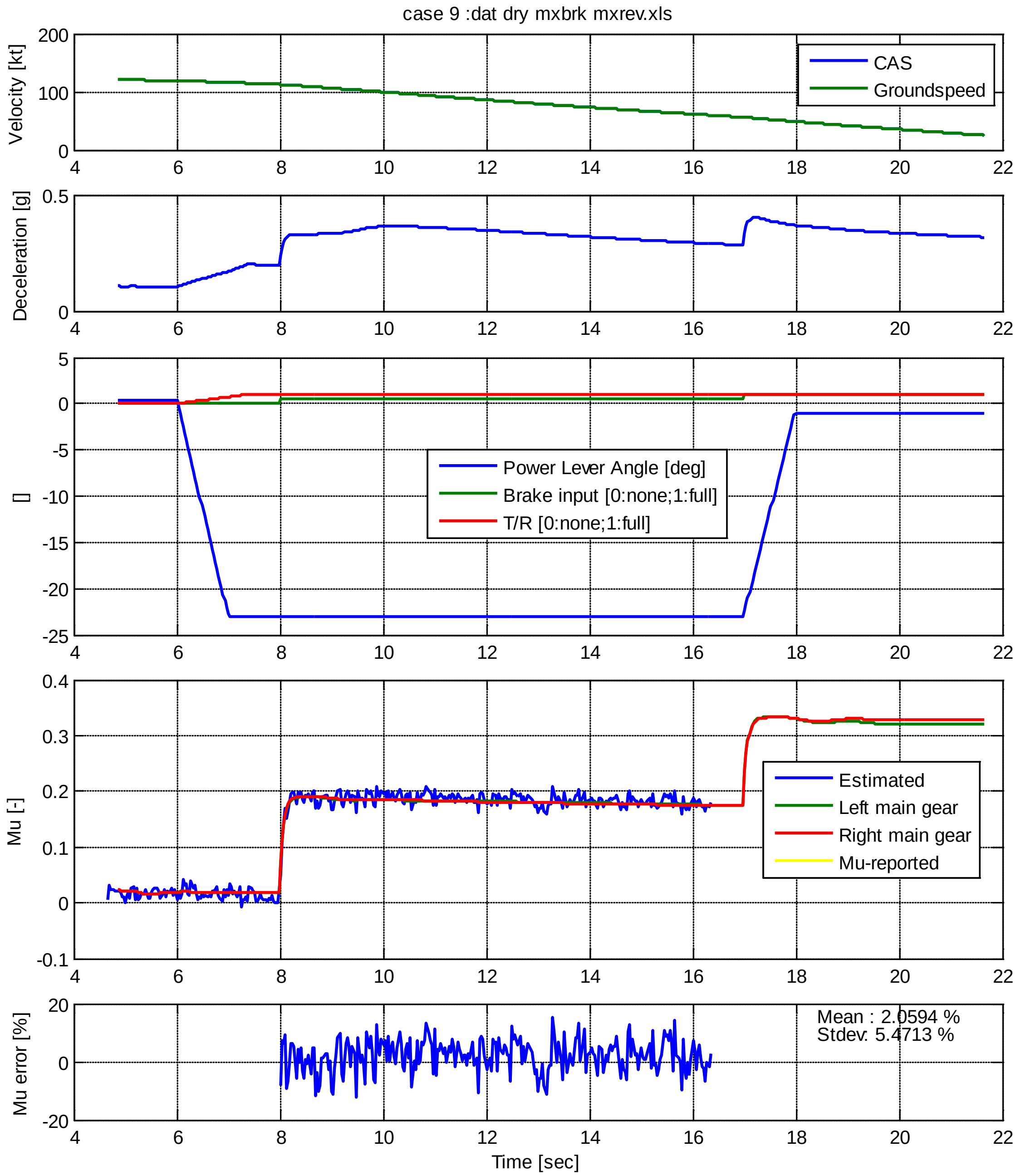

Figure C-9. Simulated Landing Run for Case 9

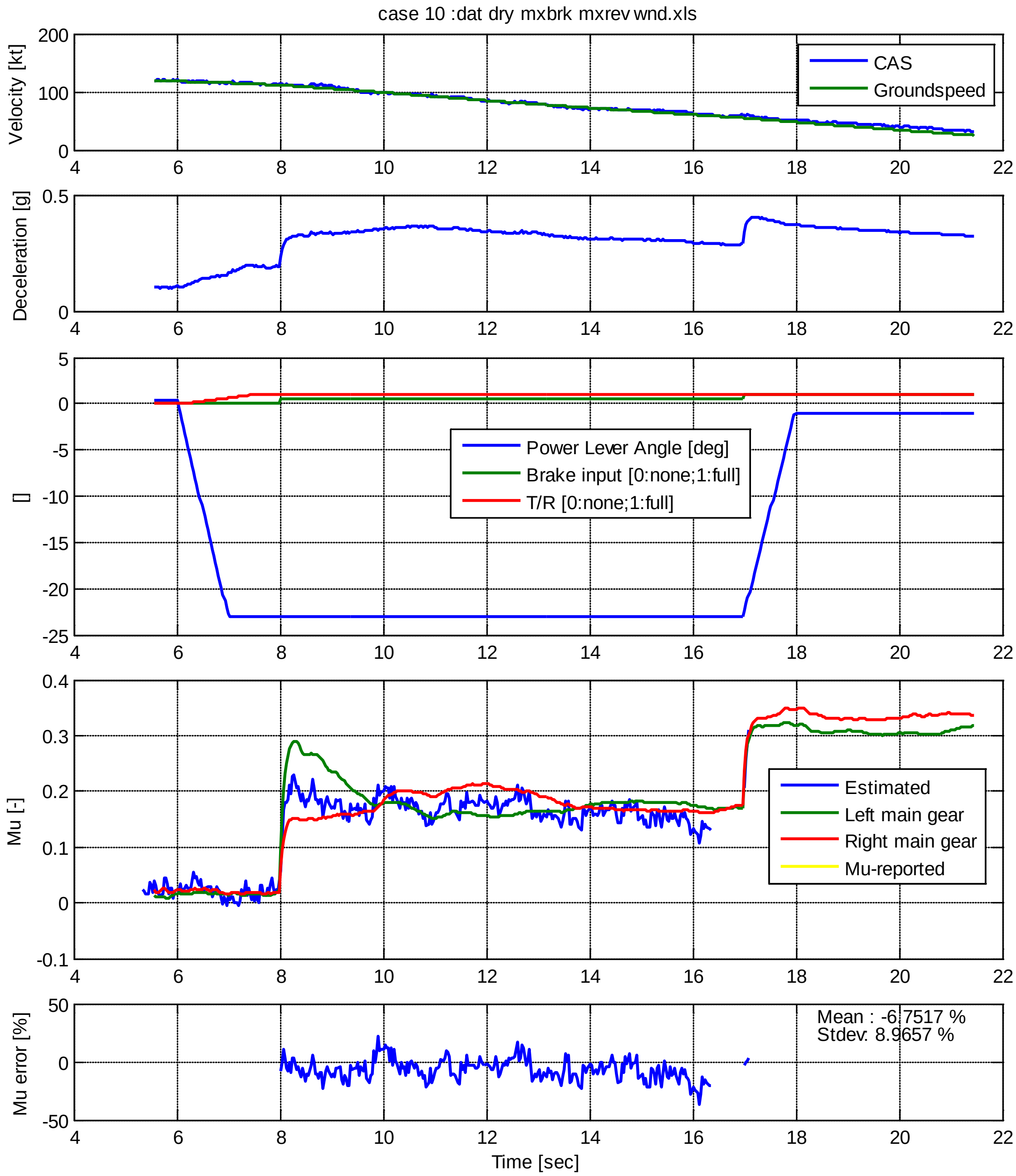

Figure C-10. Simulated Landing Run for Case 10

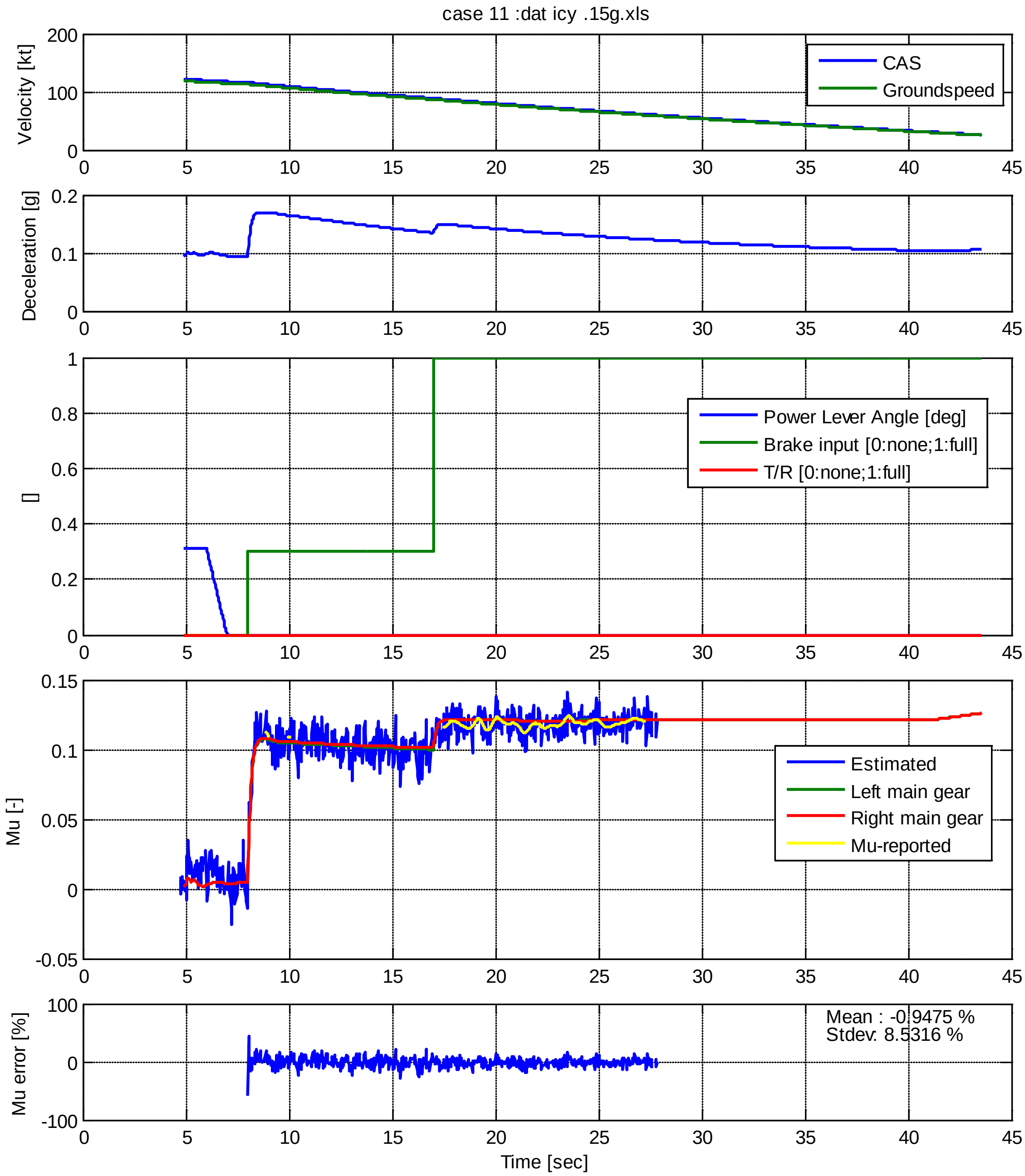

Figure C-11. Simulated Landing Run for Case 11

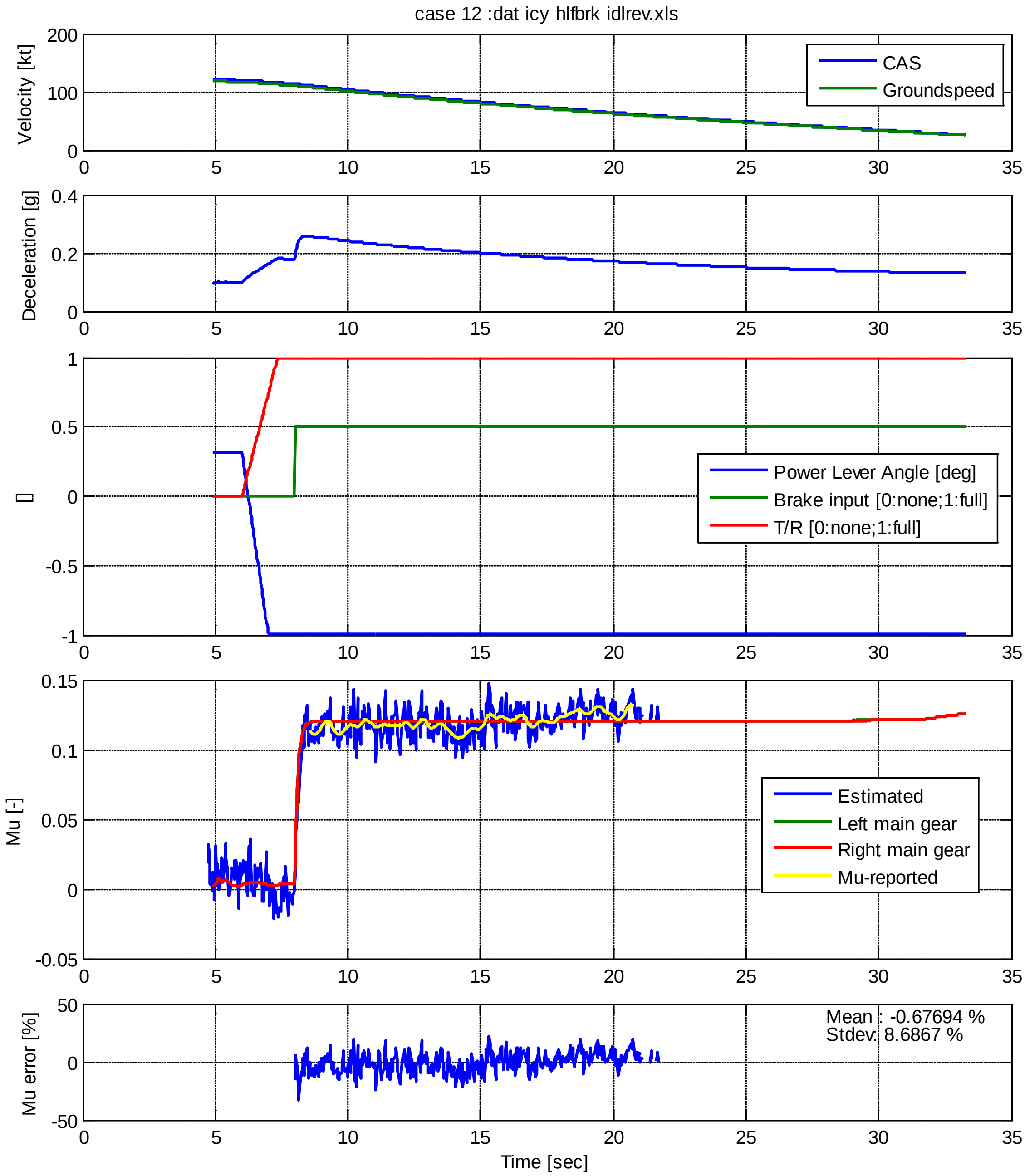

Figure C-12. Simulated Landing Run for Case 12

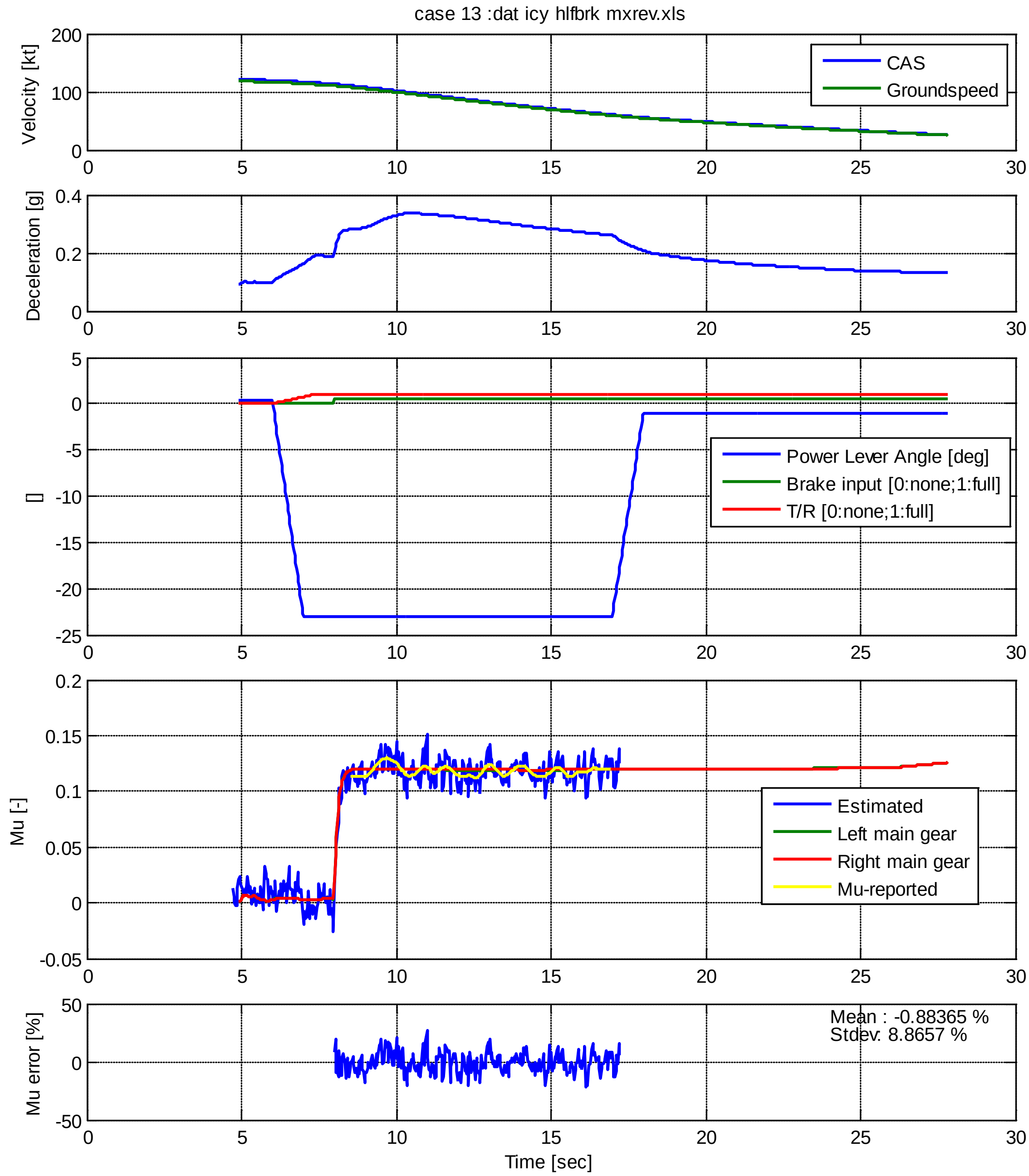

Figure C-13. Simulated Landing Run for Case 13

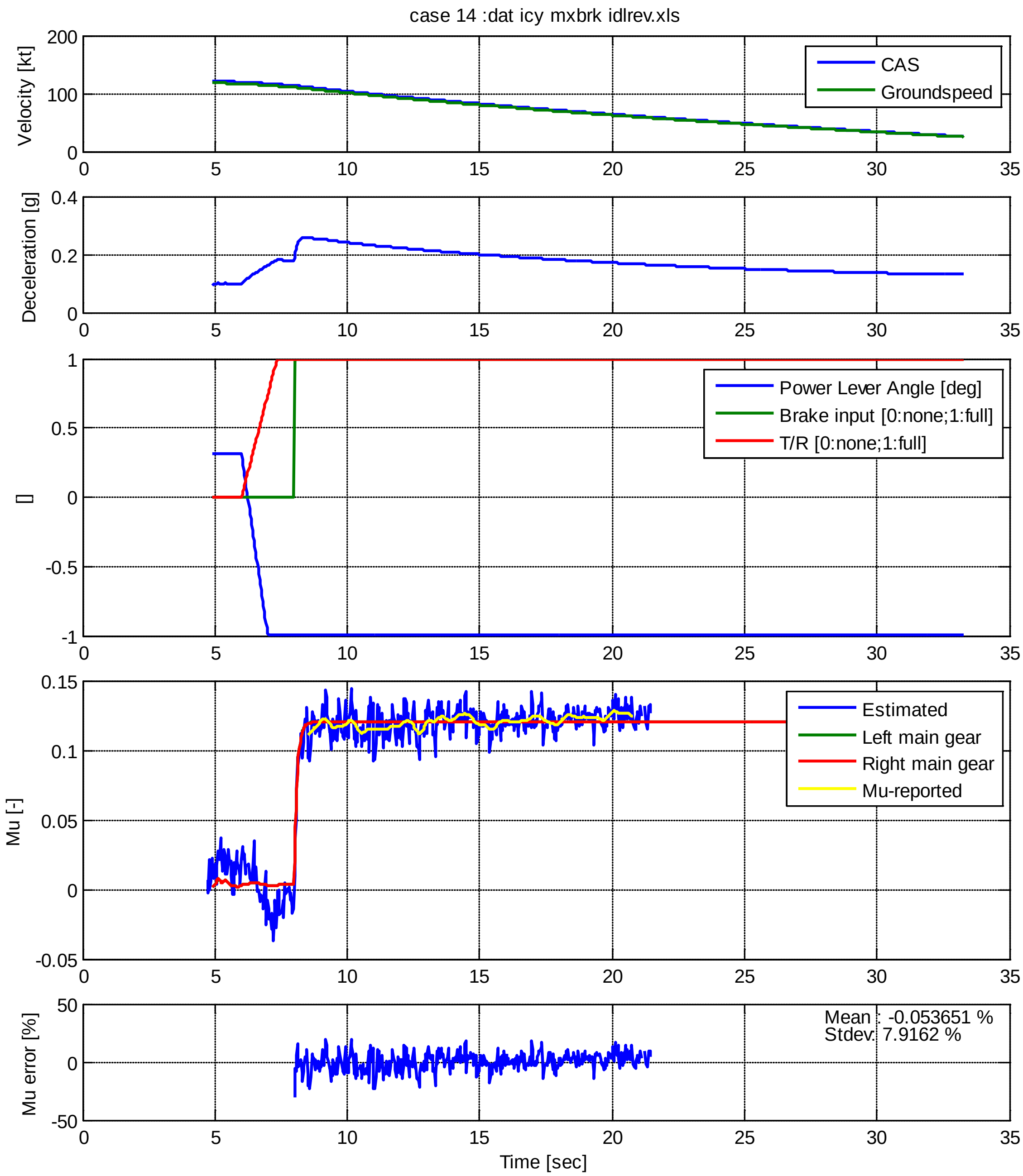

Figure C-14. Simulated Landing Run for Case 14

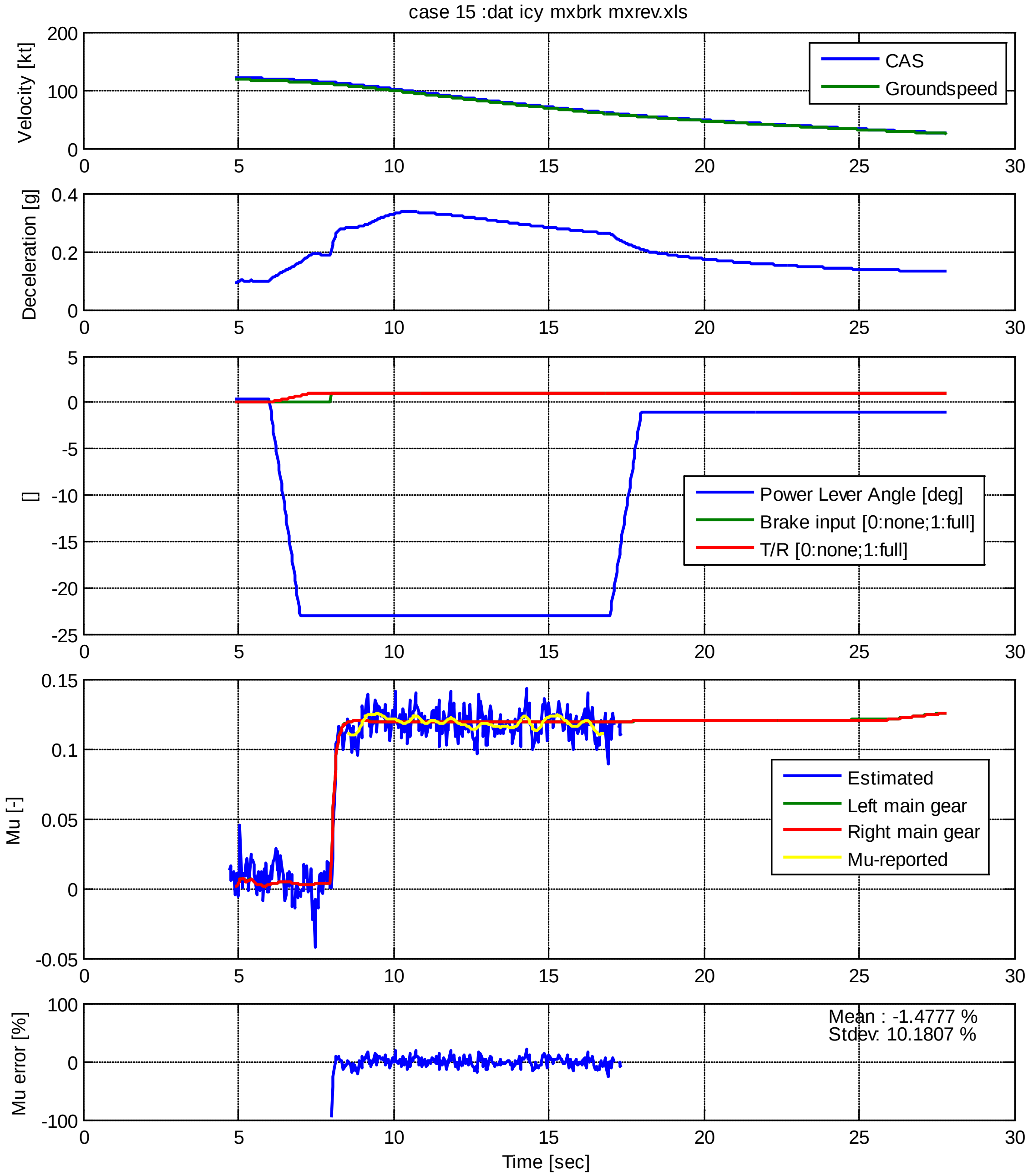

Figure C-15. Simulated Landing Run for Case 15

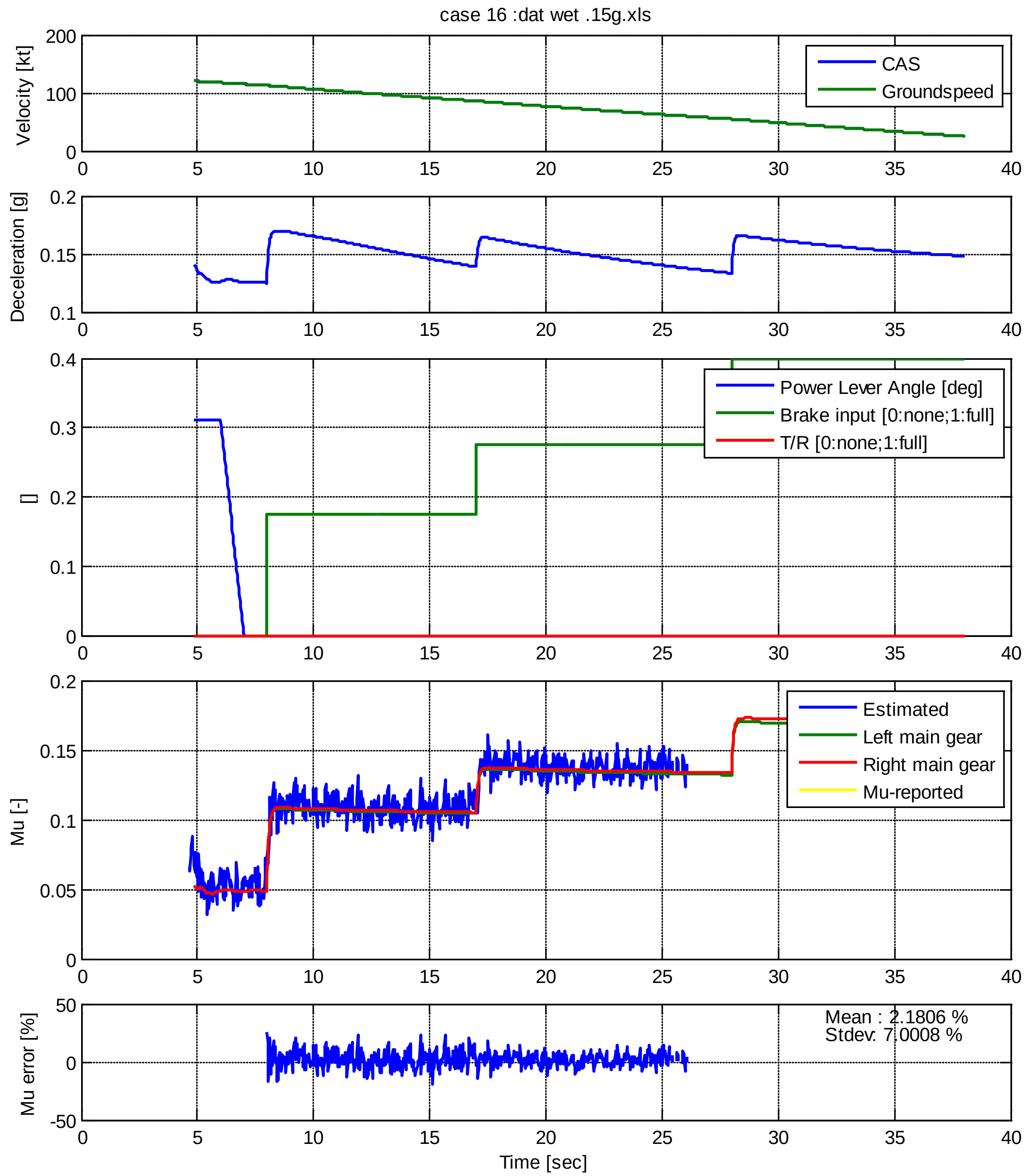

Figure C-16. Simulated Landing Run for Case 16

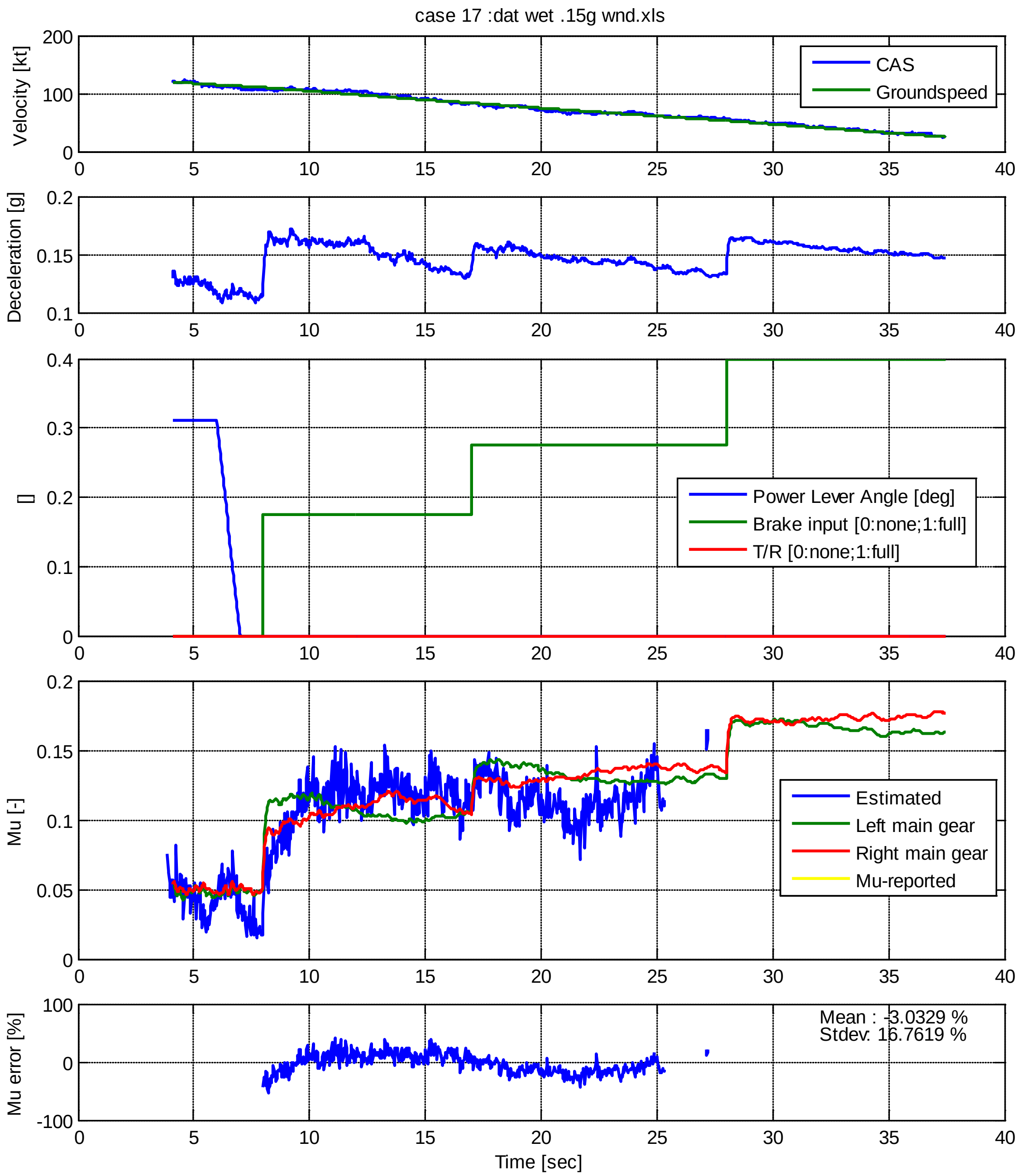

Figure C-17. Simulated Landing Run for Case 17

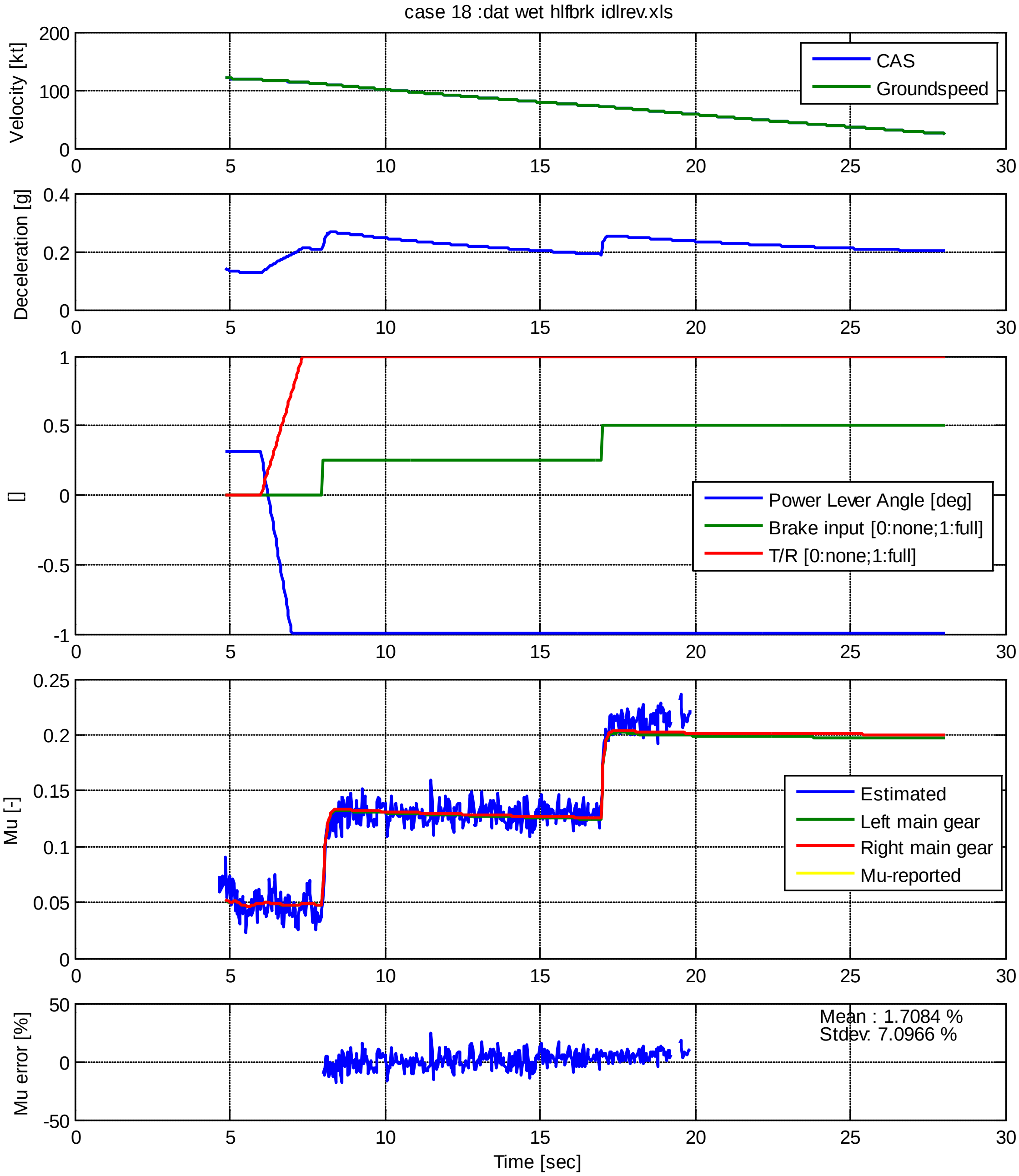

Figure C-18. Simulated Landing Run for Case 18

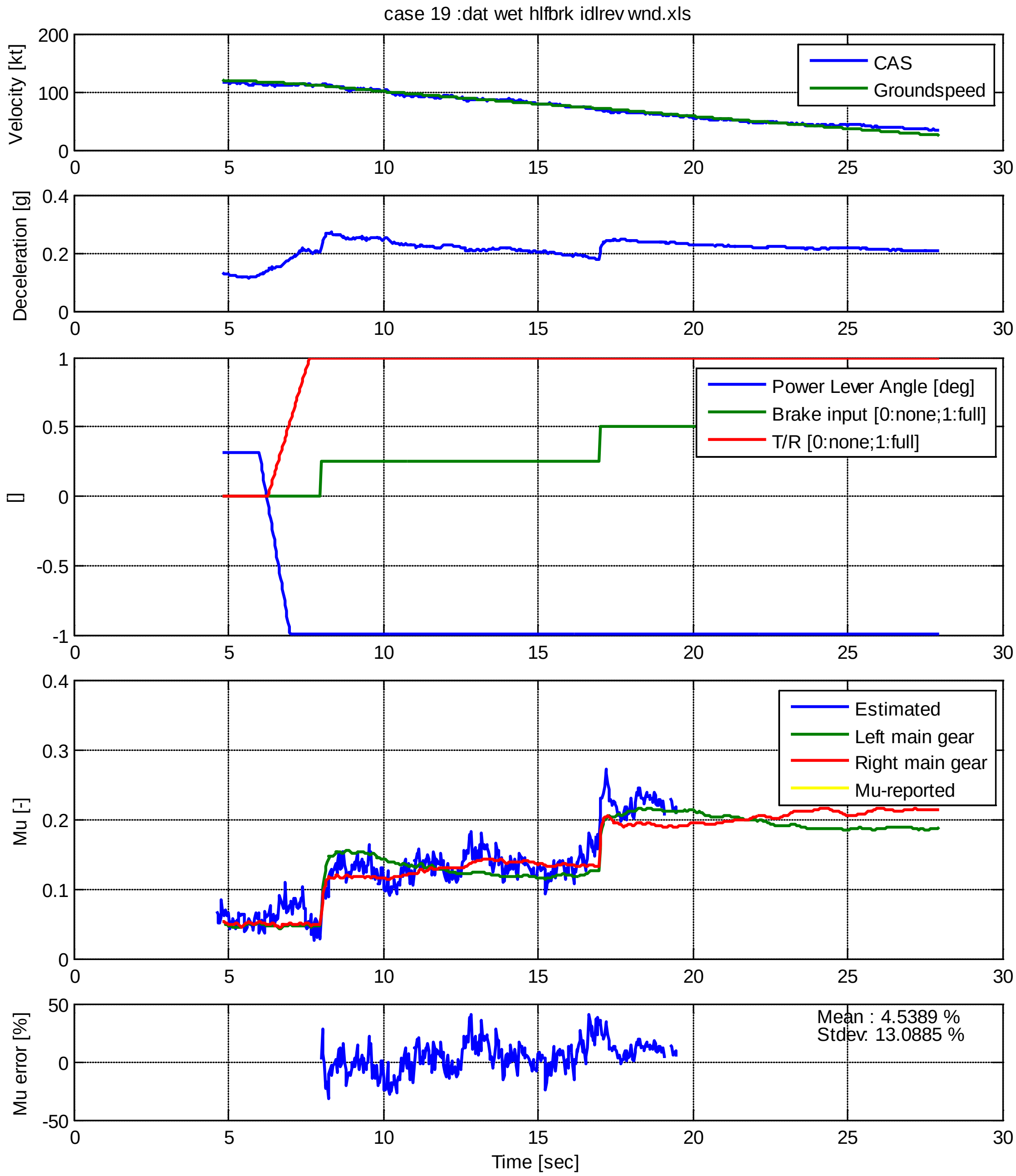

Figure C-19. Simulated Landing Run for Case 19

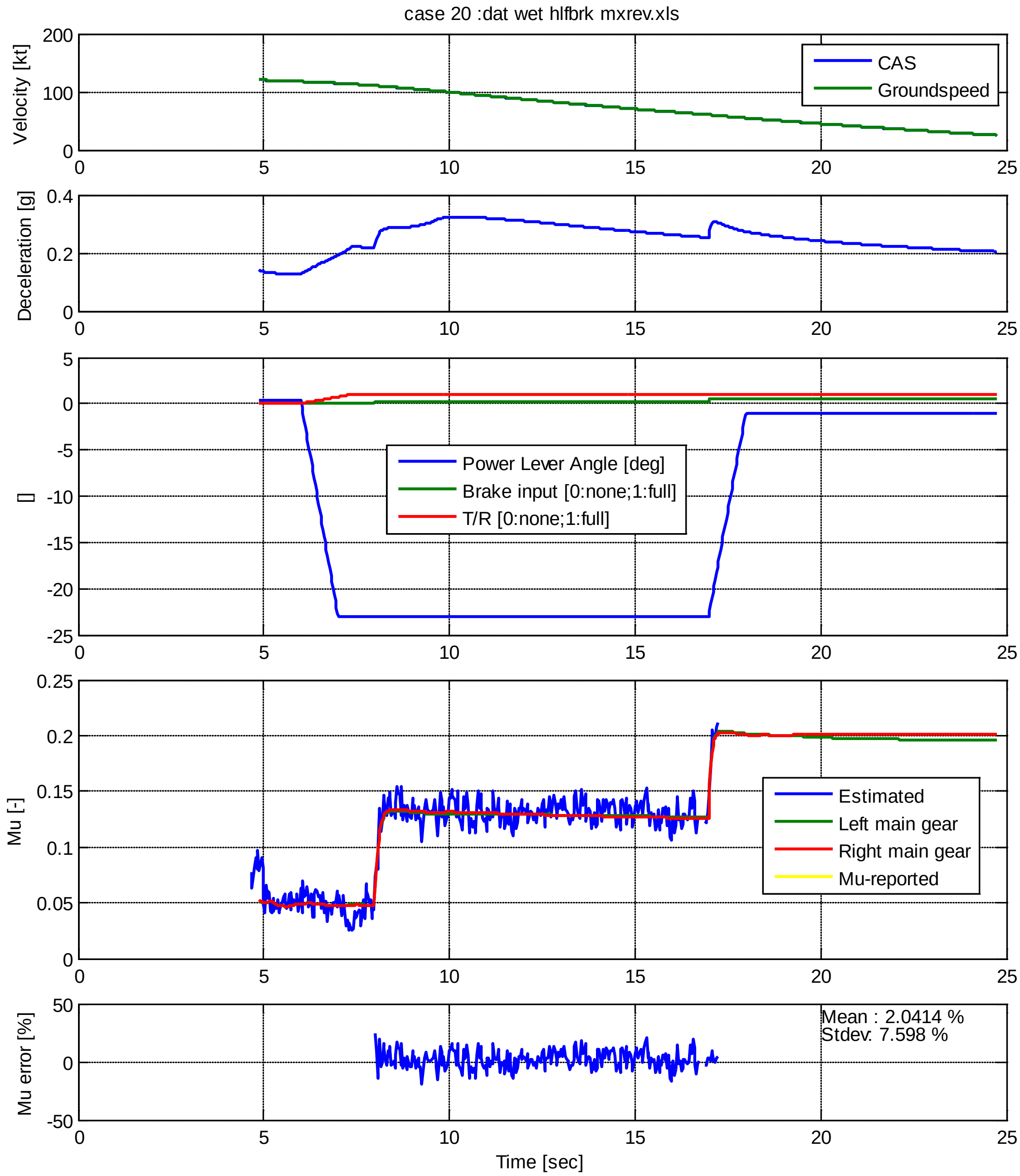

Figure C-20. Simulated Landing Run for Case 20

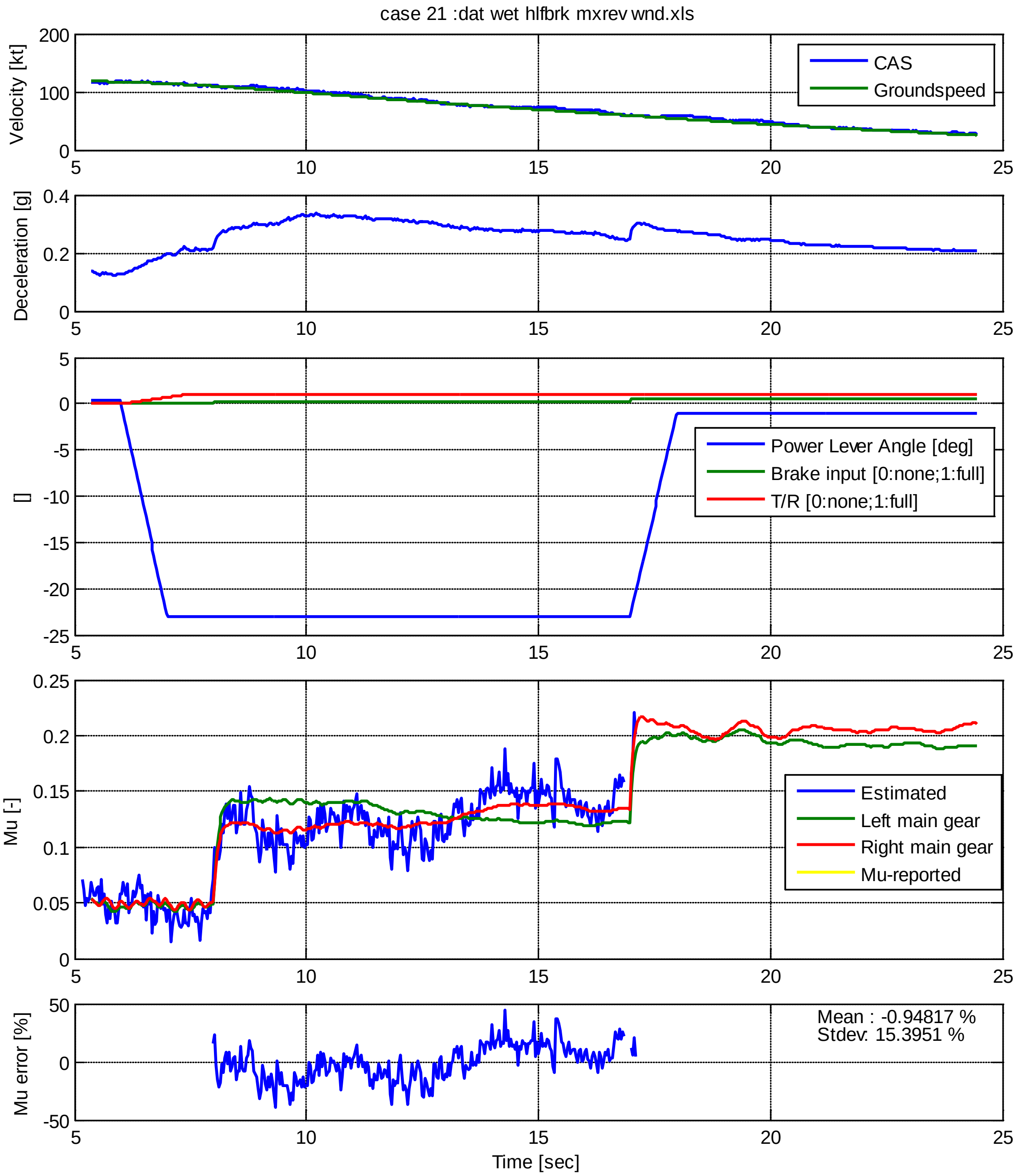

Figure C-21. Simulated Landing Run for Case 21

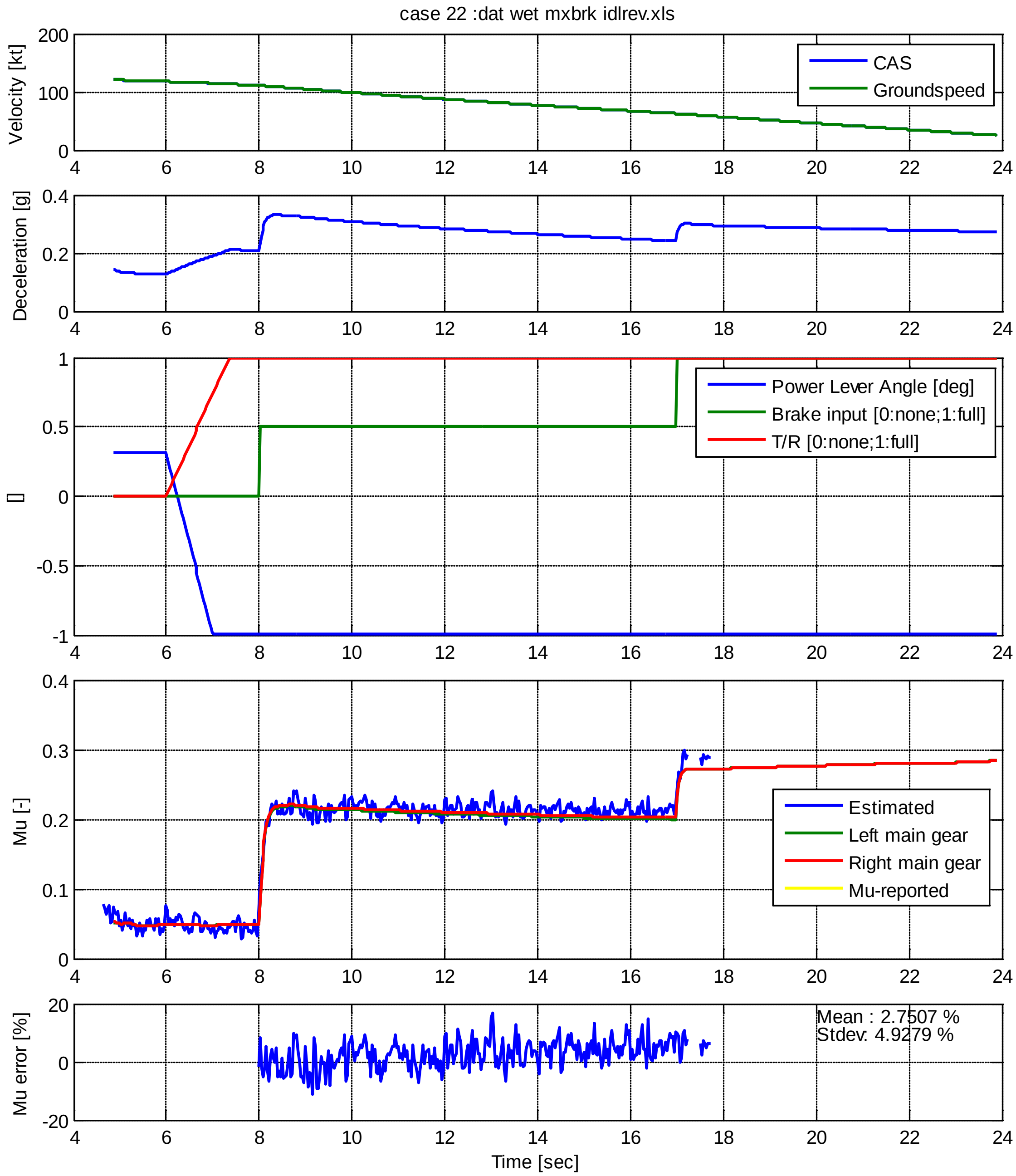

Figure C-22. Simulated Landing Run for Case 22

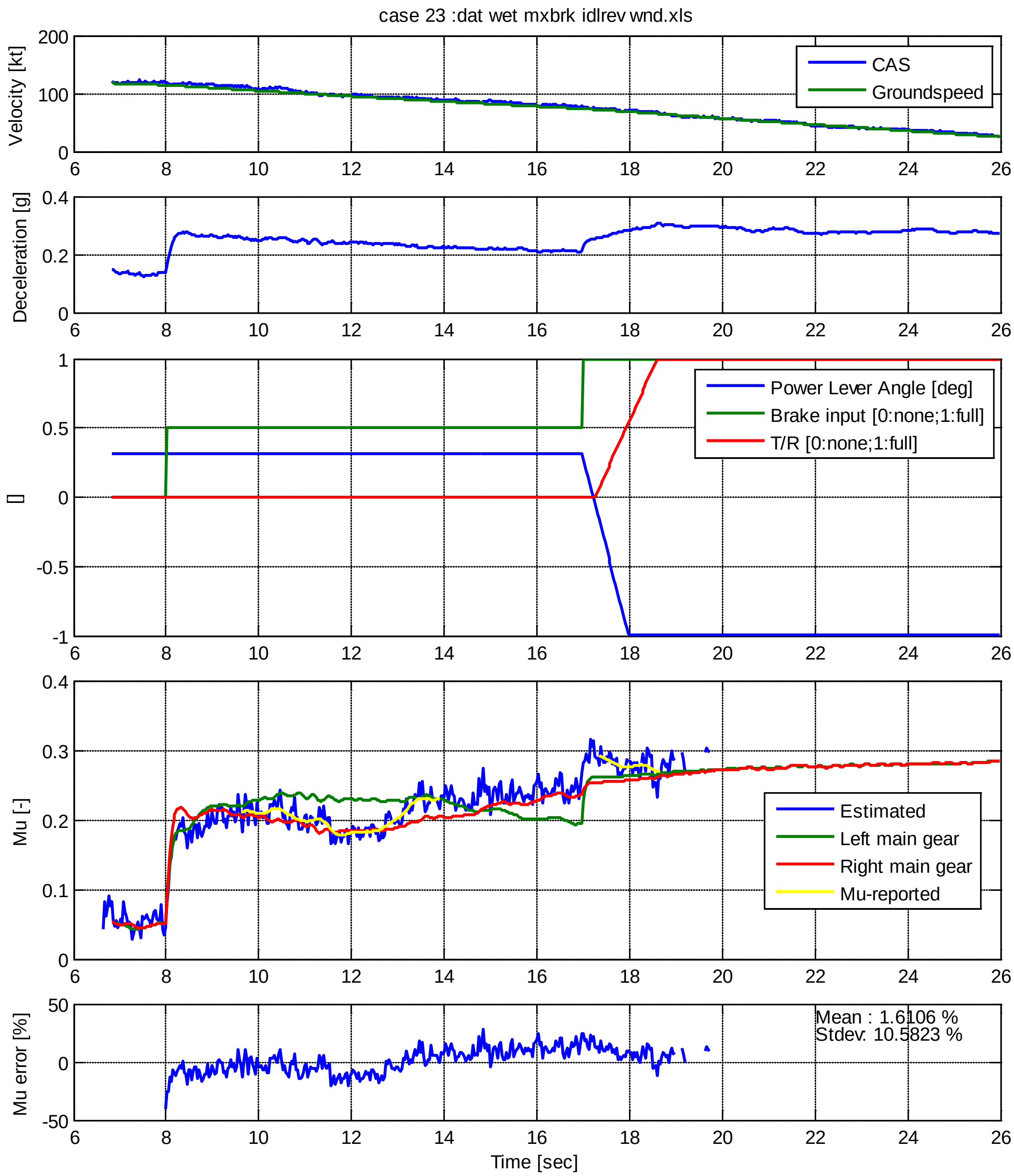

Figure C-23. Simulated Landing Run for Case 23

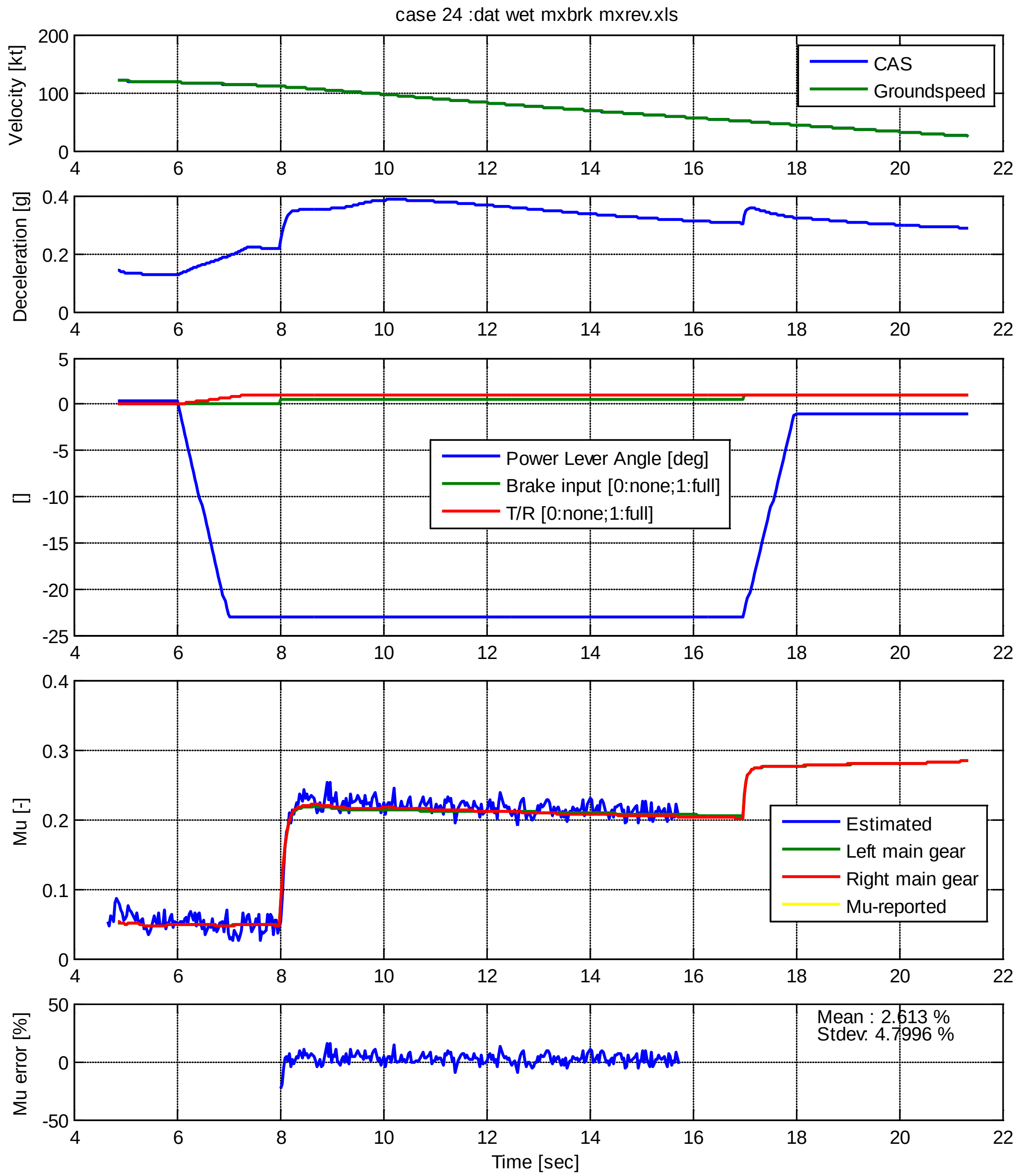

Figure C-24. Simulated Landing Run for Case 24

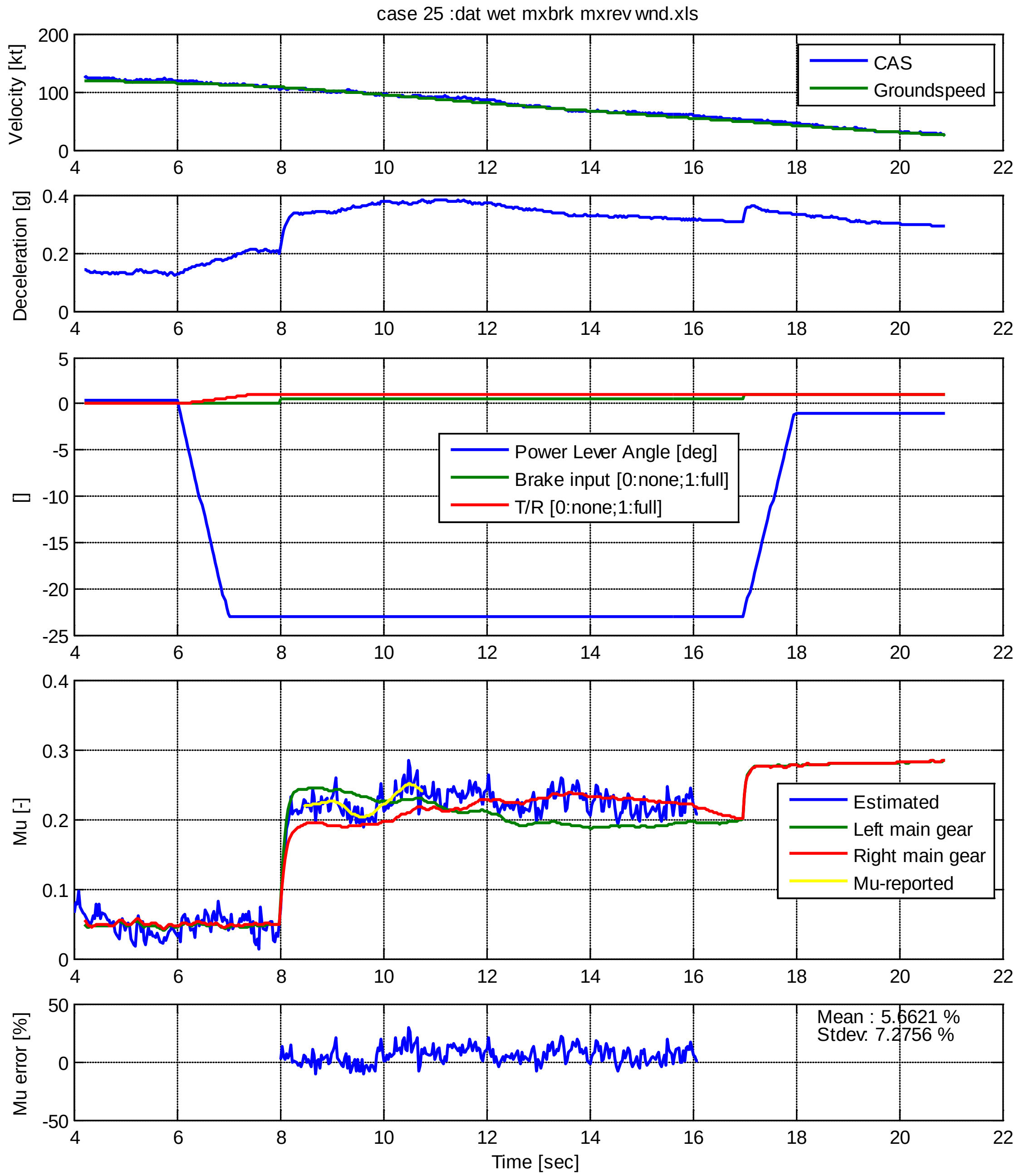

Figure C-25. Simulated Landing Run for Case 25

APPENDIX D—EXAMPLE SIMULATION RESULTS WITH MODELING ERRORS

The following charts present the algorithm outputs (estimated μ, left/right true μ, reported μ) and error in estimated μ when a few selected modeling errors are introduced in the analysis of an icy runway condition (case 13 in table 1 of the main report). Corresponding time histories of simulated landing runs in terms of velocity, deceleration, and aircraft configurations (power, brake, T/R) from touchdown to 25 kt ground speed are also displayed.

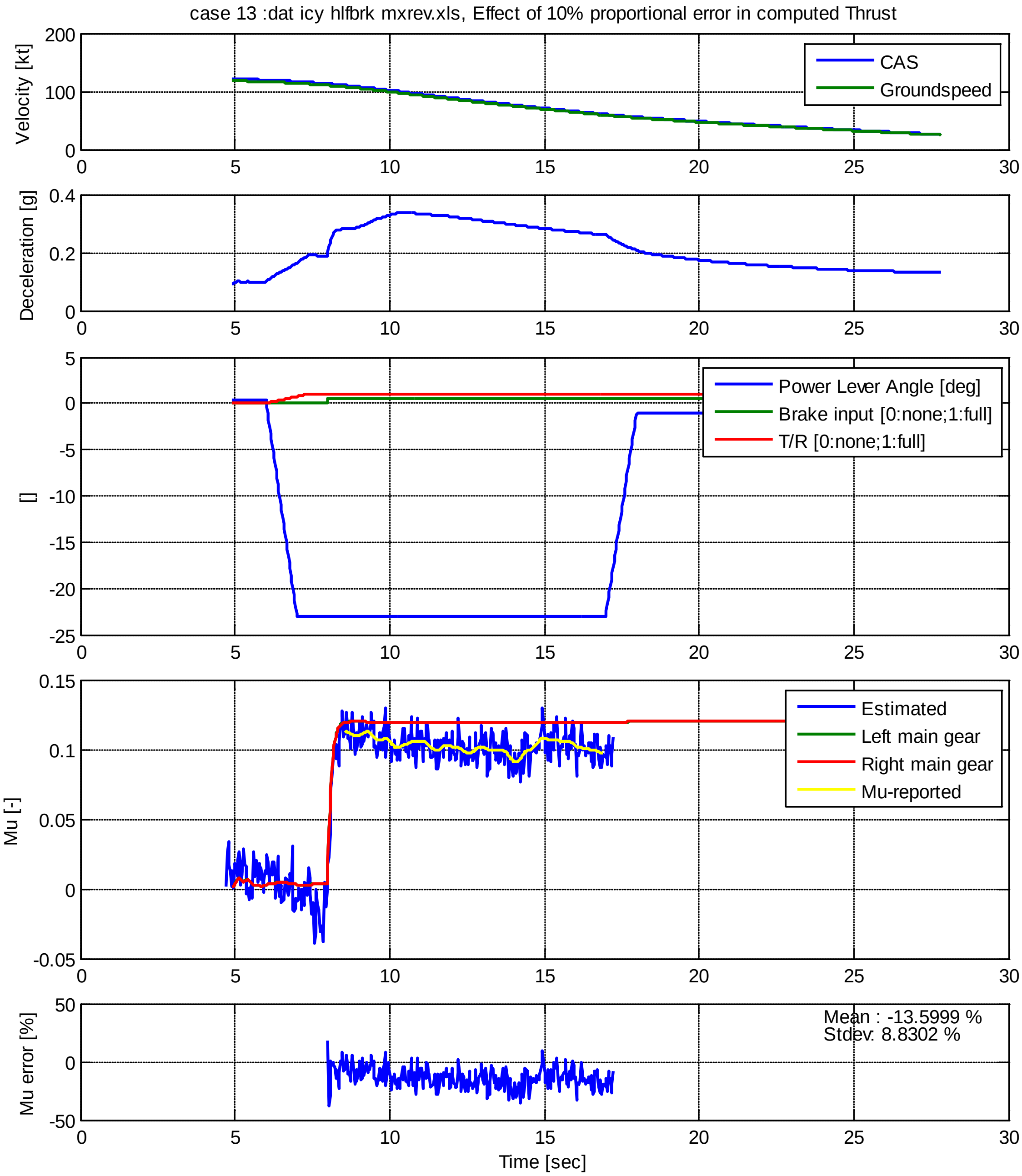

Figure D-1. Simulation Results for Modeling With 10% of Proportional Error in Computed Thrust

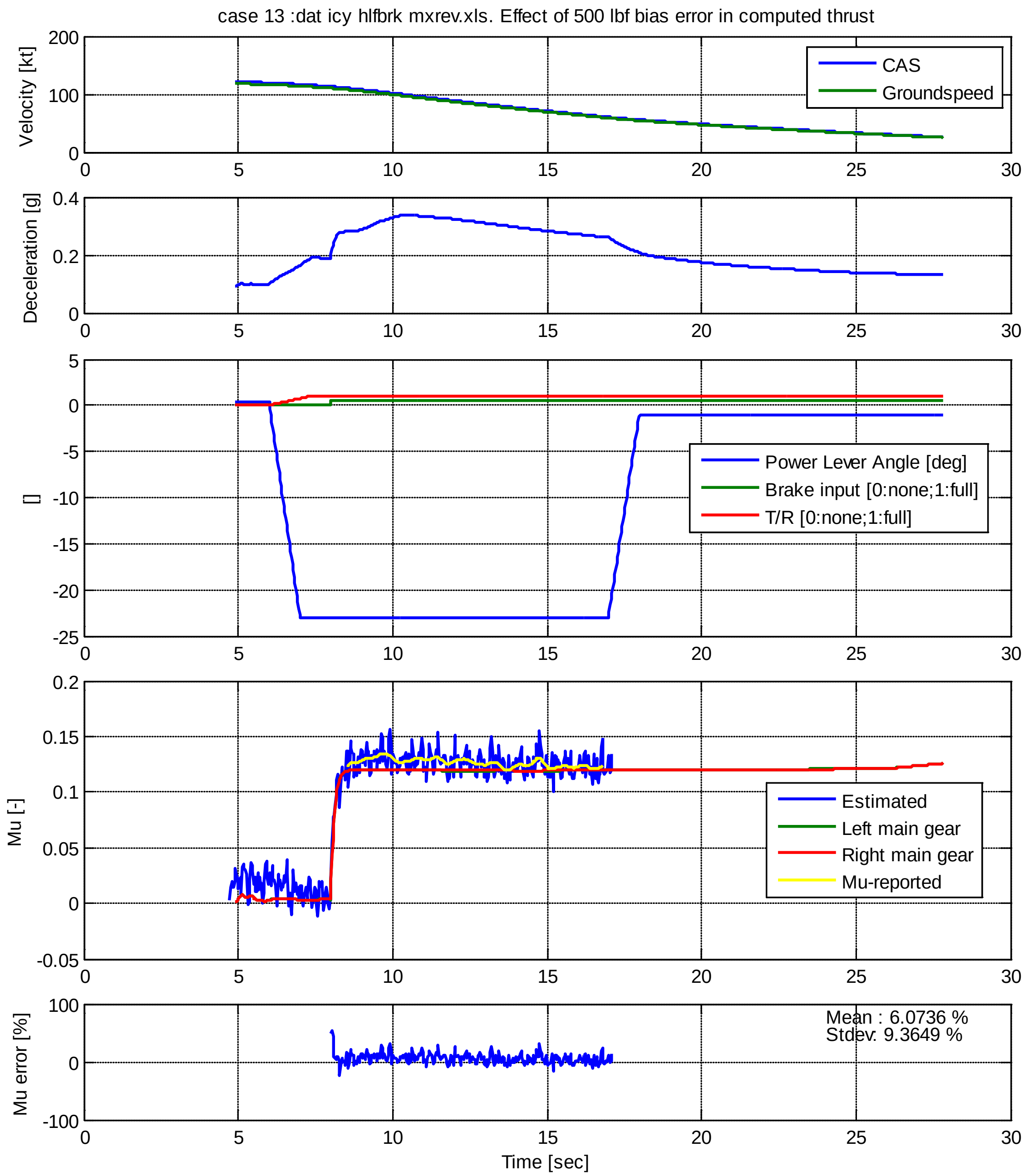

Figure D-2. Simulation Results for Modeling With a Bias of 500 lbf in Computed Thrust

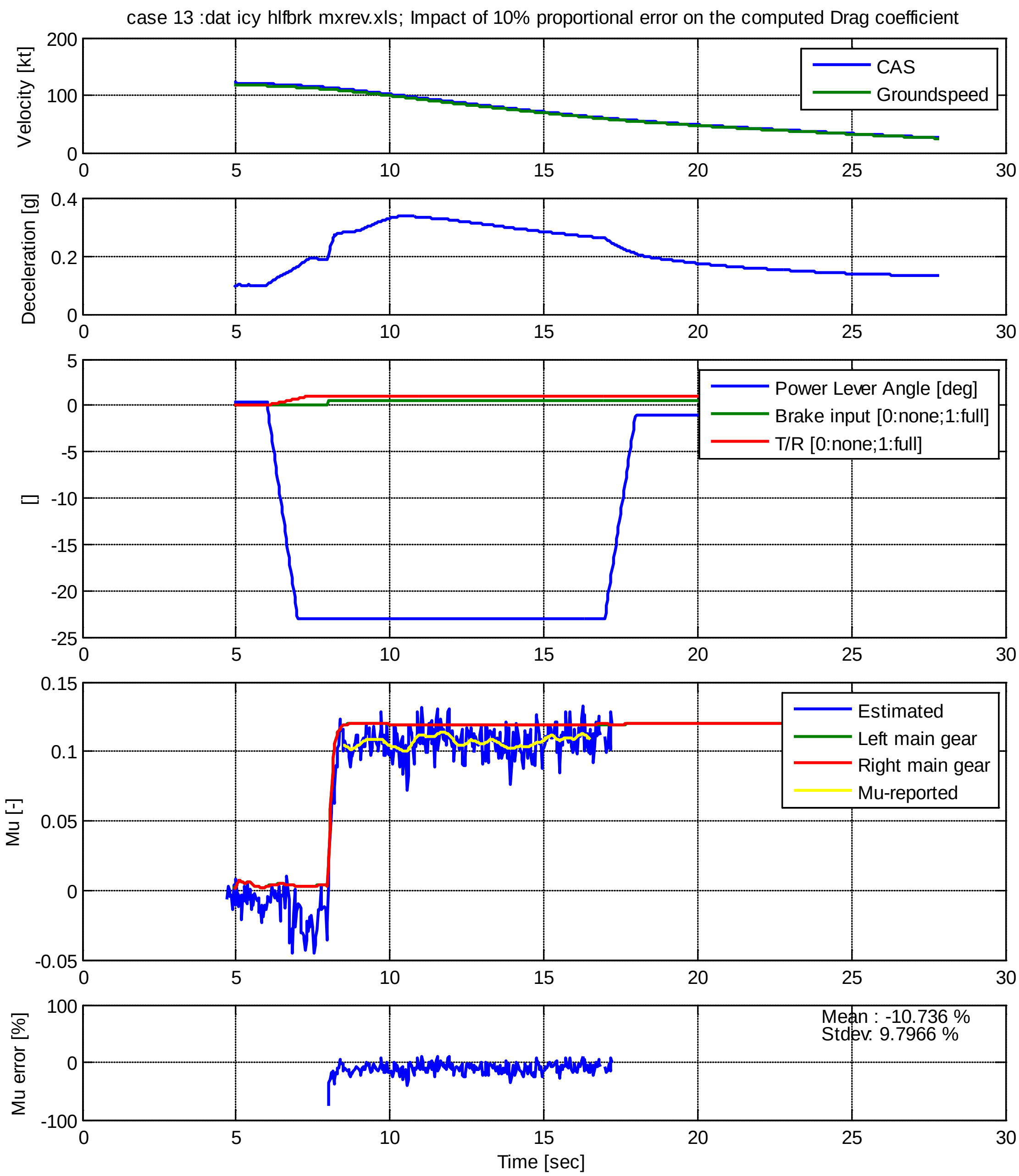

Figure D-3. Simulation Results for Modeling With 10% of Proportional Error in the Computed Drag Coefficient

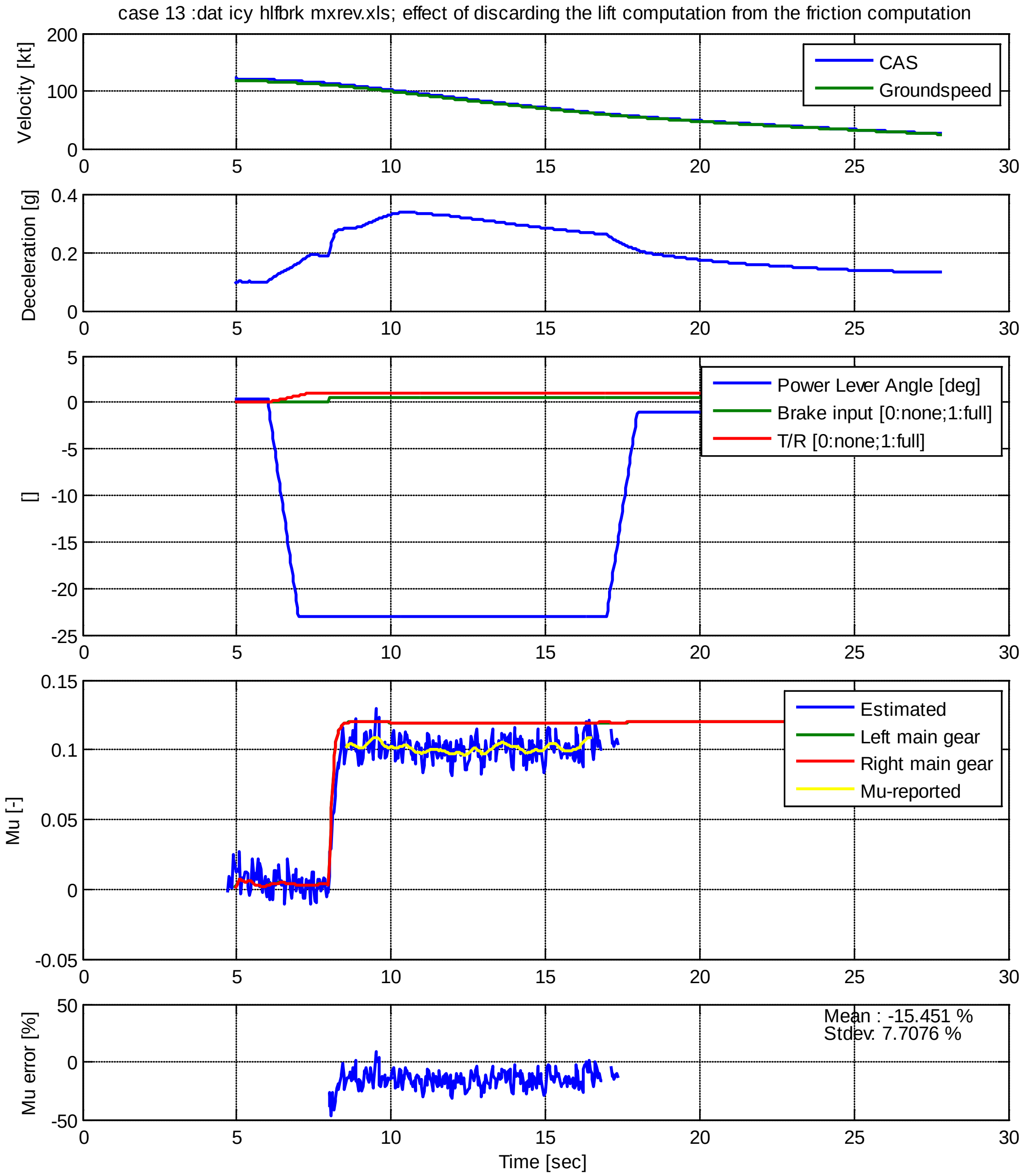

Figure D-4. Simulation Results for Modeling Without Considering Lift

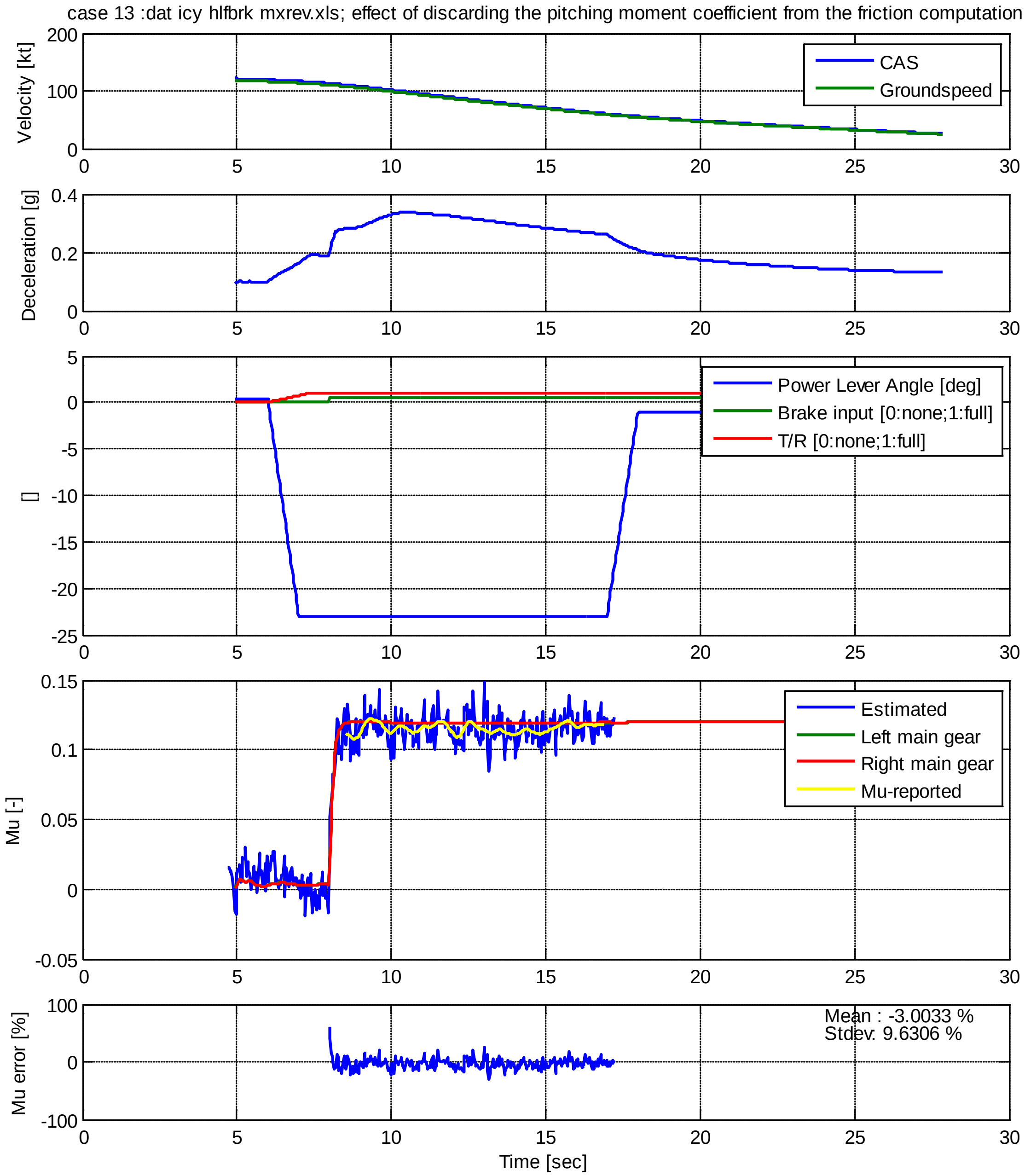

Figure D-5. Simulation Results for Modeling Without Including Pitching Moment Coefficient

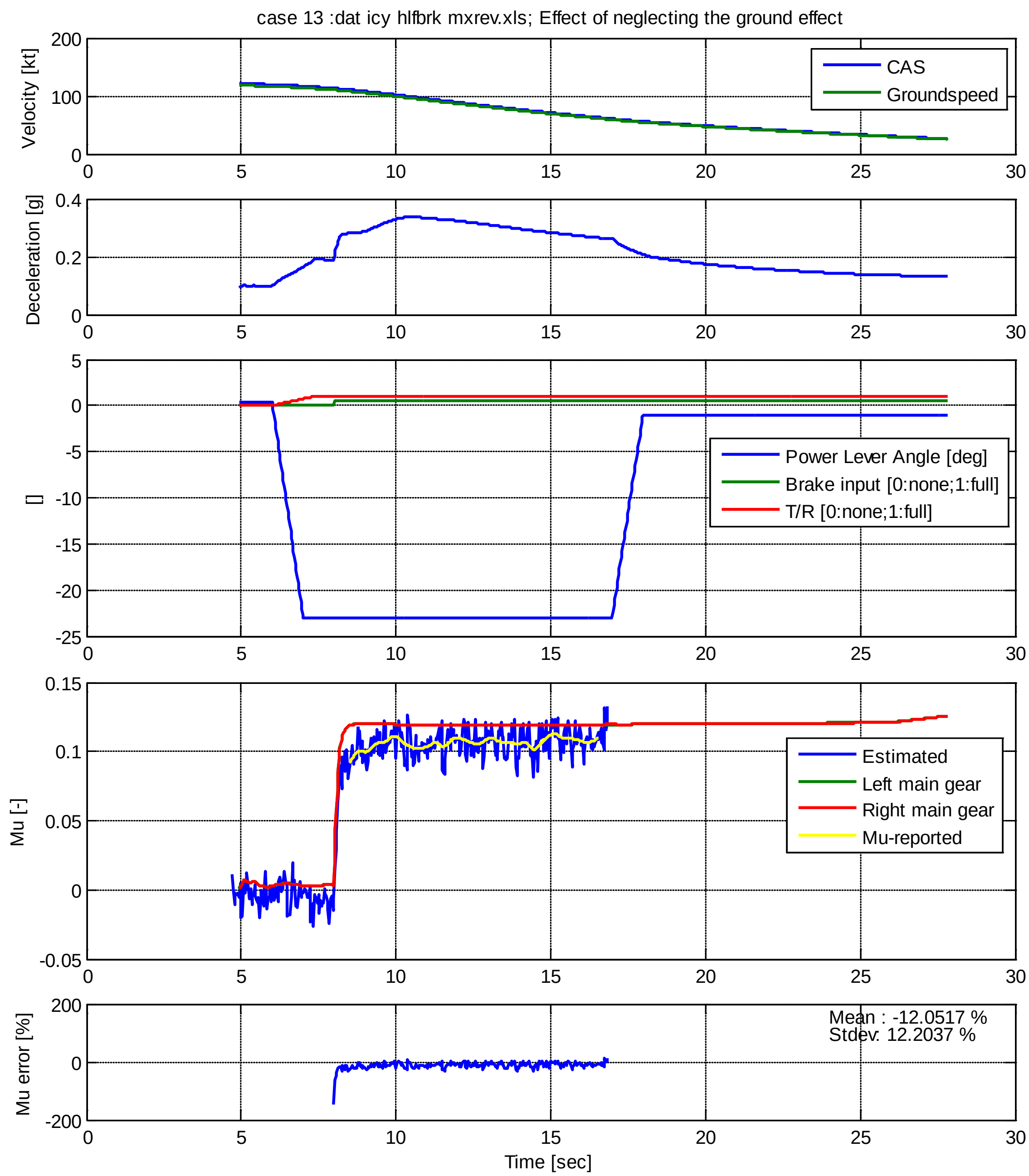

Figure D-6. Simulation Results for Modeling Without Including the Ground Effects